RETINYLIDENE IMINIUM SALTS

AND

RELATED SYSTEMS

by

GARY STEPHEN SHAW, B.Sc.

A Thesis

Submitted to the School of Graduate Studies

in Partial Fulfilment of the Requirements

for the Degree

Doctor of Philosophy

McMaster University

RETINYLIDENE IMINIUM SALTS

AND

RELATED SYSTEMS

DOCTOR OF PHILOSOPHY (1987)
(Chemistry)

McMASTER UNIVERSITY
Hamilton, Ontario

TITLE: Retinylidene Iminium Salts and Related Systems

AUTHOR: Gary Stephen Shaw, B.Sc. (McMaster University)

Supervisor: Professor R.F. Childs

NUMBER OF PAGES: xvi, 242

ABSTRACT

This thesis encompasses some investigations into the structure and chemistry of iminium salts. The interest in this work stems from previous investigations of the visual pigment rhodopsin and a related protein, bacteriorhodopsin. Both of these proteins have been shown to consist of an iminium salt linkage between the chromophore and the protein. Also, these compounds are able to absorb light in the visible region of the spectrum and undergo efficient isomerization processes.

A series of iminium salts related to these natural chromophores were prepared and characterized by a variety of spectroscopic methods in both solution and the solid states. In particular, the ground state structure of these positively charged molecules was examined in terms of charge delocalization, cation anion interactions and chromophore conformation. These properties have been previously suggested to be important in the natural chromophores. One conclusion of this study was that positive charge in these "model" systems is localized in the iminium portion of the molecule. Secondly, it was found that the conformations of these molecules may be different in the solid state from that in solution. In at least one case, the conformation of the chromophore was found to be identical to that found in the natural pigment, bacteriorhodopsin.

The photochemical and thermal reactivity of several of the prepared iminium salts was also investigated using high field ^1H NMR

spectroscopy as an analytical method to directly monitor these reactions. Using this technique, it was found that several of the iminium salts studied underwent efficient trans to cis photoisomerization reactions. In one case, the efficiency of this reaction was very close to that found for bacteriorhodopsin. Moreover, the primary photoproducts formed in these reactions were found to be stable under the experimental conditions used. This was in contrast to previously reported investigations of similar compounds, where cis/trans thermal isomerizations occurred in the reaction medium.

ACKNOWLEDGEMENTS

I would like to extend my sincere gratitude to my supervisor Dr. R.F. Childs. During the course of this work, his guidance, enthusiasm and friendship was greatfully appreciated. I would also like to thank the Natural Sciences and Engineering Council for their financial assistance.

The members of my committee, Dr. R.A. Bell and Dr. C.J.L. Lock, also supported me through much of this project and for that I am thankful. I would like to extend a special thanks to Dr. R.E. Wasylishen at Dalhousie University in Halifax for his efforts in obtaining several of the CPMAS ^{13}C NMR spectra. The many discussions with Dr. W.J. Leigh and Dr. I.D. Brown were also very rewarding.

The technical staff at McMaster offered me the best assistance I could ask for. I would especially like to thank B. Sayer for his assistance on the many NMR experiments conducted, and R. Faggiani for his expertise during crystallographic investigations. Other very important contributions were made by I. Thompson and C. Schonfeld.

During the preparation of this manuscript, many people contributed with there time and efforts. I thank Dr. M. Mahendran, N. Burke, R. Orgias, R. Perrier, J. Orlando and S. Zweep.

Finally, I would like to thank my wife Jenny for her support and encouragement during the trials and tribulations of these past few years.

For Jennifer,

TABLE OF CONTENTS

LIST OF TABLES

LIST OF FIGURES

INTRODUCTION

Chapter 1

Vision and Related Processes

Of the five human senses, perhaps vision is the most complex. Light from an object impinges on the eye and is focused on the retina at the back of the eyeball. Located within the retina is the visual pigment rhodopsin which absorbs light and triggers a chain of events that ultimately result in the sending of an electrical impulse to the brain. This apparently simple sequence allows us to see objects in near darkness or in brilliant sunshine. The human eye can depict all of the colours of the visible spectrum and permits us to see objects of every detail and size. Yet this seemingly well defined process is still largely a mystery. The mechanisms by which light energy is absorbed, and then transformed into an electrical signal are far from well understood. Central to this issue is the structure of rhodopsin, the visual pigment itself, which may contain important information in the understanding of the visual process.

A comparable process to vision occurs in the bacterium Halobacterium halobium and involves a pigment similar to the visual pigment rhodopsin. This pigment, bacteriorhodopsin, undergoes a similar chain of events to rhodopsin but allows the organism to produce energy, rather than to see. However, the structure and mechanism of action of bacteriorhodopsin, like that of rhodopsin, is still unresolved.

I. The Visual Pigment Rhodopsin

The human visual pigment rhodopsin is a membrane protein found in the receptor cells of the retina in the eye. There are two different types of receptor cells in humans, rods and cones, Figure 1-1. The smaller of these are the cones which are responsible for vision in bright light. These can be further subdivided into three types based on their absorption spectra, which provide the basis for colour discernment by absorbing light in the red, blue and green regions of the spectrum. Rods on the otherhand can not distinguish colour but can function in dim light. Because rods are more numerous and their isolation is easier most chemical and biochemical studies are carried out on them.

i. Protein Structure

The protein rhodopsin, 1, is comprised of a chromophore, 11-cis retinal (1), linked to an apoprotein opsin via a protonated Schiff base.

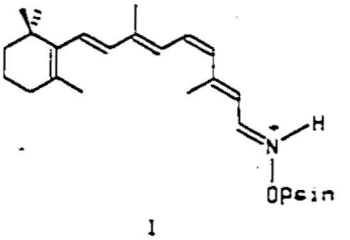

1

Only one of these chromophoric groups exist per opsin molecule (2) for all species of vertabrates. Rhodopsin has a molecular weight of about 40,000 (3) and also contains small amounts of phospholipids, carbohydrates and cholesterol (4). Recently Ovchinnikov and co-workers

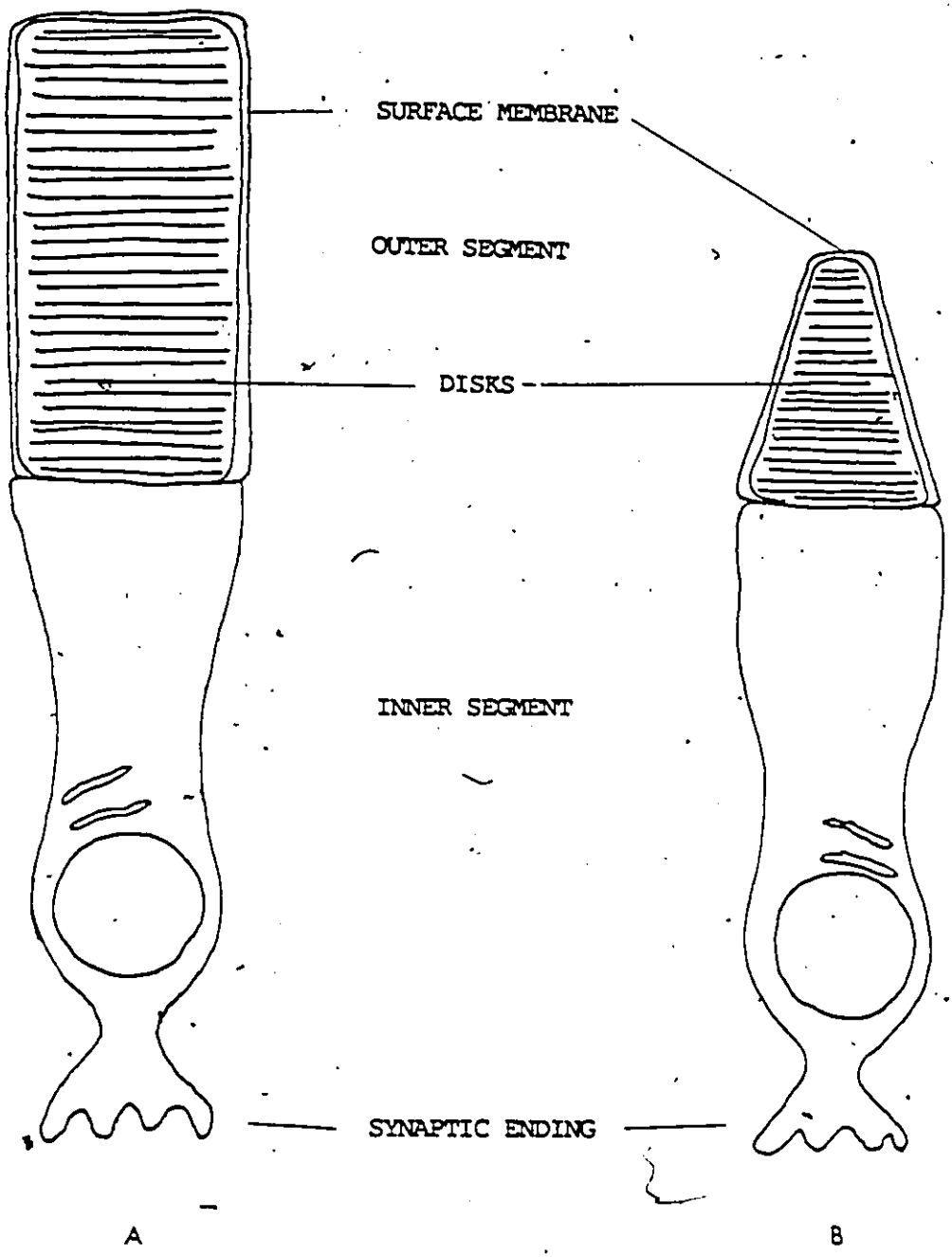

Figure 1-1: The photoreceptor cells: rod (A) and cone (B).

established the complete amino acid sequence for bovine rhodopsin (5). The polypeptide chain was found to contain 348 amino acids which transversed the rod outer segment membrane seven times. These studies also suggested that the average membrane thickness was equivalent to a peptide chain length of 40 residues. Previously it was found that the N-terminal amino acid was acetylmethionine (6) and that this portion of the molecule consisted of 39 residues which were exterior to the photoreceptor membrane (7). Similarily the carboxyl end of the protein contains 40 residues which are not within the membrane (8).

The secondary structure of rhodopsin has been studied using circular dichroism measurements and is postulated as having 30-60% α-helical content (9,10). Within the protein there also exist well defined regions of hydrophobicity which range from 30-100% (5), based on the amino acid content.

ii. The 11-cis Retinal Binding Site

The location of the binding site of the 11-cis retinal moiety to opsin was identified by mild reduction of the aldiminium bond by sodium borohydride, followed by alkaline hydrolysis and recovery of the retinal containing fragment (11,12). These studies clearly showed that 11-cis retinal is bound to position Lys 296 of the polypeptide chain towards the carboxyl end of the protein (5).

The size and shape of the binding site has been shown to be very specific in terms of breadth and longitude. Binding experiments using the various 14 stable isomers of retinal have revealed that 10 of these

form visual pigment analogues. The all-trans, 2, and 13-cis, 3, retinal isomers do not condense with opsin. This, along with the fact that 11-cis, 4 (13,14), 9-cis, 5 (15,16), and 7-cis, 6 (17), retinals form pigments has established that the retinal binding site can only accommodate a chromophore with a maximum of 2 trans C=C bonds in conjugation with the cyclohexenyl ring (18,19).

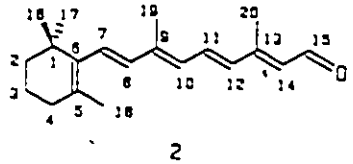

2

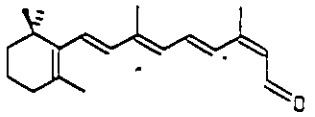

3

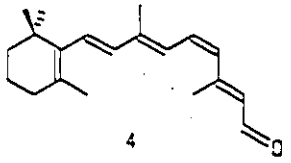

4

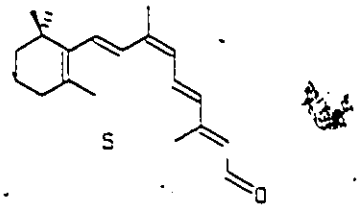

5

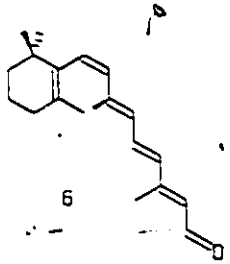

6

A further requirement of the binding site is the inclusion of the cyclohexenyl ring itself (20). It has been suggested that the cyclohexenyl ring may interact with opsin through the formation of hydrophobic bonds (21). However the stereospecificity of this portion of the binding site appears to be low since substitution about the ring system does not affect pigment generation (22). In fact, several

dihydro, and oxoretinal derivatives also form visual analogues with opsin (23-26).

iii. The Nature of the Retinal-Opsin Linkage

Bovine rhodopsin has an absorption maximum at about 500 nm (27). However, the 11-cis retinal chromophore itself absorbs at about 380 nm (28) while its Schiff base absorbs at a slightly lower value (29). Upon protonation the absorption maximum of the Schiff base is red shifted to about 450 nm (30-34). It has been suggested that the Schiff base in rhodopsin must also be protonated or strongly hydrogen bonded (35-38), in order to account for its longer wavelength absorption maximum.

Resonance Raman spectroscopy has provided the most useful information regarding the retinal opsin linkage. In rhodopsin, the stretching frequency, $\nu_{C=N}$, was found at 1655 cm^{-1} in excellent agreement with a model protonated Schiff base (39,40). Upon deuteration of the rod outer segment vesicles the $\nu_{C=N}$ shifted to lower energy by 25 cm^{-1} (41). The deuterated Schiff base model system also showed the same shift providing strong evidence that the Schiff base in rhodopsin is indeed protonated.

Nuclear magnetic resonance (NMR) spectroscopy has also provided insight into the retinal-opsin linkage in rhodopsin. The ^{13}C NMR chemical shift of C(14) in rhodopsin was found to be at 130.8 ppm by using a sample labelled with ^{13}C at this position (42). This raised some controversy over the state of protonation of rhodopsin, since it had previously been shown in studies on a model Schiff base, that the C(14)

resonance should occur near 130 ppm compared to 120 ppm in the protonated system (43). The authors concluded that the rhodopsin Schiff base was unprotonated. However, the lower field resonance of C(14) in rhodopsin compared to that in the model system was later interpreted to be a result of an interaction between the opsin protein, and the retinal chromophore at C(14). The effect of this was to deshield C(14) and shift it to lower field in rhodopsin (44).

Perhaps the most convincing argument for the Schiff base linkage being protonated in rhodopsin comes from an active site labelling experiment by Rando and Longstaff (45). In this study, a pure permethylated bovine opsin was prepared, monomethylated at Lys 296. When this modified protein was allowed to react with 11-cis retinal, a methylated Schiff base pigment was formed which had an absorption maximum at 520 nm, very near to that of bovine rhodopsin.

iv. The Structure of the Chromophore

The detailed structure of the 11-cis retinal moiety in visual rhodopsin is not known. The most accurate method for obtaining this information in rhodopsin would be x-ray crystallography. However, due to the complexity of the protein and difficulty in working with rhodopsin the general route for structural studies is to deal with model systems and compare these to the visual pigment. The model system of choice for some years now has been an n-butyl retinylidene iminium salt, 7. In this system the four carbon chain was chosen so as to mimic the free amino portion of the active site lysine in rhodopsin. A crystal structure of

this molecule has also not been attained.

Some structural information about the rhodopsin chromophore has been provided from an x-ray crystallographic study of 11-cis retinal. This has revealed that two distinct regions of the polyene chain exist (46). The atoms from C(6)-C(13) and C(12)-C(15) form two planes which are twisted by 39° about the C(12),C(13) bond. This deviation from planarity stems from the s-cis conformation of the C(12),C(13) bond resulting in a steric interaction between C(10)H and C(14)H. The C(6),C(7) bond in 11-cis retinal is also s-cis and is distorted to a dihedral angle of 41°. This is a result of crowding of the C(18) methyl group and C(8)H.

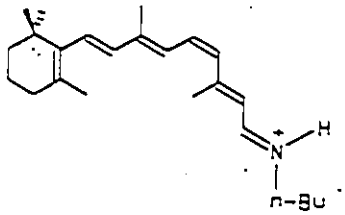

7

The structure of 11-cis retinal is not the same in solution as it is in the solid phase (39,47). Resonance Raman studies have shown that in the solid phase the C(13),C(20) stretching frequency exhibits one line at 1017 cm^{-1} due to the 12-s-cis isomer as found in the crystal structure. Recent ^{13}C NMR studies have also indicated that only one isomer is present in the solid state (48). In contrast, the solution Raman spectrum shows two bands at 1018 and 998 cm^{-1}, consistent with the presence of both the 12-s-cis, 8, and 12-s-trans, 4, conformers

respectively, equation 1. These findings were supported by ^{13}C NMR experiments which concluded that in solution the 12-s-trans form predominates at low temperatures while the 12-s-cis isomer is favoured above room temperature (49-51).

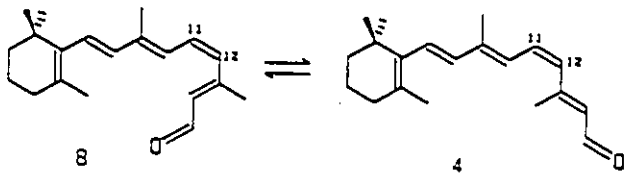

(1)

This thermal equilibrium apparently does not exist for the 11-cis retinylidene Schiff base, 9. However, it has been suggested that this compound forms the 12-s-trans isomer, 10, upon protonation, equation 2 (52).

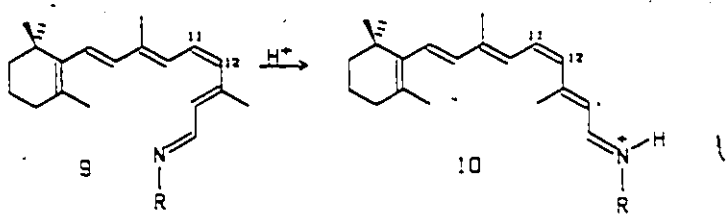

(2)

Callender et al. have concluded that the visual chromophore is also in a 12-s-trans configuration in solution based on resonance Raman data (39). This hypothesis has been verified using a retinal analogue

which was locked in the 11-cis, 12-s-trans conformation. Upon generation of a pigment with opsin, this analogue exhibited similar spectral properties to the natural chromophore (53).

It has been suggested that protonation of the Schiff base nitrogen should yield resonance structures such as those shown in equation 3. A decrease in bond alternation between single and double bonds should occur (54). This was shown to be the case in resonance Raman experiments of n-hexyl all-trans retinylidene Schiff bases and their protonated counterparts (55). The stretching frequencies for the C=C and C=N bonds in the unprotonated species were located at 1583 and 1623 cm^{-1} respectively. Upon protonation the C=C stretching frequency shifted to a lower wavenumber (energy) of 1560 cm^{-1}, suggesting a reduced double bond character. However, the C=N frequency was found at a higher energy. This has been suggested to be a result of the vibrational stretching modes for C=N bonds being altered significantly upon protonation and thus not representing the change in bond strength accurately (34,35).

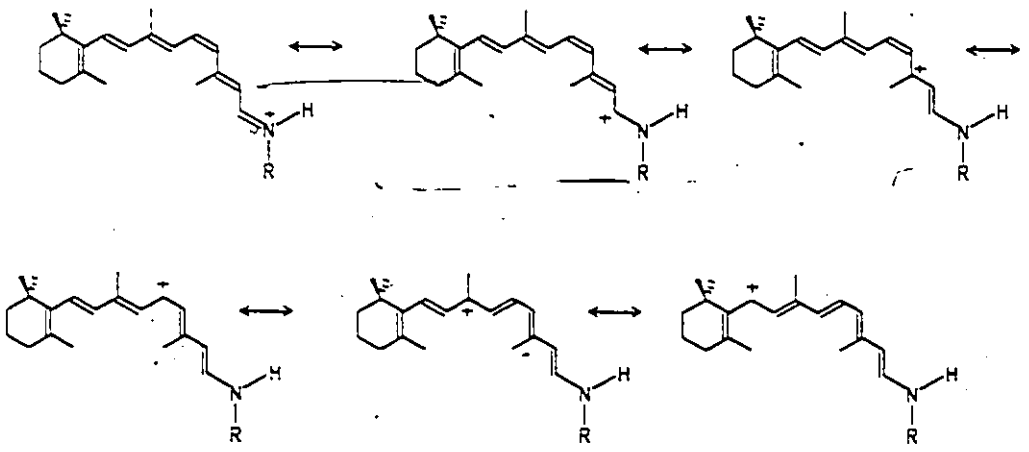

(3)

A further comparison between a retinylidene iminium salt and rhodopsin has also been made using Raman data. The C=C stretching frequency of a protonated 11-cis retinylidene Schiff base occurred at 1556 cm^{-1} (40). In contrast the same stretching mode was found at 1545 cm^{-1} in rhodopsin (39). This strongly suggested that the double bond character in the visual chromophore is somewhat less than that in the model retinylidene iminium salt. However, in order to make a statement regarding the extent of charge delocalization and thus the degree of bond alternation in rhodopsin a more detailed study of the C-C stretching frequencies is required. Such a study has recently been completed for bacteriorhodopsin and is discussed later on in this section.

An insight into the electronic distribution of the visual chromophore has been obtained from theoretical calculations. Using CNDO methods, Pullman and Mantione (56) determined the ground state charge distribution of an 11-cis retinylidene iminium ion, 11.

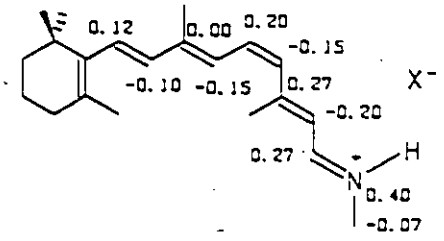

11

Several important features were present in this calculation. First, the π charge associated with the odd numbered atoms in the polyene chain was positive and decreased as one moved further from the nitrogen.

Correspondingly, the charge on the even numbered carbons was negative and became more positive further away from the nitrogen. Second, the π charge on nitrogen was quite large (+0.40), but the overall charge on nitrogen was negative. These observations are consistent with the delocalization of positive charge within the polyene chain as suggested in equation 3, and from Raman experiments. Similar calculations by Inoue (54) and Salem (57) have also shown that delocalization decreases to varying degrees with progression down the polyene chain.

A theoretical study of the bond lengths and angles in retinylidene iminium salts has also shown that a decrease in bond alternation accompanies charge delocalization. Kakitani and Kakitani (58) have determined the molecular structure of an all-trans retinylidene iminium salt, 12, by HMO calculation. They found that the C=C bond length decreased as one moved further away from the C=N fragment. Likewise the C-C bond length increased during the same progression.

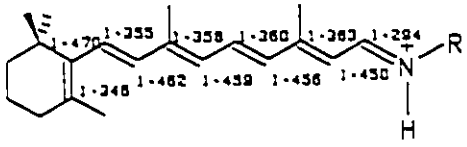

v. Bleaching of Rhodopsin

The ultimate fate of rhodopsin upon absorption of a photon is its bleaching to form dissociated all-trans retinal and opsin, equation 4.

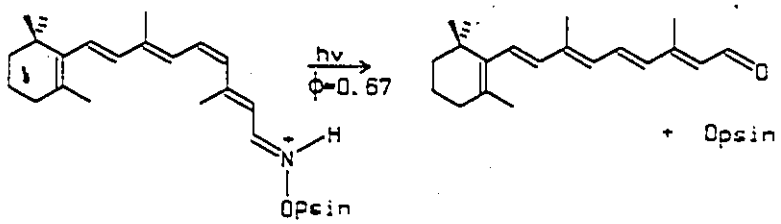

(4)

Several distinct intermediates are involved in this process, each with their own distinctive spectroscopic properties, Scheme 1-1. Most of these properties are believed to be a result of various interactions between the chromophore and the protein. The overall quantum yield for this process is 0.67 (59,60).

The primary photoproduct formed on irradiation of rhodopsin with blue light is bathorhodopsin. At 77°K, this reaction is photochemically reversible but thermally irreversible (61). Extended illumination of rhodopsin yields the photostationary state shown in equation 5. The minor photoproduct, isorhodopsin, has been suggested to contain a 9-cis chromophore and upon irradiation it too forms bathorhodopsin. Thus it was suggested that the geometry of the common photoproduct bathorhodopsin must be all-trans (62).

$$\underset{33\%}{\text{Rhodopsin}} \overset{437\ nm}{\rightleftharpoons} \underset{51\%}{\text{Bathorhodopsin}} \overset{437\ nm}{\rightleftharpoons} \underset{16\%}{\text{Isorhodopsin}} \qquad (5)$$

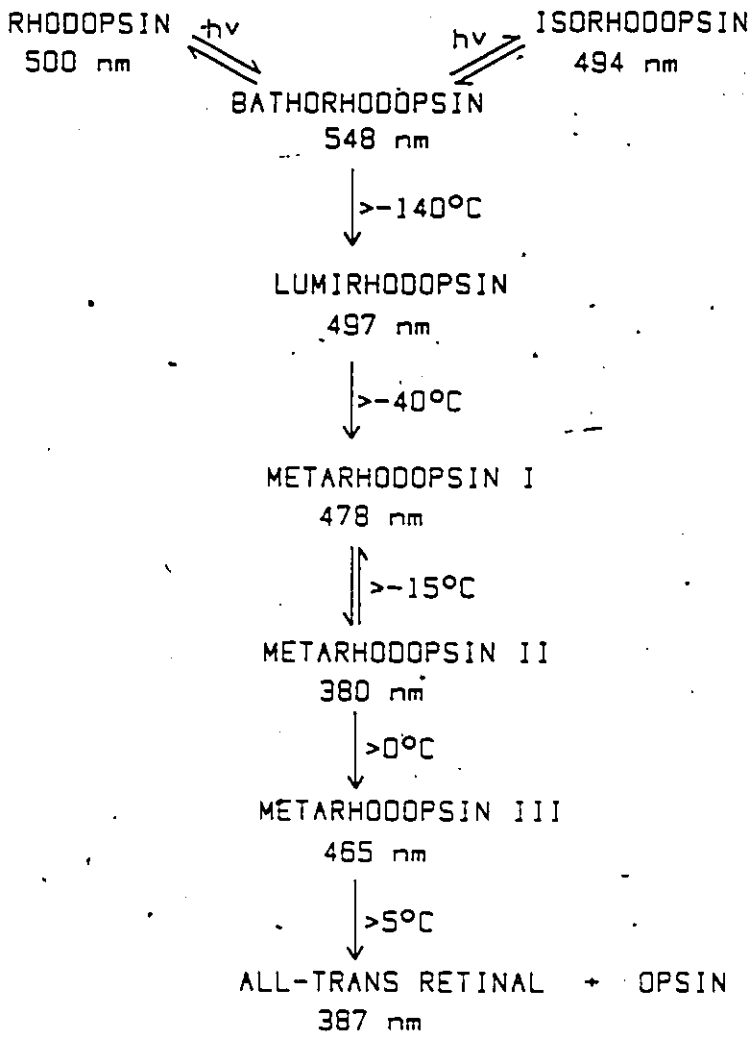

Scheme 1-1: The bleaching of rhodopsin.

The formation of bathorhodopsin as the essential process in vision was established using modified rhodopsins in which the C(11),C(12) bond of the 11-cis retinal moiety was incorporated into a ring system. This prevented isomerization of the molecule and indeed no bathorhodopsin was formed upon irradiation of these systems (53,63). This also reinforced the idea that the C(11),C(12) bond in bathorhodopsin is trans.

Bathorhodopsin decays thermally above 133°K to eventually form the long lived intermediate metarhodopsin II. It is postulated that unfolding of the protein occurs here and causes a deprotonation of the chromophore to yield metarhodopsin I (64). Resonance Raman supports these characterizations since the spectrum of metarhodopsin I is very similar to that of a protonated all-trans retinylidene Schiff base while metarhodopsin II corresponds to the unprotonated compound (65).

vi. Visual Transduction

During the visual cycle an electrical impulse is sent to the brain which then interprets the signal. This process is called visual transduction, and is postulated to occur before or during the formation of metarhodopsin II (66). It has also been determined that cis/trans isomerization is a necessary requirement for transduction to occur.

In the dark, a continuous current is present in the rods. This is the result of sodium ions passing into the rod outer segment in response to a concentration gradient. The sodium ions funnel to the far end of the rod where they are pumped out. This cycle produces a dark current of about 1 billion electron charges per second (67,68). Upon

irradiation, this current decreases by about 3% for each photon absorbed by rhodopsin and a change in membrane permeability occurs such that sodium ions no longer pass into the rod outer segment. This gives rise to the electrical impulse.

No direct correlation between the rhodopsin photocycle and the change in dark current has been observed. However, several chemical events occur at a similar time. The first is that during absorption of light by rhodopsin, cyclic guanidine monophosphate (cGMP) is hydrolysed at an enormous rate (69,70). Following this, it has been suggested that the light activated rhodopsin transforms the membrane enzyme transducin (G protein) into its active form. This in turn activates cGMP phosphdiesterase which hydrolyses cGMP (71). It has been shown that cGMP stimulates the release of calcium ions which may be responsible for blocking sodium channels and decreasing the dark current substantially (72).

II. Bacteriorhodopsin

Bacteriorhodopsin, found in the cell membrane of the bacterium Halobacterium halobium is a second biologically important protein which contains a retinal chromophore (73). Like the visual pigment rhodopsin, bacteriorhodopsin contains a protonated Schiff base linkage between the retinal and protein and exhibits photolytic activity. In the presence of oxygen this organism is capable of synthesizing ATP through a normal respiration pathway. However, anaerobically, light energy is used to produce adenosine triphosphate (ATP) via a proton pumping mechanism (74).

i. Photochemical/Thermal Cycle

Bacteriorhodopsin can exist in either dark adapted or light adapted forms. In dark adapted bacteriorhodopsin, both the all-trans, (BR_{568}), and 13-cis, (BR_{548}), retinal isomers are present (75,76). These two chromophores exist in roughly equal populations in thermal equilibrium, equation 6 (77,78). Recently, it was shown by solid state ^{13}C NMR techniques that BR_{548} contains a syn C=N bond compared to BR_{568} which is has an anti arrangement (79). In the presence of light the 13-cis isomer is efficiently converted to the all-trans (Φ=0.63), equation 7 (80,81).

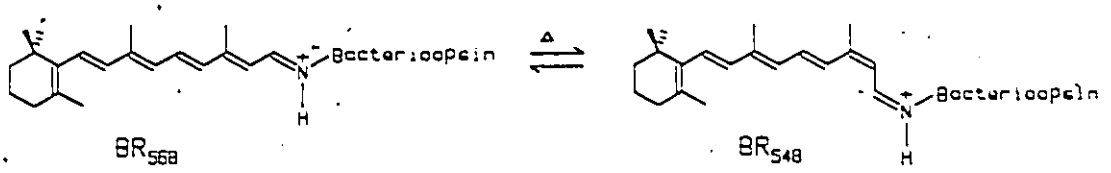

(6)

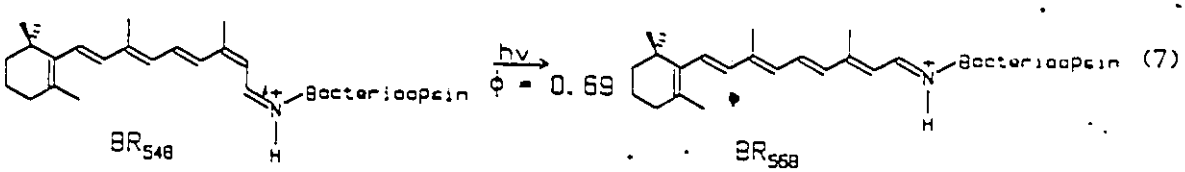

(7)

The all-trans isomer, BR_{568}, is the initial reactive species in the photochemical cycle of bacteriorhodopsin, Scheme 1-2. This process is similar to that of rhodopsin in that it involves a single C=C photoisomerization (78,82), but unlike the visual pigment, bacteriorhodopsin

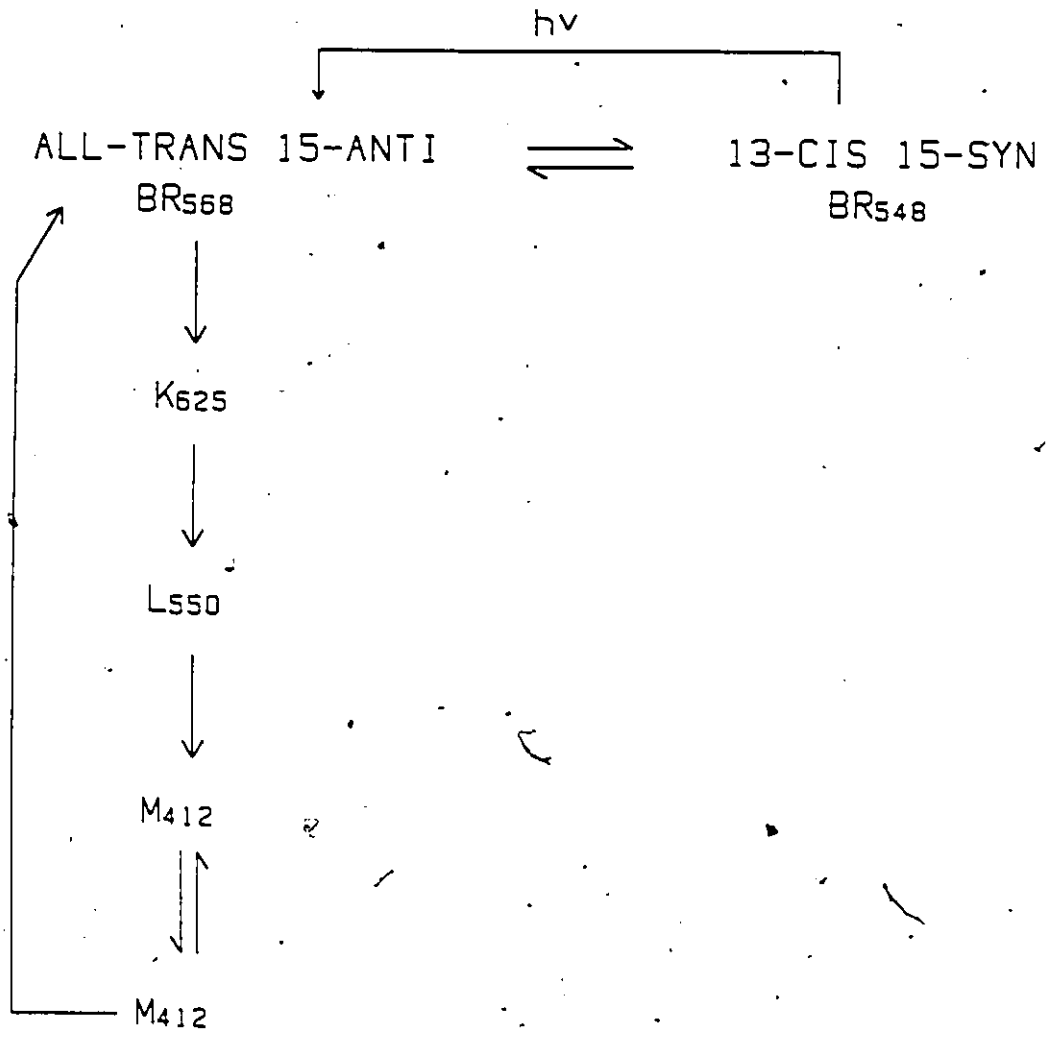

Scheme 1-2: The photocycle for bacteriorhodopsin.

is now bleached (83).

The primary step upon light absorption is the formation of the intermediate K_{625}. This process occurs in less than 40 picoseconds and has a quantum yield of about 0.30 (80,81). Resonance Raman studies have indicated that the C(13),C(14) bond of K_{625} is cis (84,85), and the C=N bond is anti (86).

The remaining steps of the cycle are thermal and involve several discrete intermediates, each named for the wavelength at which it absorbs (87-91). Decay of bacteriorhodopsin K_{625} gives rise to a structurally similar product, L_{550}, which also contains a 13-cis double bond (86,92,93). This in turn forms M_{412} which consists of two or more rapidly interconverting intermediates (94,95). The much shorter absorption maximum of M_{412} indicates that deprotonation of the nitrogen has occurred (96,97). It has been suggested that this deprotonation results from a change in the environment of the chromophore (82,98). The final intermediate formed is O_{640} in which the chromophore is now all-trans and the Schiff base has been reprotonated (99,100).

Evidence for the proton pumping activity of bacteriorhodopsin has come from kinetic measurements at low temperatures. Using analogues of bacteriorhodopsin which have either a locked C(13),C(14) bond (101) or are sterically hindered at C(11),C(12) (102,103), it was shown that the all-trans to 13-cis photoisomerization was a necessary requirement for proton pumping activity. At -40°C, it was found that the rate of proton release parallels that of the formation of intermediate M_{412} (104,105). Reprotonation occurs rapidly and coincides with the formation of O_{640}

(106). One estimate has suggested that two protons may be pumped per cycle (107,108).

ii. Protein Structure

Bacteriorhodopsin is a structurally simpler protein than rhodopsin. It contains only 248 amino acids, 100 fewer than the visual pigment (109,110). X-ray and electron diffraction studies (111-115) have provided a wealth of structural information about the protein and have enabled researchers to propose a detailed three dimensional model.

The polypeptide chain of bacteriorhodopsin consists of seven "rods", approximately 40 Å each in length and with 10 Å spacings. Three of these "rods" are parallel to the lipid bilayer and the remainder are slightly tilted. There are about 25 amino acids in each rod and 70 amino acids which connect the "rods" together. The protein has been estimated to be 70% hydrophobic, based on its amino acid composition (109).

Experiments aimed at determining the secondary structure of bacteriorhodopsin have found that the peptide backbone is quite rigid. Based on solid state ^{13}C measurements, no motions greater than 10° and faster than 100 s^{-1} could be observed (116).

iii. The Binding Site

Bacteriorhodopsin has a binding site which is quite different from that of rhodopsin. Both the all-trans and 13-cis retinal isomers form pigments with bacterioopsin, while the 11-cis and 9-cis isomers do not (117). This suggests that the pocket in which the chromophore is

located is long and narrow. Many different bacteriorhodopsin analogues can be formed including ones that have an extended (118) or truncated polyene chain (119), or lack a cyclohexenyl ring (120).

The retinal moiety is deeply buried within the protein. It is estimated to be about 8 Å from the membrane surface (121) and bound to Lys 216 (109,122).

Resonance Raman experiments have shown that the Schiff base linkage between retinal and bacterioopsin is protonated (78,88,100,123). This has been verified by solid state ^{15}N NMR experiments in which Lys 216 was ^{15}N enriched. It was found that the ^{15}N chemical shift of the labelled bacteriorhodopsin was very near that of a model protonated Schiff base. These resonances also had comparable line-widths and tensor values (124).

iv. The Structure of the Retinal Chromophore in Bacteriorhodopsin

The exact structure of the chromophore in bacteriorhodopsin, like that of rhodopsin, is still unknown. However, a more detailed structure of the retinal chromophore in bacteriorhodopsin compared to that in rhodopsin exists largely because of the ease in working with an all-trans chromophore rather than the 11-cis isomer. A large portion of evidence for the structure of bacteriorhodopsin comes from the ability to synthesize derivatives labelled specifically at one or more positions (125).

All of the single bonds from C(8)-C(15) in BR_{568} have been shown to be s-trans by resonance Raman spectroscopy (87). These findings were

previously suspected from an x-ray crystallographic study of all-trans retinal (126). In addition, the crystal structure showed that the polyene chain of all-trans retinal was markedly bent from linearity and bowed from planarity. Similar to the crystal structure of 11-cis retinal, the all-trans isomer is s-cis about the C(6),C(7) bond. It has been assumed that this conformation does not change upon formation of bacteriorhodopsin. The dihedral angle about C(6),C(7) in all-trans retinal is 62°, somewhat larger than that in 11-cis retinal, while solution experiments have shown that this angle is about 32° using nuclear overhauser experiments (NOE) (49). Theoretical studies of bacteriorhodopsin have also shown that the conformation about the C(6),C(7) bond is 6-s-cis (127), however the predicted dihedral angle is 82°.

Recently, it has been suggested that the C(6),C(7) bond in bacteriorhodopsin may not have a twisted 6-s-cis conformation. Evidence for this has come from solid state ^{13}C NMR experiments using both labelled retinal derivatives, and systems with known C(6),C(7) conformations obtained from crystal structure data (128). Using these data, Harbison and co-workers have shown that the C(6),C(7) bond in bacteriorhodopsin is in a perturbed 6-s-trans conformation, 13.

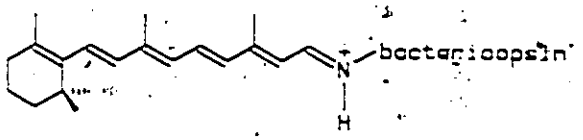

13

Delocalization in bacteriorhodopsin has been shown to very extensive. In resonance Raman experiments using deuterium and/or carbon labelled chromophores, Smith and co-workers were able to unequivocally identify each C-C stretch in the chomophores of bacteriorhodopsin and a model retinylidene iminium salt (87,123). In each case, the specific C-C stretching frequencies of the polyene chain for bacteriorhodopsin are at higher energy than the comparable one in the model compound, corresponding to a more delocalized structure in bacteriorhodopsin.

Schulten and Tavan have also shown that bond alternation in the bacteriorhodopsin chromophore is reduced near the C=N bond and increases steadily as one moves further down the polyene chain (127). Accompanying this is an increase in charge delocalization. Overall, the highest positive charge is located on C(15), C(13) and C(11) and the most negative charge was found on N, C(14) and C(12). In the model system used to determine these values an anion was placed 3.0 Å from the nitrogen and as a result a significant portion of the positive charge was found on the nitrogen proton.

III. Rhodopsin and Bacteriorhodopsin Model Systems

The complex nature of the binding site and protein in both rhodopsin and bacteriorhodopsin has made detailed structural examination of the chromophores in these systems very difficult. As has already been shown there appears to be a significant structural difference between the natural chromophores and simple protonated retinylidene Schiff base models. It is now widely accepted that these differences result from

anionic/cationic interactions between the protein and the chromophore within the binding sites (129,130). It has also been suggested that the binding sites of rhodopsin and bacteriorhodopsin play a large role in the photochemistry and thermal chemistry of these systems. As a result, model systems have been developed to mimic the absorption spectra of rhodopsin and bacteriorhodopsin in an effort to understand the environments of the chromophores and their overall structures. Model systems have also been used to probe the mechanisms of photochemical and thermal isomerization in these systems.

i. Models Based on Absorption Spectra

A protonated retinylidene Schiff base exhibits a broad, featureless absorption spectrum that is the result of a π-π^* electronic transition. The lack of fine structure in these spectra suggests that a large number of vibrational levels exist with similar energy in the first excited singlet state, S_1 (131).

A linear relationship between the reciprocal of the anion radius and the absorption maximum exists for protonated n-butyl retinylidene Schiff bases, 14a-f, Table 1-1. In this study it was found that retinylidene iminium salts prepared with different anions had absorption maxima in non polar solvents. The shortest absorption maximum was observed with a chloride anion and the longest was with perchlorate. Based on this data (32), it was suggested that a small anion such as chloride forms a strong hydrogen bond with the nitrogen proton and tends to move the anion closer to the nitrogen. In contrast, larger anions

such as iodide or perchlorate possess a weaker hydrogen bond, and are located further from the nitrogen. Thus the absorption maximum increases as the anion size increases. In a more recent study (132), encompassing retinylidene salts with a greater range of anions based on pKa, this finding was corroborated for strong mineral acids using ^1H NMR spectroscopy.

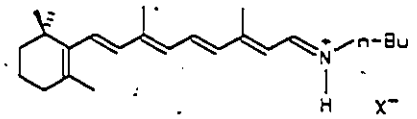

14a: X = Cl
b: X = NO_3
c: X = HSO_4
d: X = Br
e: X = I
f: X = ClO_4

The binding sites of rhodopsin and bacteriorhodopsin are very confined and it is highly unlikely that the distance between the anion and nitrogen would be greater than 4.0 Å. Thus the simple cation/anion distance relationship for retinylidene iminium salts has been ruled out in accounting for the longer wavelength absorptions of bacteriorhodopsin (570 nm) or rhodopsin (500 nm). As a result, further models for bacteriorhodopsin and rhodopsin were developed which could mimic possible secondary anionic (point charge) interactions between the protein and the chromophore. The charged species of the protein would most likely be in the form of amino acid residues which contain zwitterionic groups such as carboxylate or ammonium ions.

The first suggestion that the opsin protein could modify the spectral properties of the 11-cis retinal chromophore in rhodopsin was

Table 1-1

Absorption Spectra Data[a] for Retinylidene Iminium Salts[b]

Compound	X^-	λ_{max} ($CHCl_3$)
14a	Cl^-	460
14b	NO_3^-	464
14c	HSO_4^-	466
14d	Br^-	468
14e	I^-	478
14f	ClO_4^-	480

a in nm.

b ref. 32

made by Hubbard (129). Theoretical evidence for this interaction, presented by Pullman and Mantione, indicated that the placement of an anion along the polyene chain of the chromophore could alter the ground and excited state properties of the molecule (56). This electrostatic interaction was capable of mimicking the longer wavelength absorption of rhodopsin better as compared to the model retinylidene compounds 14a-f. However, the exact nature of the interaction and the specific location of the anion in the opsin protein remained uncertain.

Some time later, Nakanishi and co-workers showed, using a series of dihydro-retinals, that the section of the retinal chromophore most responsible for the long wavelength absorption of rhodopsin was the region from C(11) to nitrogen (133). Using this information, it was calculated that a negative "point charge" placed approximately 3 Å from C(12) and C(14) could reproduce the absorption maximum of bovine rhodopsin, Figure 1-2. It was also suggested that this model could be modified by employing one or more external charges to reproduce the three absorption maxima of human cone rhodopsins (44,134). A series of modified diene iminium salts were used to show that in addition to a red shift from external negative charge interactions, 15, a blue shift could also be obtained, 16 (135). Retinal analogues with "built-in point charges" have since been synthesized in an effort to reproduce the absorption properties of rhodopsin (136,137).

In bacteriorhodopsin the absorption maximum is more than 100 nm red shifted from that of the n-butyl retinylidene iminium salts, 14a-f. It was therefore suggested that a different mechanism from that of

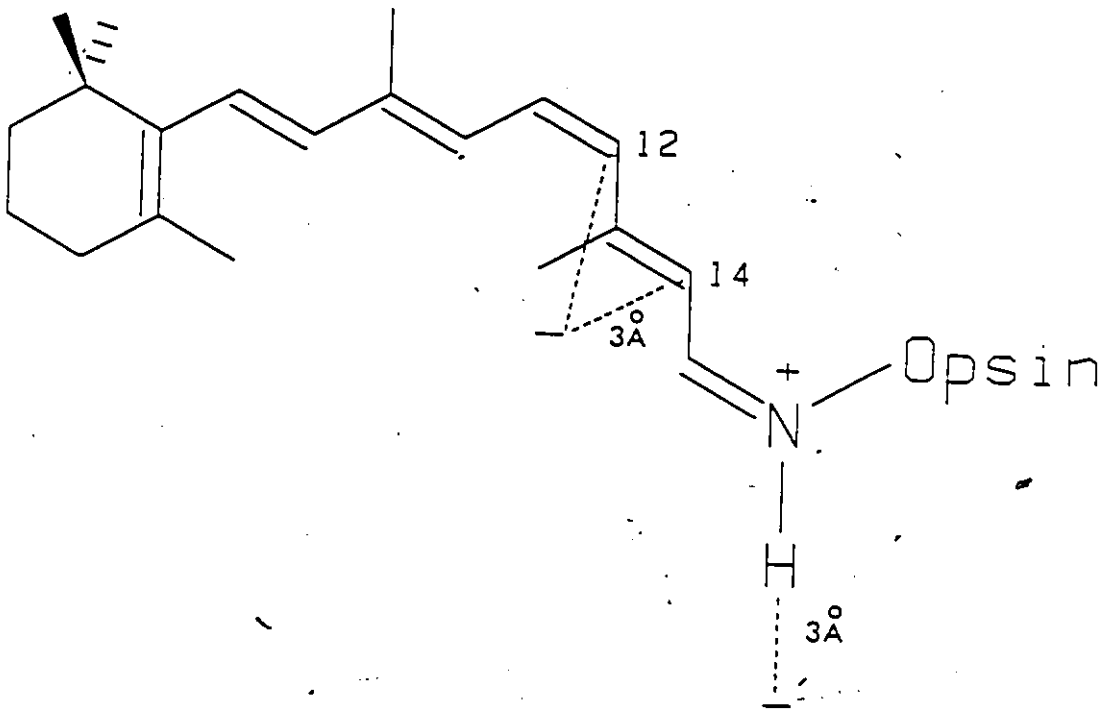

Figure 1-2: The point charge model for rhodopsin.

rhodopsin must be operating to account for this large difference. Using the same principles as employed in the visual pigment, Nakanishi developed a second "point charge" model for bacteriorhodopsin. It was found that a negative charge above C(5) in the β-ionone ring could account for the long wavelength absorption of bacteriorhodopsin (136, 138,139).

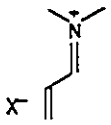

15

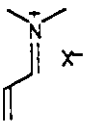

16

A recent re-examination of the dihydro-retinal derivatives used for the bacteriorhodopsin model system (140,141), showed that the difference in absorption maxima between the 7,8 dihydro bacteriorhodopsin 17 and its corresponding retinylidene ion was too large to arise from a simple anionic charge near C(5) as was originally proposed. It was suggested that a planar 6-s-trans retinal configuration (128,142) in bacteriorhodopsin, rather than the previously suspected twisted 6-s-cis conformer may exist in addition to a negative charge above C(5). A model containing a 6-s-trans chromophore had previously been considered by Honig et al. who calculated the dependence of the absorption maximum on the C(6),C(7) twist angle in retinylidene iminium salts (143).

Recently, a retinal derivative with a fixed 6-s-trans configuration was synthesized. When combined with bacterioopsin, an

absorption maximum of 564 nm was obtained, in excellent agreement with the actual absorption maximum of bacteriorhodopsin (144). This experiment clearly showed that the retinal chromophore in bacteriorhodopsin is 6-s-trans. The currently accepted model for bacteriorhodopsin is shown in Figure 1-3.

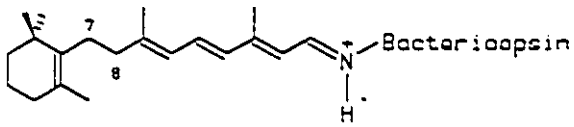

17

ii. Photochemical Models

Absorption of a photon by the retinylidene iminium salt 7, produces its first excited singlet state, S_1. Decay to a ground state species S_o, can be achieved by the emission of light (fluorescence) or through a radiationless process. In addition, the S_1 state can undergo intersystem crossing to the lowest excited triplet state; T_1 which can relax to the ground state through phosphorescence or radiationless means, Scheme 1-3.

Within each energy manifold are several vibrational levels, Scheme 1-3. Conversion within a manifold from a higher vibrational level to a lower one is attained through collisional transfer of energy, to produce the lowest energy vibrational state, ν_0. This process occurs in approximately 10^{-9}-10^{-12} seconds.

It is also possible for higher singlet states than S_1 to become

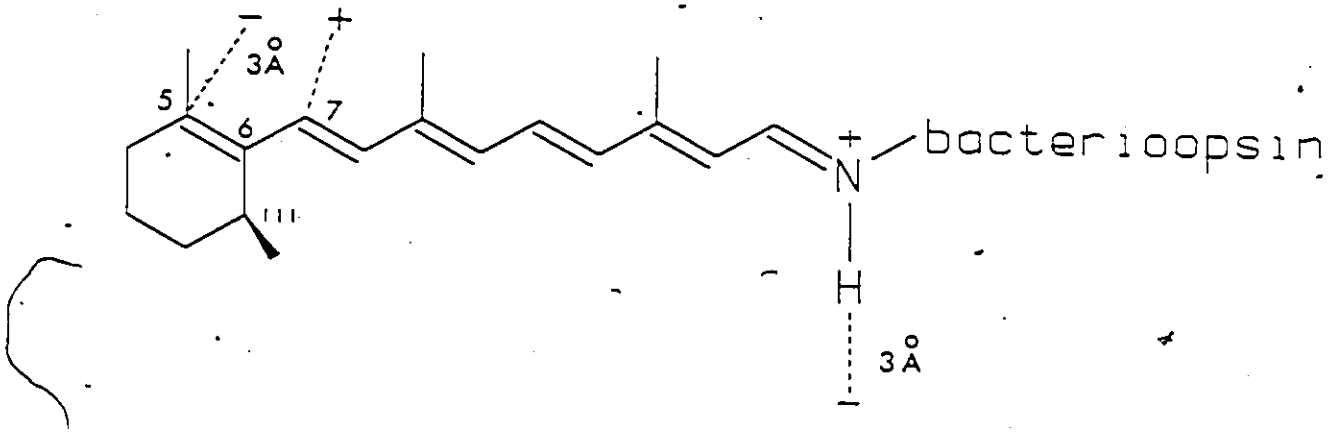

Figure 1-3: The point charge model for bacteriorhodopsin.

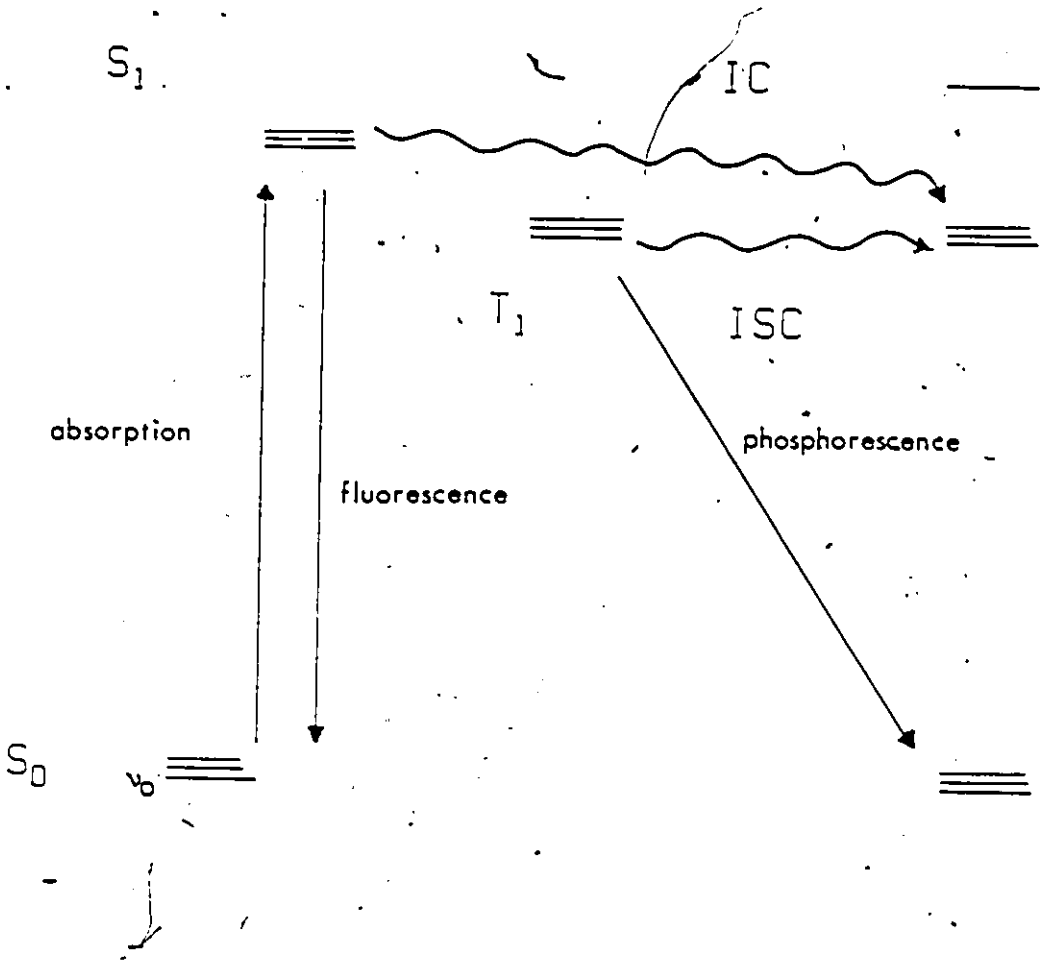

Scheme 1-3: Modified Jablonski diagram.

populated upon absorption of light. When this occurs, rapid internal conversions (10^{-14} seconds) to a lower singlet state occur. These reactions are isoenergetic and result in a higher vibrational level in the lower excited state.

Many possible radiationless processes are possible for a highly conjugated system such as 7. Fluorescence of model systems such as 7, rhodopsin and bacteriorhodopsin is very weak and only observable at low temperatures. Quantum yields for intersystem crossing are also very low, Table 1-2. Thus it has been suggested that photoisomerization reactions of these iminium salts are occurring from the S_1 excited state (145).

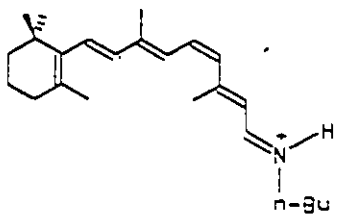

7

The detailed course of a photoisomerization can be described in terms of an energy surface(s) which the molecule may follow enroute to its return to its ground state energy and conformation (150). Such an energy surface is shown in Figure 1-4. The S_1 energy surface for an isomerization reaction has an energy minimum or "funnel" which the molecule can follow. The "deeper" or lower in energy this "funnel" is, the more probable it is for a molecule to follow this pathway. Thus, in the case where several isomerization pathways may be present, such as in rhodopsin and bacteriorhodopsin, the molecule will choose the path of

Table 1-2

Quantum Yields for Fluorescence and Intersystem Crossing of Retinylidene Iminium Salts

Compound	Φ_f	Φ_{ISC}
Rhodopsin	0.000012[a]	-
Bacteriorhodopsin	0.00025[b]	-
7	0.001[c]	0.01[c]
14	0.001[d]	~<0.001[c]

Φ_f = quantum yield for fluorescence, Φ_{ISC} = quantum yield for intersystem crossing

a ref. 146

b ref. 147

c ref. 148

d ref. 149

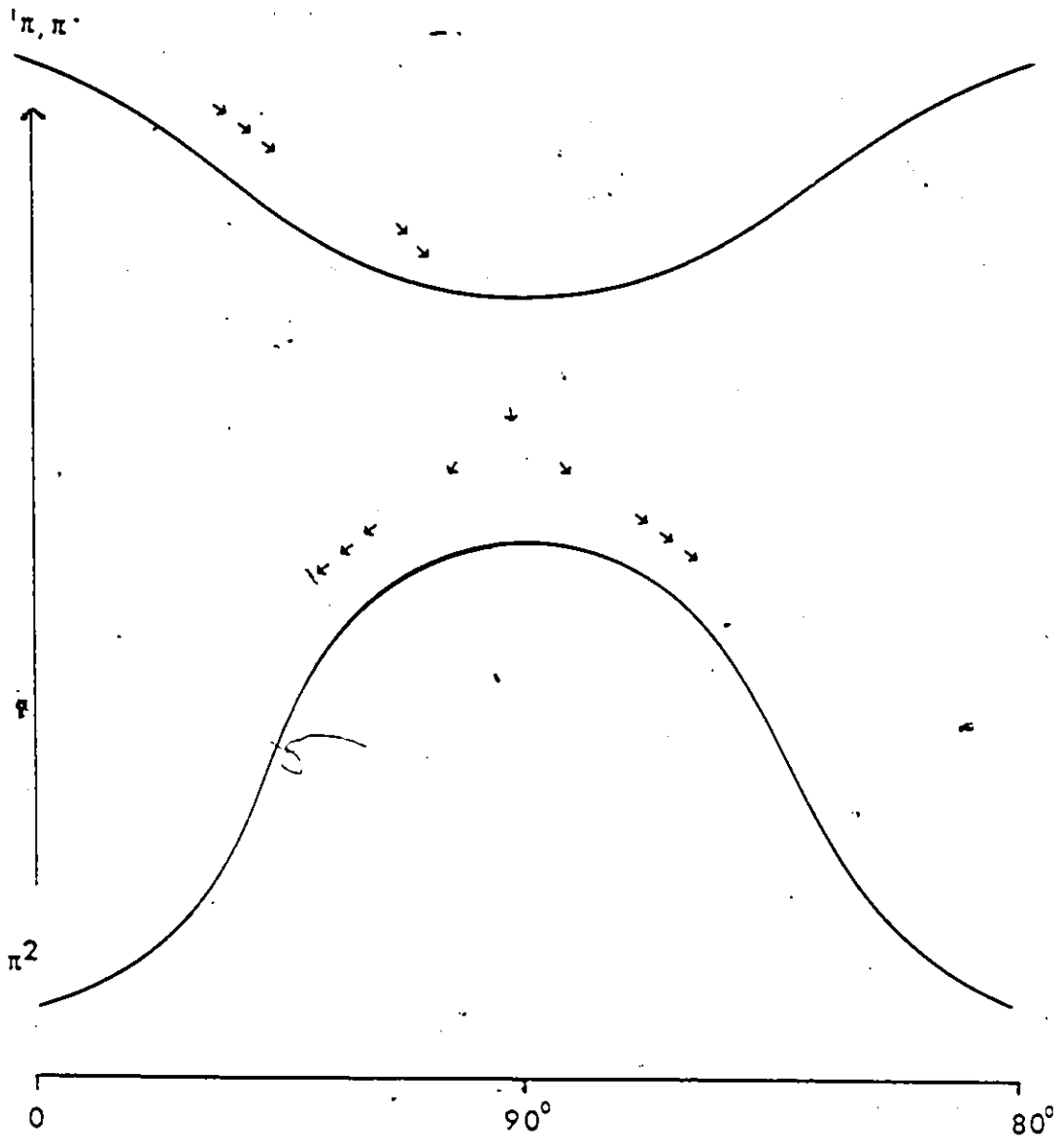

Figure 1-4: Energy surfaces and crossing points for photoisomerization.

steepest descent (ie. the path with the deepest "funnel"). In addition, if the excited state energy surface has an energy barrier between the initial position of the excited molecule and the "funnel", the probability of the molecule following this pathway will be reduced. This can often result in the molecule choosing a radiational pathway such as fluorescence. Once the molecule reaches the bottom of the "funnel" (usually at $\Theta=90^{\circ}$), it crosses over to the ground state energy surface, and continues its course until an energy minimum is achieved.

Proposing a photochemical model for rhodopsin or bacteriorhodopsin is difficult. The model must be able to account for several experimental observations in addition to the high quantum yield for the 11-cis to all-trans isomerization (151). These are;

i) the photoisomerization must be regiospecific; only one double bond is involved,

ii) the photoisomerization must be reversible,

iii) the isomerization is extremely rapid. Pulsed laser experiments have shown that bathorhodopsin, the primary photoproduct of rhodopsin is formed in the order of psec.

iv) both forward and reverse photoisomerizations must occur from a common energy minimum in the excited singlet state.

The sudden polarization model, Scheme 1-4, proposed by Salem and Bruckmann, is perhaps one of the most popular theories in detailing the cis/trans photoisomerization in rhodopsin (152-156). This theory implies that in the ground state approximately 80% of the positive charge in the retinylidene chromophore is found in the C(12) to nitrogen region of the

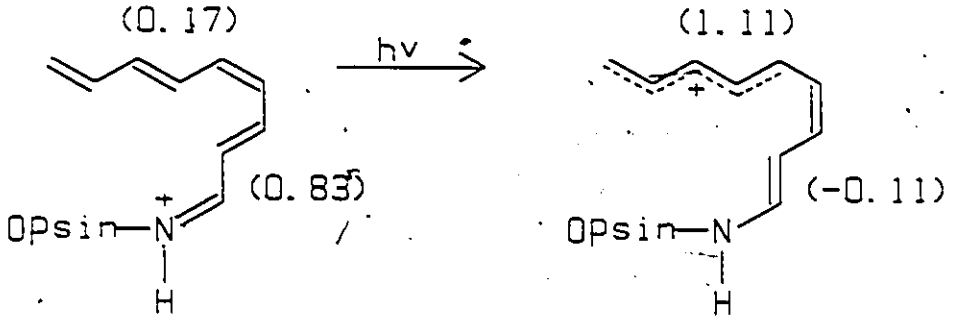

Scheme 1-4: The sudden polarization model.

molecule. Upon excitation of the molecule to the lowest excited singlet state, a highly polarized intermediate is formed. The polarization of this species becomes a maximum at a twist angle of 90° about C(11),C(12), where a zwitterionic intermediate forms such that more than a full positive charge is found in the C(7) to C(11) region and a small negative charge is located in the C(12) to nitrogen portion of the molecule. This allows for facile C(11),C(12) isomerization, however, this model does not account for the high quantum yield in rhodopsin. A second flaw in this theory is that it does not account for for the regioselectivity of the photoisomerization of either rhodopsin or bacteriorhodopsin.

Semiclassical trajectory calculations have been used by Warshel (157-159) and by Birge (160) in an effort to explain the efficiency and the extremely fast rate of cis/trans isomerization in rhodopsin. The calculated quantum yield using this approach can be as high as 0.61, very near to that of rhodopsin (0.67). In these studies a "surface crossing probability" per oscillation, Θ, from the excited state minimum was estimated. If Θ is small, many oscillations would occur in a given time frame (ie. the molecule will have equilibrated in the minimum of the excited state "funnel"). Equal probability should exist, at this point, for the molecule to cross over to the ground state potential curve and follow a course to yield either the starting isomer of an isomerized product. The quantum yield should be about 0.5 for this process. If Θ is large, few oscillations occur (ie. the molecule will not have equilibrated in the excited state "funnel"). This will favour the molecule crossing over to the ground state and following a course forming

the isomerized material. The quantum yield would be greater than 0.5. This proposal also uses a common energy minimum for photoisomerization and allows for reversibility. However one criticism of this model is that it allows for the direct interconversion of isorhodopsin (9-cis) and rhodopsin - a process which has not been shown to occur in nature (61).

A non-mathematical, photochemical model which is applicable to bacteriorhodopsin and rhodopsin was developed recently by Liu and co-workers (161-163). This model was based on the premise that photo-isomerization in either of these systems should be governed by volume constraints of the binding sites within each protein. In each case the retinal moiety was "tethered" at each end, by the lysine linkage of the nitrogen and by hydrophobic interactions near the cyclohexenyl ring. Thus isomerization had to occur through movement of the polyene chain only. The exact mechanism of this motion was determined through computer simulation and was found to involve not only the double bond of interest but also an adjoining single bond, equation 8. This process was dubbed the "Hula Twist" (H.T.). Thus in bacteriorhodopsin, the suggested mechanism for the photoisomerization of all-trans BR_{568} to its 13-cis intermediate, K_{625}, involves a trans/cis isomerization of the C(13),C(14) bond and conversion of the C(14),C(15) from s-trans to s-cis. This intermediate would then decay thermally, via the intermediates shown in Scheme 1-2, enroute to the completion of the cycle and reformation of the all-trans species. A similar mechanism could occur in rhodopsin involving the photoisomerization of the 10-s-trans, 11-cis chromophore to the 10-s-cis, 11-trans isomer (bathorhodopsin, Scheme 1-1), in the

primary step of the visual process.

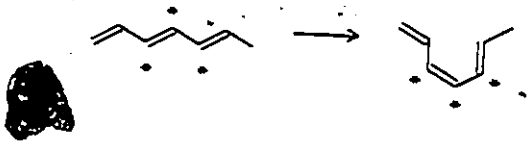

(8)

Although the "Hula Twist" model is an elegant approach to account for the specificity of the photoisomerizations in both rhodopsin and bacteriorhodopsin, it is inconsistent with other existing experimental evidence (164-167). Recently it was shown by Mathies et al. using resonance Raman techniques, that the primary photoproduct of rhodopsin, bathorhodopsin, has a 10-s-trans, 11-trans conformation (164) and the first photochemical intermediate, K_{625}, of bacteriorhodopsin is 13-cis, 14-s-trans (165). Both of these results are inconsistent with the structures proposed by Liu for the "Hula Twist" mechanism.

Information on the photoisomerizations of rhodopsin and bacteriorhodopsin has been obtained using various cis-retinal isomers (168-173), retinylidene imines (172-176) and retinylidene iminium salts (173-177), Table 1-3. Photoisomerization of either the 11-cis or 13-cis isomers of these compounds results, in most cases, in the formation of the corresponding all-trans isomers, equation 9. The exception to these cis to trans processes is the photoisomerization of 11-cis retinal which also forms small amounts of the 11-cis, 13-cis retinal, equation 10. Overall, the regioselectivity of these photoisomerizations is in good

Table 1-3

Photoisomerization Data for Cis-Retinylidene Derivatives

Compound	R	Products	Φ_{ISO}	Solvent
11-cis	O	trans/11,13-dicis (5:1)	0.24[a]	3-MP
		trans	0.04[a]	MeOH
"	NR'	trans	0.01[b]	Hexane
		trans	0.24[b]	MeOH
"	NHR'	trans	0.16[c]	Acetone
		trans	0.28[c]	Hexane
13-cis	O	trans	0.21[a]	3-MP
"	NR'	trans	0.01[b]	Hexane
		trans	0.03[b]	MeOH
"	NHR'	trans	0.05[b]	Hexane

Φ_{ISO} = quantum yield for photoisomerization

a ref. 168

b ref. 175

c ref. 174

agreement with that found in the natural pigments. However, the quantum yields for the isomerizations of these model compounds are significantly lower than found in either rhodopsin or bacteriorhodopsin, Table 1-3.

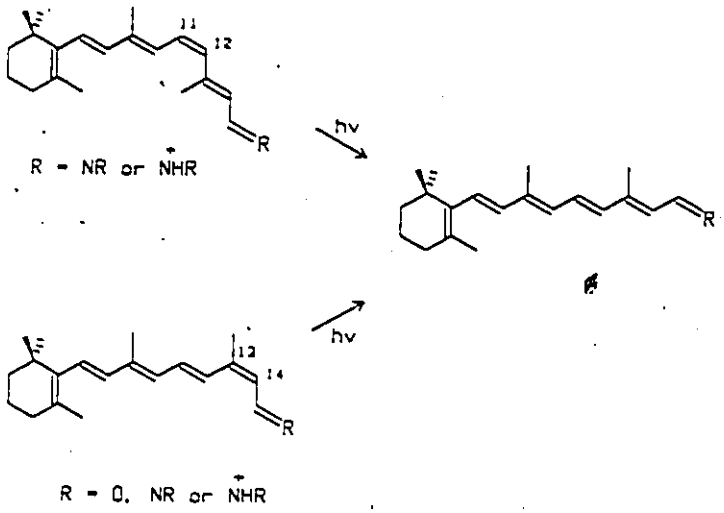

(9)

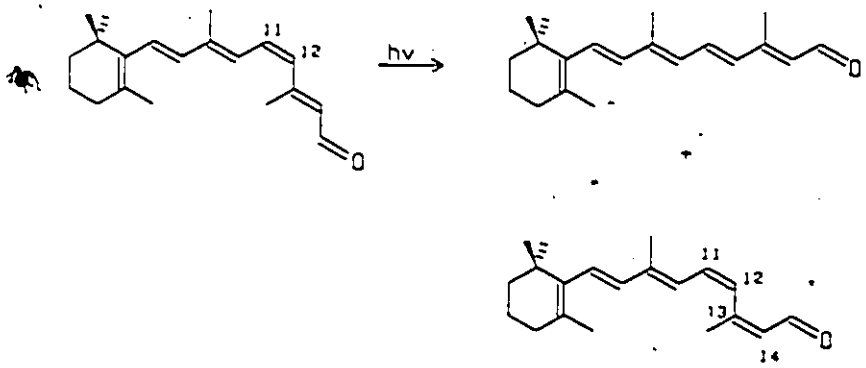

(10)

In bacteriorhodopsin, a photoisomerization from the all-trans form (BR_{568}) to the 13-cis isomer (K_{625}) occurs. Thus many photoisomerizations of all-trans retinals, retinylidene imines and retinyli-

Table 1-4

Photoisomerization Data for All-Trans Retinylidene Derivatives

Compound	λ_{ex}	Product Ratio 13cis	11-cis	9-cis	7-cis	Φ_{ISO}	Solvent
Aldehyde	350	1	-	-	-	0.04	3-MP[a]
"	350	1	-	-	-	0.006	MeOH[a]
"	350	11	4.5	1	t	0.33	EtOH[b]
Imine	355	1	-	-	-	0.01	Hexane[c]
"	355	1.9	5.7	1	t	0.12	MeOH[c]
Iminium Salt	355	1.7	6.4	1	t	0.14	Hexane[c]
"	355	1.8	14	3	1	0.13	MeOH[c]
"	436	2.3	4.6	1	t	0.14	Hexane[d]
"	468	4.2	-	1	-	0.17	MeOH[d]
"	436	9.3	4.3	1	t	0.36	Hexane[d]

Φ_{ISO} = total quantum yield for photoisomerization, t = trace

a ref. 168

b ref. 171

c ref. 175

d ref. 177

dene iminium salts have been investigated, Table 1-4. In contrast to photoisomerization studies of the 13-cis and 11-cis retinal derivatives, the regioselectivity of photoisomerization of the all-trans compounds is much lower. In many cases, several isomeric products are formed and the quantum yields are extremely low in all examples, Table 1-4.

iii. Thermal Chemistry

Dark adapted bacteriorhodopsin exists as an approximate 50:50 mixture of 13-cis, 15-syn (BR_{548}) and 13-trans, 15-anti (BR_{568}) retinal isomers in thermal equilibrium, equation 11. This interconversion of isomers involves a C=C and a C=N isomerization - two relatively high energy processes (178). Typically, rotation about a C=C bond requires about 50 kcal/mol (127), while rotation about the C=N bond in $CH_2=NH_2^+$ has been calculated to be about 70 kcal/mol in the gas phase (179). However, the barrier to C=C isomerization has been shown to be significantly lower in the presence of differing anions (180-182). In some cases this barrier can be lowered to as little as 11.6 kcal/mol. In bacteriorhodopsin, the energy barriers to these two isomerizations must be <20 kcal/mol for rapid interconversion to occur at temperatures above 0°C. This intriguing aspect of bacteriorhodopsin has prompted many studies of C=C and C=N isomerizations using model compounds (183-188).

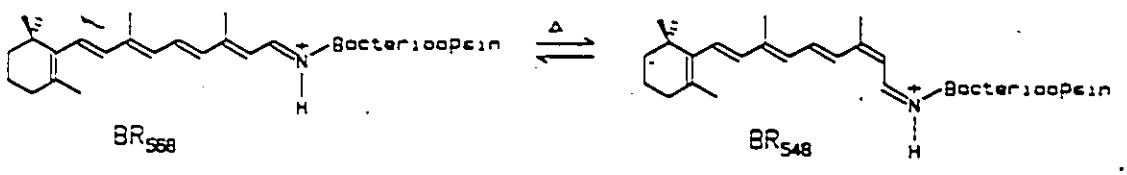

BR_{568} BR_{548} (11)

Recently, a systematic approach to the mechanism of C=N isomerization was taken by Pankratz and Childs (186), using a series of N-aryl 3-arylpropenylidene iminium salts, 18a-e, equation 12, in strong acid solutions. It was found that E/Z isomerizations in these molecules required an activation energy of 28-32.7 kcal/mol, and that two different mechanisms were operating depending on the substituent on the 3-aryl ring. As shown in Scheme 1-5, an electron donating substituent ($X=OCH_3$) favoured an N-protonation mechanism while an electron withdrawing group ($X=NO_2$) lead to a nucleophilic addition mechanism. This latter mechanism may be occurring in bacteriorhodopsin. The protonation mechanism is not probable in bacteriorhodopsin, however this study provides important evidence that a simple rotational mechanism about the C=N bond in bacteriorhodopsin is unlikely.

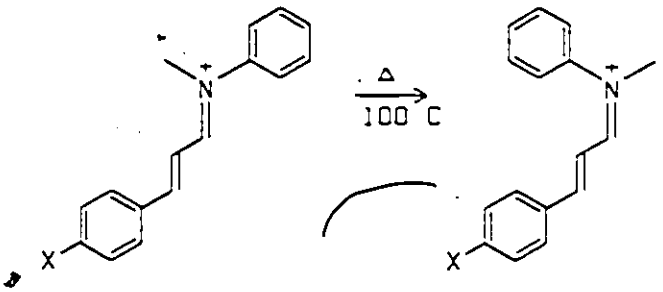

(12)

18a: X = NO_2
b: X = Cl
c: X = H
d: X = CH_3
e: X = OCH_3

19c-e

The mechanism by which the C(13),C(14) bond in bacteriorhodopsin isomerizes has been more extensively researched than that of C=N

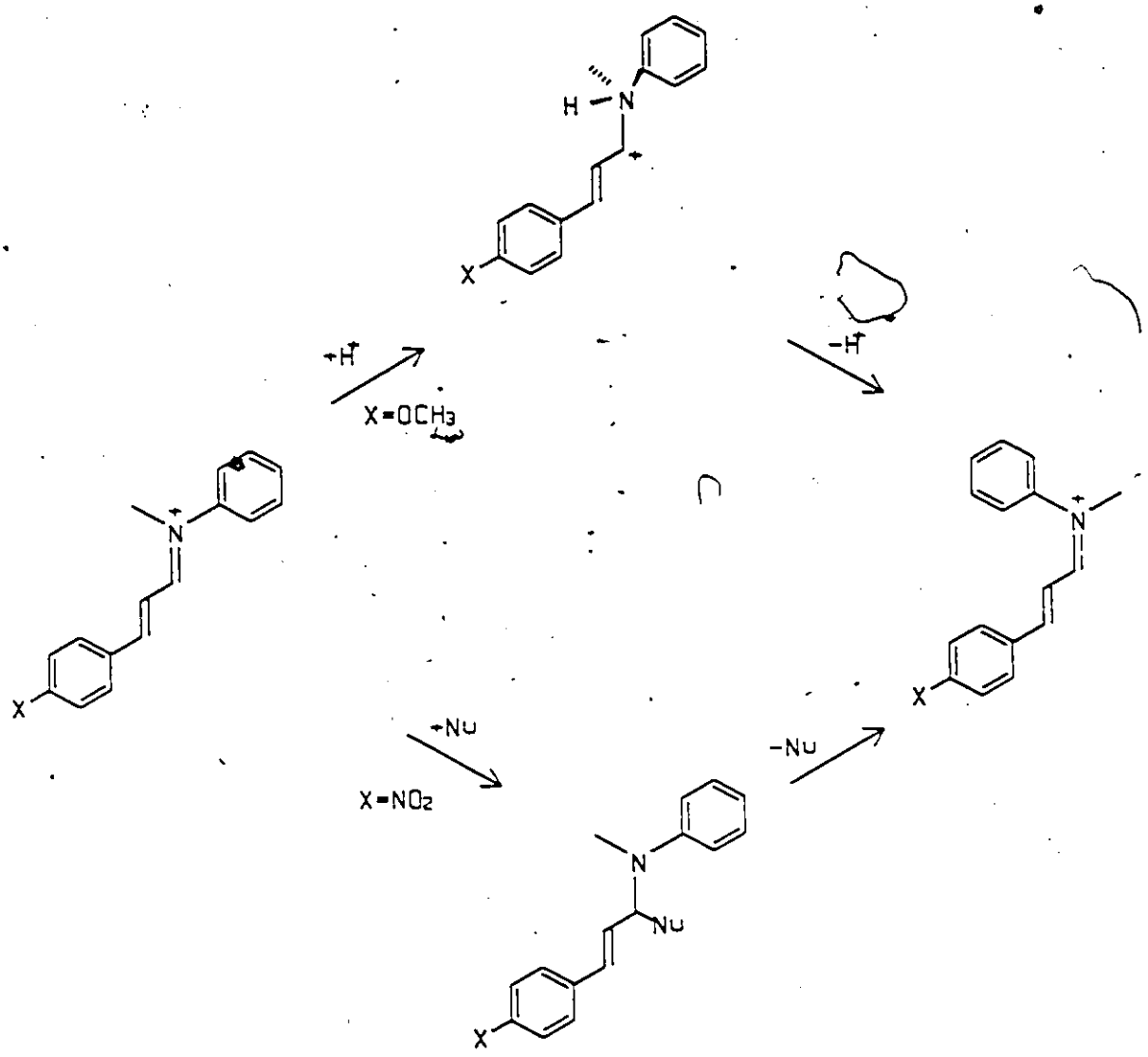

Scheme 1-5: Protonation vs. nucleophilic addition mechanisms for thermal isomerization in iminium salts.

isomerization (185,187). Rando and Lukton have investigated the mechanisms for C=C isomerization in a series of retinals, retinylidene imines and retinylidene iminium salts (189,190). In 11-cis retinal, the activation energy for isomerization about the C(11),C(12) bond was found to be about 25 kcal/mol, in good agreement with a previous study (191). However, the corresponding 11-cis retinylidene imine isomerized about three times faster than the aldehyde, and moreover, this rate was decreased by nearly ten fold in the presence of excess amine. Rando suggested that the excess amine was able to neutralize trace quantities of acid in the solvent, which was involved in the imine isomerization. This theory was tested by studying the rates of isomerization of various cis-retinylidene imines in the presence of HCl.

In excess HCl the rates of isomerization were found to be 13-cis > 11-cis > 9-cis at 25°C, with an approximate activation energy for the 13-cis isomer of 19.6 kcal/mol. It was further determined that trifluoroacetic acid also catalysed this reaction, but that the rate of isomerization was nearly 10^4 times slower than with HCl. Based of these experiments, Rando suggested that the isomerization of retinylidene iminium salts was proceeding via a nucleophilic addition mechanism, Scheme 1-6. This may also be occurring in bacteriorhodopsin. A similar mechanism had been proposed earlier by Childs and Dickie (188) for the C=C isomerization of a series of 3-aryl propenylidene iminium salts, 20a-e, equation 13.

A study of the isomerization rate of an 11-cis retinylidene imine in a lipid dispersion has provided information that the lipids may

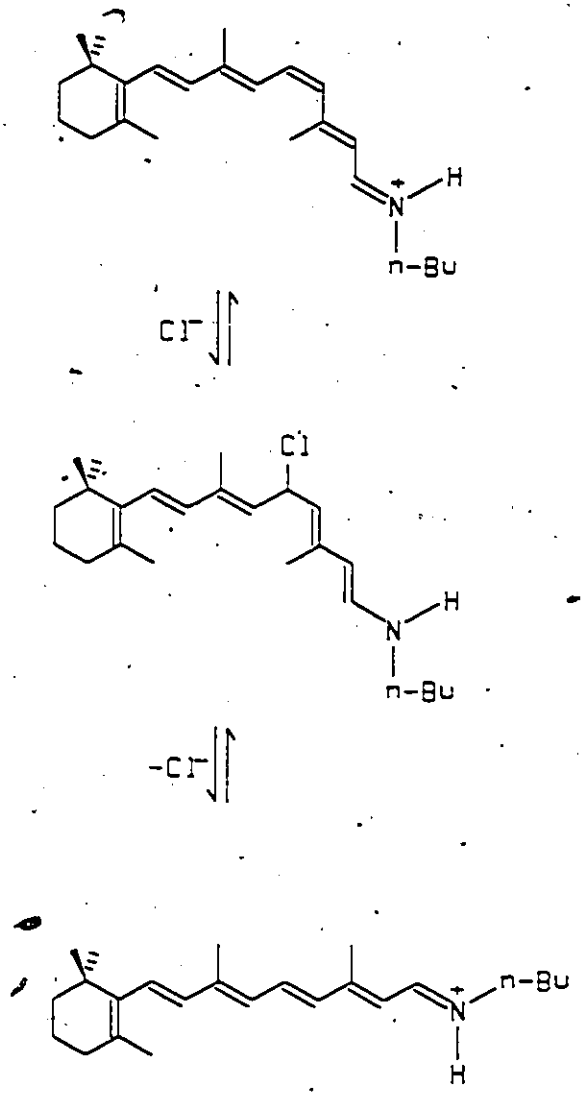

Scheme 1-6: Nucleophilic addition mechanism for thermal cis/trans isomerization of retinylidene iminium salts.

catalyse isomerization through a similar mechanism (192). The imine 22 was found to isomerize 10^3 times faster in a lipid matrix than in n-heptane. A pH study of this isomerization suggested that a possible nucleophilic catalysis was occurring and that only a single proton was involved in the isomerization.

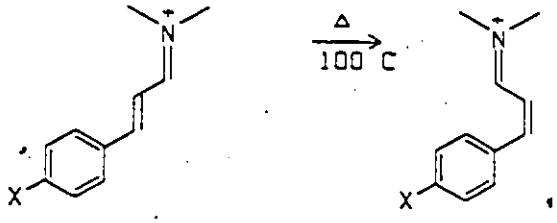

(13)

20a: X = NO_2
b: X = Cl
c: X = H
d: X = CH_3
e: X = OCH_3

21a-e

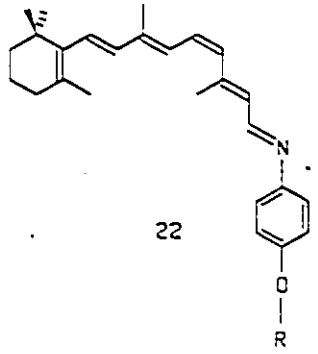

22

The thermal barrier for rotation about the C(13),C(14) bond in bacteriorhodopsin model system 23, is approximately 46 kcal/mol, based on

quantumchemical MNDOC calculations (127). Upon protonation of 23 this value is reduced to about 11.5 kcal/mol, in the absence of a counter-anion, 24. This barrier to rotation increases to about 21.6 kcal/mol when an anion is placed 3.0 Å from nitrogen. A similar study (180) found that 24 had a C=C barrier to rotation of 15.8 kcal/mol in the absence of a counteranion. This increased significantly to 38.0 kcal/mol when an anion was placed 2.5 Å from nitrogen. Since the presently accepted model for bacteriorhodopsin also contains a second anion near C(5), the C(13),C(14) barrier to isomerization was also calculated by Schulten and was found to be only 5.8 kcal/mol. This second cation/anion interaction produces of a significant amount of charge delocalization in the polyene chain and thus a lower bond order between the C(13),C(14) bond, allowing for facile isomerization. This interaction also represents the initial stages of a nucleophilic addition reaction as suggested by Childs and by Rando. It was suggested, by Schulten, that these interactions allow for C=C isomerizations to occur on the millisecond time scale, consistent with those observed in dark-adapted bacteriorhodopsin.

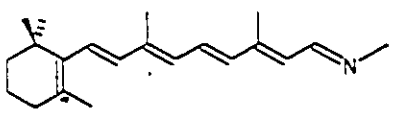

23

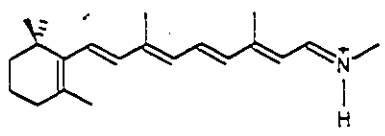

24

iv. Problems With Retinylidene Iminium Salt Photochemical Studies

Studies on the photoisomerization of all-trans retinal compounds are difficult because the all-trans molecules possess five potential isomerization sites. Typically, photoproducts are analysed by HPLC techniques (168-170). However, in the case of the retinylidene iminium salts, the problem is complicated by the inability of HPLC to resolve each isomer as its iminium salt. The usual technique for the quantitative analysis of these compounds is to hydrolyse them to their corresponding aldehydes and analyze by HPLC. Difference absorption spectroscopy (173-176), although a practical method, is also extremely difficult in these cases since all isomeric retinylidene iminium salts have a very similar absorption spectrum and the extinction coefficients vary by as much as 30% for any one isomer (177).

These problems seem to be manifested in the reported photoisomerization of the bacteriorhodopsin model system 25 in two independent studies (175,177), shown in Scheme 1-7 and Table 1-4. Though studied at two different wavelengths, it is clear from these reactions that this photoisomerization is neither regioselective nor as efficient as in bacteriorhodopsin. A striking difference between these studies is the primary site of the photoisomerization of 25. In one case the 13-cis isomer is formed preferentially (177), while in the second case the 11-cis isomer is formed to a larger extent (175). In neither case is the reaction regioselective and the quantum yields are only reported as a total for the entire photoisomerization. The reactions would seem to be extremely sensitive to the wavelength of irradiation, a property not

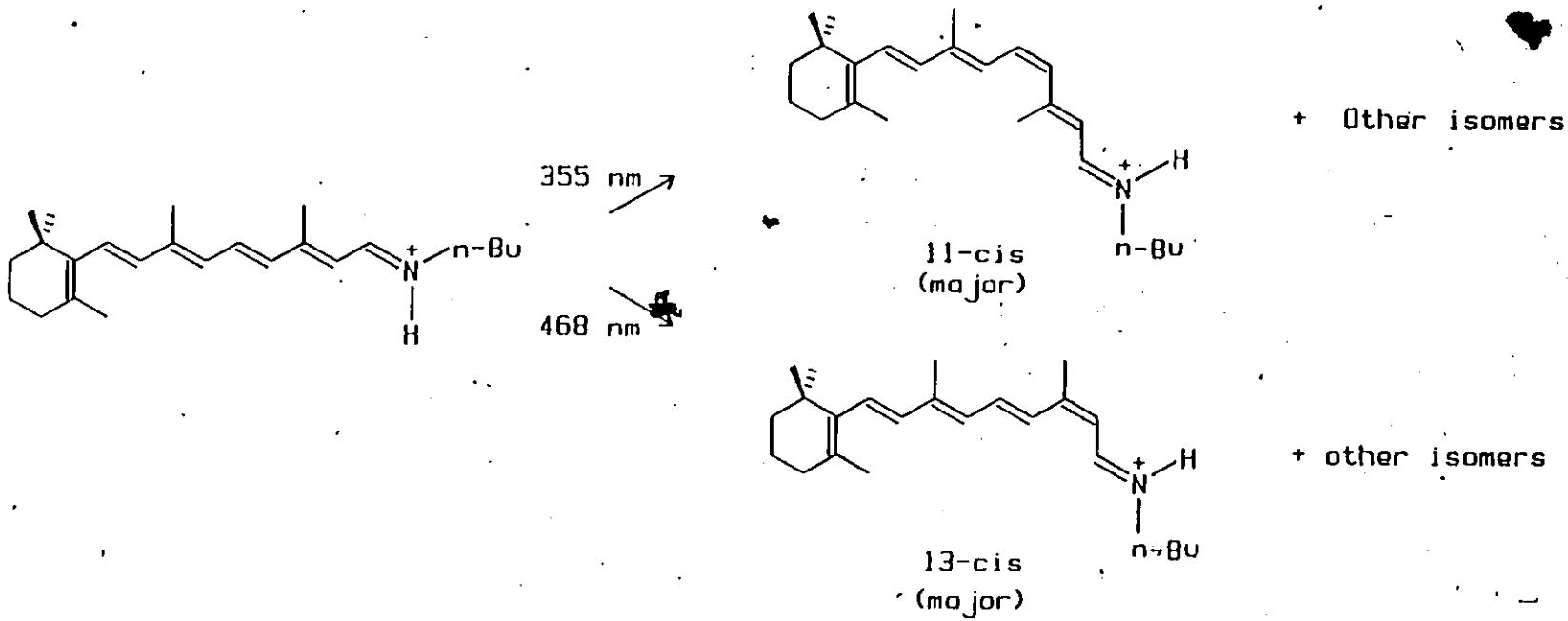

Scheme 1-7: Primary photoproducts from the photoisomerization of a N-n-butyl-retinylidene iminium salt at two different wavelengths.

found in the natural pigments.

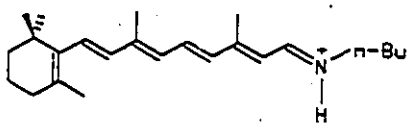

25

A second major problem encountered in photochemical studies of all-trans retinylidene iminium salts is the competing thermal reactions which may occur. Indeed, it has been shown by several groups (186,188-190) that photochemically formed cis isomers are extremely susceptible to nucleophilic catalysis reactions which reform the trans starting materials. In the case of retinylidene iminium salts, catalysis by chloride ion is extremely rapid for the isomerization of the 13-cis and 11-cis isomers to the all-trans compound. These reactions also occur with trichloroacetate, but at a reduced rate. In the photochemical studies shown in Scheme 1-7, either chloride or trichloracetate anions were present in excess amounts during the photoreactions. The presence of a nucleophilic catalysed reaction such as those observed by Rando and by Childs could severely influence the isomer content and efficiency of these photoreactions.

It was suggested some years ago that the best method to directly identify and quantitate this photoreaction, ^1H NMR spectroscopy, was not practical due to the complexity of the resulting spectra and the small quantities involved in the photoreaction. In order to address this problem I undertook a high field ^1H NMR spectroscopic examination of the

photochemical isomerizations of a series of conjugated iminium salts including several all-trans retinylidene iminium ions. Included in this investigation was an in-depth assessment of the thermal stabilities of each retinylidene photoisomer. The aim of this study was to accurately identify all of the photoproducts generated from the irradiation of these iminium ions directly by ^{1}H NMR spectroscopy, and determine the regioselectivity and efficiency of these photoisomerizations as compared to rhodopsin and bacteriorhodopsin. This study should give significant insight into the differences in retinylidene iminium ion photochemistry in solution and within the binding sites of rhodopsin and bacteriorhodopsin.

Related to this photochemical study is one which details the structures of some model systems of the visual chromophore and bacteriorhodopsin. Some uncertainty of the conformation and electronic distribution in these simplified chromophores still remains. Moreover the majority of the previous studies of retinylidene ions have been done in polar solvents, conditions which do not mimic the hydrophobic environment of the binding sites of the natural pigments. In an effort to gain structural information about retinylidene ions in such an environment, ^{13}C NMR, FT-IR and UV spectroscopic techniques were employed in both the solution (CH_2Cl_2) and in the solid state. This analysis is of particular importance since it is now generally accepted that the conformation in bacteriorhodopsin is 6-s-trans. This conformation has not been shown to exist in model retinylidene iminium salts. Close attention in this work has also been given to the effect the counterion

has on the ^{13}C chemical shifts of a retinylidene ion and whether these are indicative of charge delocalization.

The most direct route for the structure determination of a conjugated iminium salt, such as a retinylidene ion, is through x-ray crystallographic techniques. Despite the immense interest in these compounds, there are surprisingly few crystal structures of them in the literature. One approach in this work investigated the x-ray structures of an α,β unsaturated iminium salt and its corresponding imine. From these data, a comparison could be made between these two compounds in an effort to determine the effect of protonation on bond alternation, conformation and electronic distribution. X-ray crystallography also allows for the study of interactions which occur between the iminium ion and its counterion exactly, in analogy to the protein-chromophore interactions which occur in the visual pigments. To my knowledge, such a study has only been carried out on theoretical grounds before, but has not been reported using a crystallographic basis.

RESULTS AND DISCUSSION

Chapter 2

Structural Studies of Conjugated Iminium Salts

The most direct method which can been used to assess the structure of a conjugated iminium salt is x-ray crystallography. Unfortunately, this approach has been used sparingly and there are few structures of these compounds reported in the literature. Hence, alternative means to analyse the structures of iminium ions have been used, including ^{1}H and ^{13}C NMR spectroscopy, infrared, resonance Raman and absorption spectroscopy, and theoretical techniques.

The determinations of the structures of a simple α,β unsaturated imine and iminium salt, using a variety of techniques are presented in this chapter. The goal of this work is to determine the differences in structure between an imine and a related iminium salt. The relationship that exists between the cation and anion in the iminium salt and its effect on the electronic distribution in the molecule is developed.

A major concern in the chemistry of rhodopsin and bacteriorhodopsin is the degree of charge delocalization in these molecules. In the previous section it was shown that the position of the counteranion has a large effect on charge delocalization in these molecules and their thermal barriers for bond rotation. To probe this phenomenon, charge delocalization in a series of model retinylidene iminium salts has been probed in this work by analysing the correlation between ^{13}C NMR chemical

shifts and the distance of various counteranions. Absorption spectroscopy is also used to determine the extent of delocalization as it relates to the counteranion. These studies also include, for comparison, several protonated unsaturated aldehydes.

A third facet of iminium salt structure which is examined is conformation. In bacteriorhodopsin solid state ^{13}C NMR spectroscopy has recently been used to show that this chromophore exists in a 6-s-trans conformation. In this thesis, solid state ^{13}C NMR spectroscopy and absorption spectroscopy have been used to show that the 6-s-trans conformation is also present in some retinylidene iminium salts.

RESULTS

I. Preparation of Iminium Salts

Imines 26-29 were prepared by the same general method (32). The appropriate aldehyde or ketone was condensed with either n-butyl or t-butyl amine as indicated in equation 14. In the case of the β-ionone derivative 28, the n-butyl imine was prepared because t-butyl amine showed no reaction with the ketone. Imines 26-29 were found to be extremely sensitive to both temperature and moisture and best results occurred when they were protonated immediately after formation.

Protonation of these imines was accomplished using a dilute ethereal solution of perchloric acid or fluorboric acid to yield the iminium salts 30-33, equation 15. Iminium salt 34 was prepared by reacting dimethyl ammonium perchlorate with 2,4 hexadienal (193),

equation 16. Imines 28 and 29 contained minor isomeric impurities which disappeared upon protonation. All of the iminium salts prepared were assumed to retain the all-trans configuration which was present in the starting aldehyde or ketone. This was substantiated by ^1H NMR spectroscopy as shown in Tables 2-1 to 2-4.

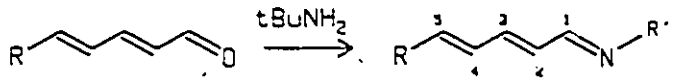

26 R=CH_3, R'=tBu
27 R=CH_3(CH=CH), R'=tBu

(14)

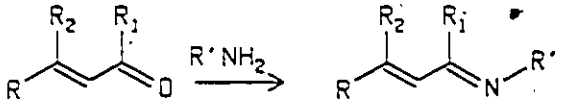

28 R= , R_1=CH_3, R_2=H, R'=nBu
29 R=  , R_1=H, R_2=CH_3, R'=tBu

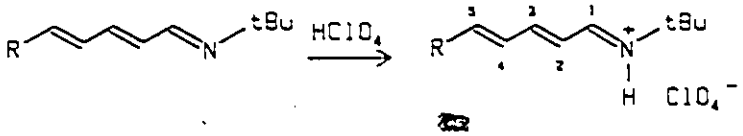

30 R=CH_3
31 R=CH_3(CH=CH)

(15)

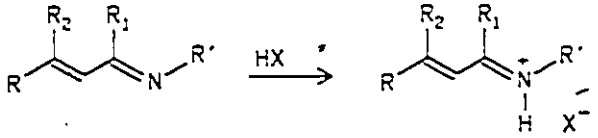

32 R= , R_1=CH_3, R_2=H, R'=nBu, X=BF_4
33 R=  , R_1=H, R_2=CH_3, R'=tBu, X=ClO_4

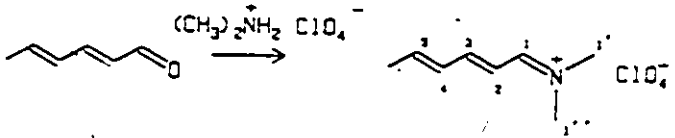

(16)

For comparison purposes pertaining to charge delocalization, the aldehydes 35 and 36 were cleanly protonated by extraction from CH_2Cl_2 into FSO_3H at -78°C, to form 38 and 39, equation 17. An attempt to protonate the aldehyde 37 by this method, to form 40, yielded at least two rearranged products. These were not identified[1].

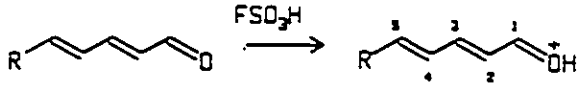

(17)

35 R=CH_3 38
36 R=CH_3(CH=CH) 39
37 R=CH_3(CH=CH)$_2$ 40

The iminium salts 41-44 were prepared by stirring equimolar amounts of the appropriate aldehyde with N-methyl aniline and either perchloric or trichloroacetic acid in ether (186), equation 18. The imine 45 was synthesized by condensing aniline with p-chloro-cinnamaldehyde, equation 19.

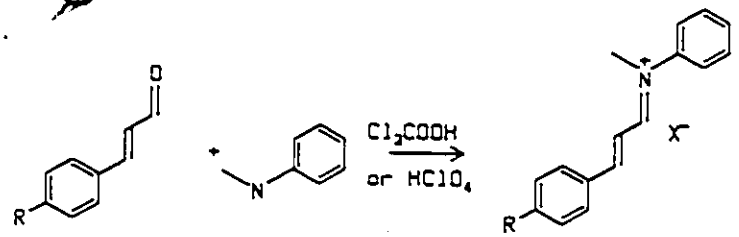

(18)

41 R=H, X=Cl_3COO
42 R=H, X=ClO_4
43 R=Cl, X=Cl_3COO
44 R=Cl, X=ClO_4

[1]This work was completed as part of a collaborative project with P. Yates, J. Krepinsky and I. Gupta of the Department of Chemistry and The Ludwig Cancer Institute, University of Toronto, Toronto, Ontario.

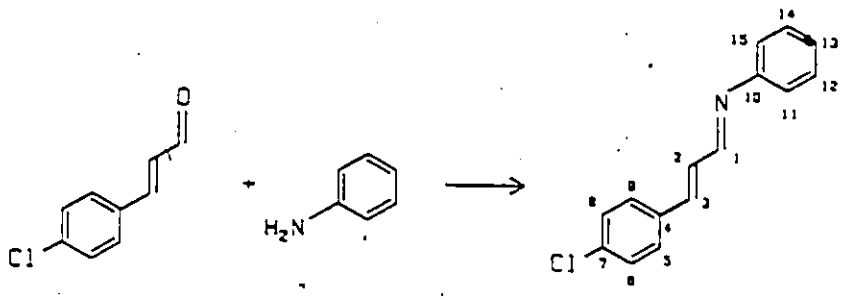

45 (19)

The retinylidene imines 46 and 47 were synthesized using literature methods (32). All-trans retinal was allowed to condense with the appropriate amine in the absence of light, equation 20. The desired iminium salts 48-53 were prepared by adding slightly less than an equimolar amount of an ethereal acid solution to the freshly prepared imine, equation 21.

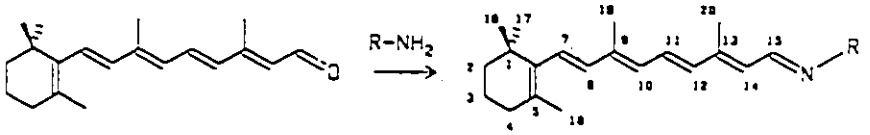

(20)

46 R=n-Bu
47 R=t-Bu

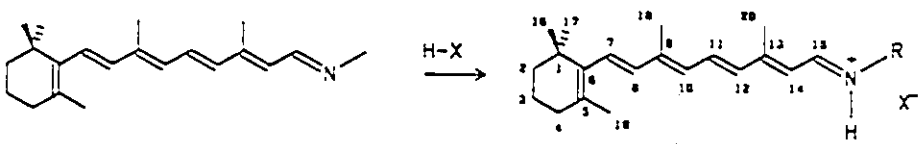

(21)

48 R=nBu. X=Cl_3CCOO
49 R=nBu. X=ClO_4
50 R=tBu. X=I
51 R=tBu. X=BF_4
52 R=tBu. X=ClO_4
53 R=tBu. X=CF_3SO_3

The dimethyl retinylidene iminium perchlorate salt 54 was made by a condensation of dimethyl ammonium perchlorate with all-trans retinal (193), equation 22. All retinylidene iminium salts synthesized possessed an all-trans geometry as indicated by ^{1}H NMR spectroscopic data shown in Tables 2-5 and 2-6.

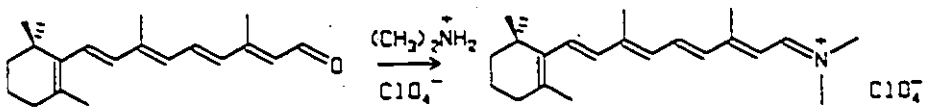

(22)

54

II. ^{1}H NMR Spectroscopy

The chemical shifts and coupling constants of all imines and iminium salts are listed in Tables 2-1 through 2-6. Assignment of the resonances was accomplished by a variety of methods. In several cases literature comparisons were made using salts with similar structures or in some cases the same cation but differing counteranions (34,52,184, 186,188,194-198). The remainder of the assignments were based on first order coupling constant information at either 250 or 500 MHz. In one case, 31, the 250 MHz ^{1}H NMR spectroscopy spectrum yielded several complex spin systems which were very difficult to assign directly. In this case, assignments were made using a spectral simulation technique, Figure 2-1.

The ^{1}H NMR data for aldehydes 35 and 36 and protonated aldehydes 38 and 39 are shown in Table 2-7. Identification of the resonances for

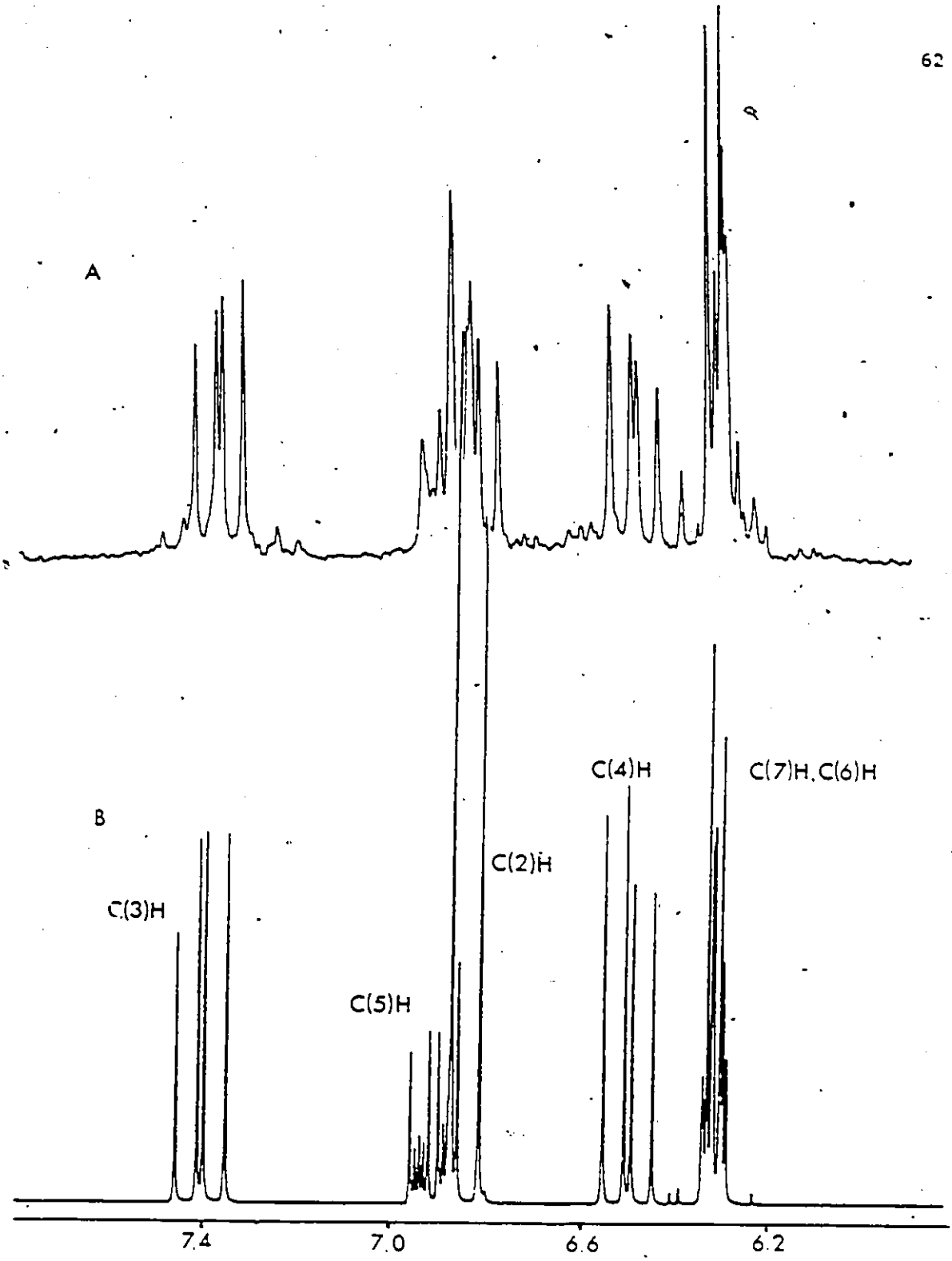

Figure 2-1: Vinyl region of 250 MHz ^{1}H NMR spectrum of N-t-butyl-2,4,6-octatrienylidene iminium perchlorate, 31, (A) and simulated (B), with coupling to Cl(H) removed.

Table 2-1

^{1}H NMR Chemical Shift[a,b,c] Data For Aliphatic Imines and Iminium Salts

	Compound			
Position	26	30	31	34
C(1)H	7.84d	8.13dd	7.96dd	8.38d
C(2)H	6.18dd	6.74dd	6.84dd	6.55dd
C(3)H	6.53dd	7.49dd	7.40dd	7.63dd
C(4)H	6.18dd	6.48dd	6.50dd	6.49dd
C(5)H	5.90dq	6.65dq	6.90dd	6.70dq
C(6)H	-	-	6.31dd	-
C(7)H	-	-	6.32dq	-
CH_3	1.78d	1.99d	1.92d	2.02d
C(1')H	-	-	-	3.49s
C(1'')H	-	-	-	3.68s.
C(2')H	1.16s	1.51s	1.51s	-
N-H	-	11.00bs	11.04bs	-

a s = singlet, d = doublet, dd = doublet of doublets, dq = doublet of quartets, bs = broad singlet.
b in ppm. Numbering of carbons as in text.
c referenced to CD_2Cl_2, 5.32 ppm. Measured at 21°C.

Table 2-2

Coupling Constant Data (Hz) For Aliphatic Imines and Iminium Salts

	Compound			
	26	30	31	34
$J_{1,N}$	-	16.64	16.47	-
$J_{1,2}$	8.79	10.39	10.43	10.54
$J_{2,3}$	15.24	14.71	14.60	14.43
$J_{3,4}$	10.87	10.65	11.34	10.87
$J_{4,5}$	15.11	15.07	15.11	14.93
$J_{5,6}$	6.14	6.64	12.03	6.87
$J_{6,7}$	-	-	17.65	-
$J_{7,8}$	-	-	5.43	-

Table 2-3.

^{1}H NMR Chemical Shift[a,b] Data For Aliphatic Imines and Iminium Salts

	Compound			
Position	28[c]	29[d]	32[e]	33[d]
C(2)H	1.50t	1.46t	1.43t	1.48t
C(3)H	1.67m	1.62m	1.70m	1.64m
C(4)H	2.06t	2.03t	2.13t	2.12t
C(7)H	6.66d	6.36d	7.73d	7.13d
C(8)H	6.13d	6.14d	6.51d	6.49d
C(10)H	-	6.19d	-	6.82d
C(11)H	-	8.34d	-	8.28dd
1,1 CH_3	1.01s	1.02s	1.01s	1.08s
5 CH_3	1.70s	1.69s	1.81s	1.80s
9 CH_3	1.97s	2.03s	2.40s	2.32s

a s = singlet, d = doublet, t = triplet, dd = doublet of doublets, m = multiplet
b in ppm at 21°C. Numbering of carbons as in text.
c referenced to $CDCl_3$, 7.28 ppm.
d referenced to CD_2Cl_2, 5.32 ppm.
e referenced to $(CH_3)_4NBF_4$, 3.10 ppm, in TFA.

Table 2-4

Coupling Constant Data (Hz) For Aliphatic Imines and Iminium Salts

	Compound			
	28	29	32	33
$J_{7,8}$	17.05	15.88	15.01	16.01
$J_{10,11}$	-	8.38	-	11.08
$J_{11,N}$	-	-	-	16.17

Table 2-5

^1H NMR Chemical Shift[a,b,c] Data For Retinylidene Imines and Iminium Salts

	Compound							
Position	46	47	48	49	51	52	53	54
C(2)H	1.50t	1.50t	1.47t	1.53t	1.61t	1.50t	1.61t	1.51t
C(3)H	1.62m	1.62m	1.62m	1.65m	1.61m	1.61m	1.61m	1.61m
C(4)H	2.03t	2.05t	2.05t	2.09t	2.06t	2.06t	2.06t	2.09t
C(7)H	6.25d	6.28d	6.51d	6.56d	6.53d	6.47d	6.53d	6.36d
C(8)H	6.13d	6.16d	6.24d	6.27d	6.26d	6.21d	6.25d	6.31d
C(10)H	6.15d	6.19d	6.29d	6.33d	6.31d	6.29d	6.32d	6.36d
C(11)H	6.86dd	6.91dd	7.40dd	7.51dd	7.48dd	7.43dd	7.45dd	7.59dd
C(12)H	6.37d	6.41d	6.56d	6.56d	6.57d	6.58d	6.55d	6.62d
C(14)H	6.19d	6.33d	6.74d	6.72d	6.74d	6.65d	6.86d	6.64d
C(15)H	8.30d	8.32d	8.20d	8.34dd	8.22dd	8.19dd	8.20dd	8.56d
C(16)H C(17)H	1.03s	1.05s	1.04s	1.08s	1.05s	1.05s	1.05s	1.08s
C(18)H	1.71s	1.73s	1.73s	1.77s	1.74s	1.74s	1.74s	1.78s
C(19)H	1.99s	2.01s	2.09s	2.13s	2.10s	2.10s	2.10s	2.16s
C(20)H	2.09s	2.14s	2.29s	2.36s	2.33s	2.32s	2.31s	2.46s
C(1')H	3.47t	-	3.70t	3.74dt	-	-	-	3.74s
C(1")H	-	-	-	-	-	-	-	3.47s
C(2')H	1.62m	1.28s	1.78m	1.81m	1.50m	1.51m	1.50m	-
C(3')H	1.33m	-	1.41m	1.43m	-	-	-	-
C(4')H	0.93t	-	0.96t	0.99t	-	-	-	-
N-H					10.94bs	10.82bs	11.60bs	-

a s = singlet, d = doublet, t = triplet, dd = doublet of doublets, dt = doublet of triplets, bs = broad singlet.

b in ppm. Numbering of carbons as in text.

c referenced to CD_2Cl_2, 5.32 ppm. Measured at 21°C.

Table 2-6

^1H, ^1H Coupling Constant Data[a] For Retinylidene Imines and Iminium Salts

	Compound							
	46	47	48	49	51	52	53	54
$J_{7,8}$	16.32	16.28	16.18	15.95	16.62	15.90	16.01	15.96
$J_{10,11}$	11.48	11.21	11.74	11.81	11.72	11.99	11.71	11.77
$J_{11,12}$	15.12	15.13	14.84	14.70	14.83	14.90	14.84	14.68
$J_{14,15}$	9.86	9.90	11.11	11.28	11.10	11.32	11.10	11.79
$J_{15,N}$	-	-	-	15.71	16.19	15.41	15.86	-

a in Hz. Numbering of carbons as in text.

Table 2-7

^1H NMR Chemical Shift[a,b] Data For Aldehydes and Protonated Aldehydes

	Compound			
Position	35[c]	26[c]	38[d]	39[d]
C(1)H	9.63d	9.55d	8.82d	8.58d
C(2)H	6.07dd	6.17dd	6.85dd	6.81dd
C(3)H	7.13dd	7.13dd	8.48t	8.41t
C(4)H	6.30m	6.20m	7.05t	7.00t
C(5)H	6.30m	6.63dd	7.70m	7.83dd
C(6)H	-	6.38dd	-	6.71t
C(7)H	-	6.10m	-	7.18m
CH_3	1.93d	1.85d	2.32d	2.17d

a s = singlet, d = doublet, t = triplet, dd = doublet of doublets, m = multiplet

b in ppm. Numbering of carbons as in text.

c referenced to $CDCl_3$ 7.24 ppm. Measured at 19°C.

d referenced to CD_2Cl_2 5.32 ppm in FSO_3H/CD_2Cl_2. Measured at -60°C.

C(2)H, C(4)H and C(6)H in 39 was made on the basis of ^1H decoupling experiments. The remainder of the spectrum was assigned using coupling constant information.

The ^1H NMR data shown in Tables 2-1, 2-3 and 2-5 indicated that in all cases protonation of the imines 26-29 and 46,47 produces a general downfield shift of the odd numbered proton resonances. This is consistent with protonation occurring on nitrogen. A similar trend is found in the protonated aldehydes suggesting protonation on oxygen. In the iminium salts 30, 31, 33, and 49-53 the aldiminium proton appears as a doublet of doublets, Figure 2-2. The larger of the two coupling constants in this spin system results from coupling across the C=N bond of 15.4-16.6 Hz to the proton on nitrogen (184). This coupling constant is indicative of an anti C=N arrangement (199).

Since coupling is observed in these systems between the aldiminium proton and the N-H proton, exchange of the nitrogen proton must be slow relative to the NMR time scale. Thus the equilibrium for proton exchange, equation 23, lies far to the right in these systems, at room temperature. This is in marked contrast to previously reported studies using trifluoroacetic acid as a protonating agent where a 1:1 complex only exhibited this coupling below -61°C (184).

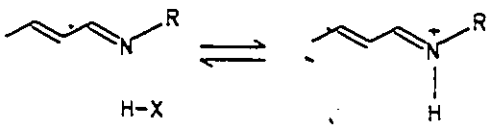

(23)

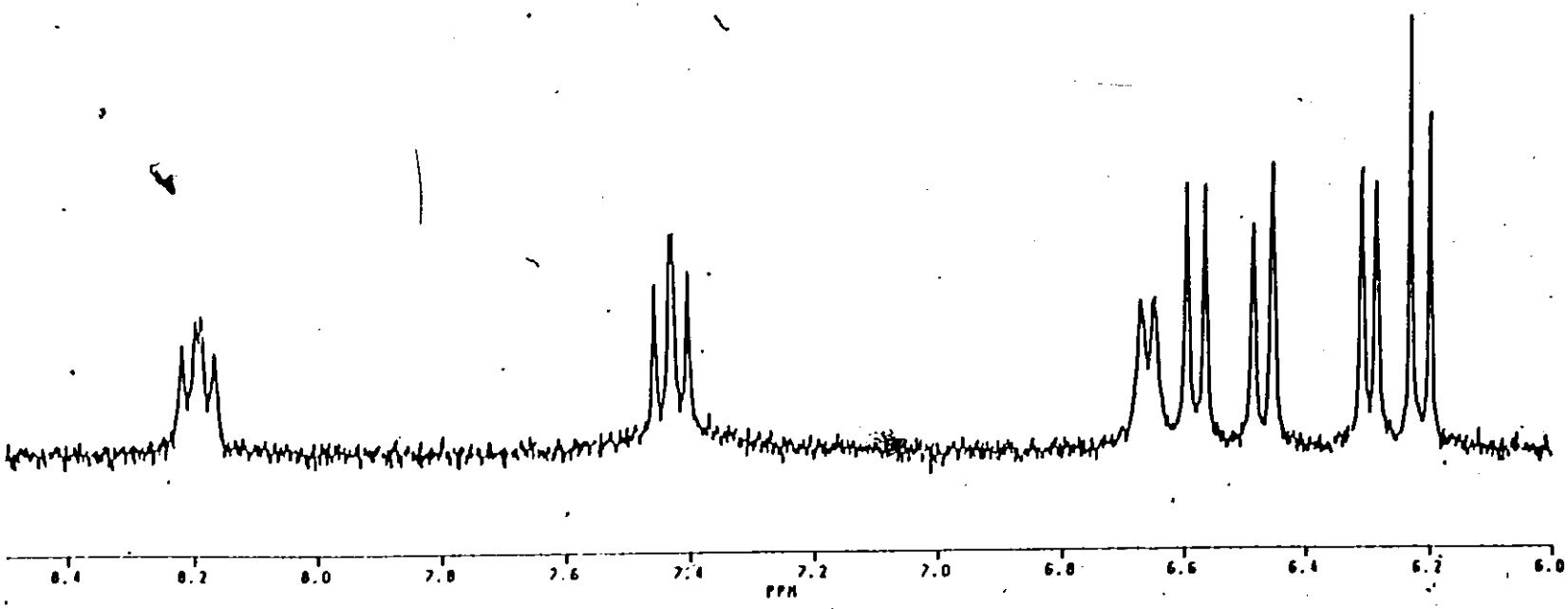

Figure 2-2: Vinyl region of 500 MHz ^{1}H NMR spectrum of N-t-butyl-retinylidene iminium perchlorate, 52.

III. Solution ^{13}C NMR Spectroscopy

The ^{13}C NMR spectroscopic data shown in Tables 2-8 to 2-10 are of the all-trans iminium salts as determined by the ^{1}H NMR experiments. Chemical shifts of the various resonances were found to depend slightly on the acquisition temperature. For example, the resonances of 52 showed a general, but small (<0.5 ppm) shift to higher field on lowering the temperature from -10°C to -40°C.

Assignments of the various ^{13}C resonances of imines 26-29, iminium salts 30-34, and protonated aldehydes 38 and 39 were made by comparison with published data (43,52,54,132,184,198,200), proton off-resonance decoupling or $^{13}C\{^{1}H\}$ shift correlation experiments. The latter method is shown for the iminium salt, 31, in Figure 2-3, where all of the vinylic carbons occur in a confined region of the spectrum. All of the resonances of the retinylidene imines 46,47 and iminium salts 48-54 were assigned using J-modulated spin echo experiments and comparison with literature data. The use of spin echo experiments was required since the chemical shifts of C(13) and C(15) were found to be extremely anion dependent, Table 2-10.

Protonation of imines 26-29 results in a general shift of the odd numbered vinylic carbons to lower field and the even numbered carbons to slightly higher field. The retinylidene imines 46,47 and iminium salts 48-54 show the same trend as exemplified in Figure 2-4.

Table 2-8

^{13}C NMR Chemical Shift[a,b] Data For Aliphatic Imines and Iminium Salts

	Compound						
Position	26	27[c]	30	31	32	33	34
C1	157.05	164.53	166.12	164.96	35.01	34.71	171.01
C2	131.26	132.53	120.46	120.90	41.02	40.26	117.53
C3	141.13	141.20	160.68	160.33	20.53	19.29	163.36
C4	131.56	132.97	131.25	128.35	35.21	34.28	131.54
C5	134.22	138.20	151.11	150.39	146.44	138.76	152.98
C6	18.59	134.00	19.11	131.73	137.59	137.74	19.94
C7	-	135.27	-	143.25	151.63	143.05	-
C8	-	-	-	19.26	124.94	134.82	-
C9	-	-	-	-	181.62	160.55	-
C10	-	-	-	-	-	119.82	-
C11	-	-	-	-	-	166.40	-
1,1 CH_3	-	-	-	-	28.93	29.57	-
5 CH_3	-	-	-	-	15.55	14.68	-
9 CH_3	-	-	-	-	22.27	22.20	-
C1'	57.20	-	61.65	60.49	47.99	60.16	-
C1''	-	-	49.63	-	-	-	-
C2'	28.87	28.40	-	28.43	30.48	28.57	-

a in ppm. Numbering of carbons as in text.
b referenced to CD_2Cl_2, 53.8 ppm. Measured at 21°C.
c from ref. 48

Table 2-9

^{13}C NMR Chemical Shift[a,b] Data For Retinylidene Imines and Iminium Salts

	Compound								
Position	46	47	48	49	50	51	52	53	54
C1	34.71	34.22	34.21	34.24	34.78	34.69	34.21	34.66	34.32
C2	40.21	37.74	39.46	39.47	40.30	40.16	39.44	40.15	39.82
C3	19.78	19.29	19.13	19.11	19.70	19.56	19.10	19.55	19.20
C4	33.57	33.10	33.27	33.34	33.80	33.76	33.32	33.74	33.41
C5	130.18	129.64	131.74	132.40	132.37	132.59	132.26	132.44	133.94
C6	138.35	137.78	137.45	137.47	138.13	138.02	137.45	137.97	137.63
C7	128.13	127.37	131.74	132.79	132.89	133.20	132.60	132.90	132.90
C8	138.00	137.52	137.19	136.91	137.32	137.23	136.94	137.18	136.61
C9	138.35	137.78	145.24	147.17	146.82	147.42	146.86	146.95	148.20
C10	130.43	130.76	129.60	129.69	129.93	129.97	129.68	129.92	129.52
C11	128.29	127.70	137.19	139.42	138.76	139.57	139.08	139.02	140.41
C12	136.56	136.25	133.63	133.33	132.89	133.75	133.41	133.67	133.49
C13	144.02	143.21	163.27	165.73	163.56	165.53	164.98	164.57	168.30
C14	130.18	130.01	120.35	119.27	119.16	119.83	119.47	119.74	116.43
C15	159.36	153.50	164.64	164.20	158.43	159.28	158.96	159.02	163.81
C16	29.20	28.75	28.76	28.79	28.95	28.60	28.78	28.59	28.82
C17									
C18	21.89	21.43	21.77	21.82	21.98	21.97	21.79	21.95	21.61
C19	13.01	12.58	13.11	13.27	13.54	13.44	13.16	13.40	13.22
C20	13.20	12.88	13.90	14.40	14.47	14.92	14.47	14.83	14.54
C1'	62.27	57.32	c	58.80	60.23	59.72	59.49	59.58	49.90
C1''	-	-	-	-	-	-	-	-	40.53
C2'	33.79	29.58	31.33	31.15	29.25	29.16	28.15	29.14	-
C3'	20.97	-	19.87	19.66	-	-	-	-	-
C4'	14.10	-	13.59	13.50	-	-	-	-	-

a in ppm. Numbering of carbons as in text.
b referenced to CD_2Cl_2, 53.8 ppm. Measured at 21°C.
c under solvent peak.

Table 2-10

^{13}C NMR Chemical Shift[a] Data For Aldehydes and Protonated Aldehydes

	Compound			
Position	35[b]	36[b]	38[c]	39[c]
C1	193.82	193.27	198.20	190.89
C2	129.79	130.46	122.92	132.14
C3	152.55	152.25	184.87	183.51
C4	130.03	127.42	134.57	122.21
C5	141.88	142.94	174.96	171.89
C6	-	131.00	-	134.37
C7	-	136.94	-	164.10
CH_3	18.87	19.06	22.15	21.01

a in ppm. Numbering of carbons as in text.
b referenced to $CDCl_3$ 77.3 ppm. Measured at 19°C.
c referenced to CD_2Cl_2 53.8 ppm in FSO_3H/CD_2Cl_2. Measured at -60°C.

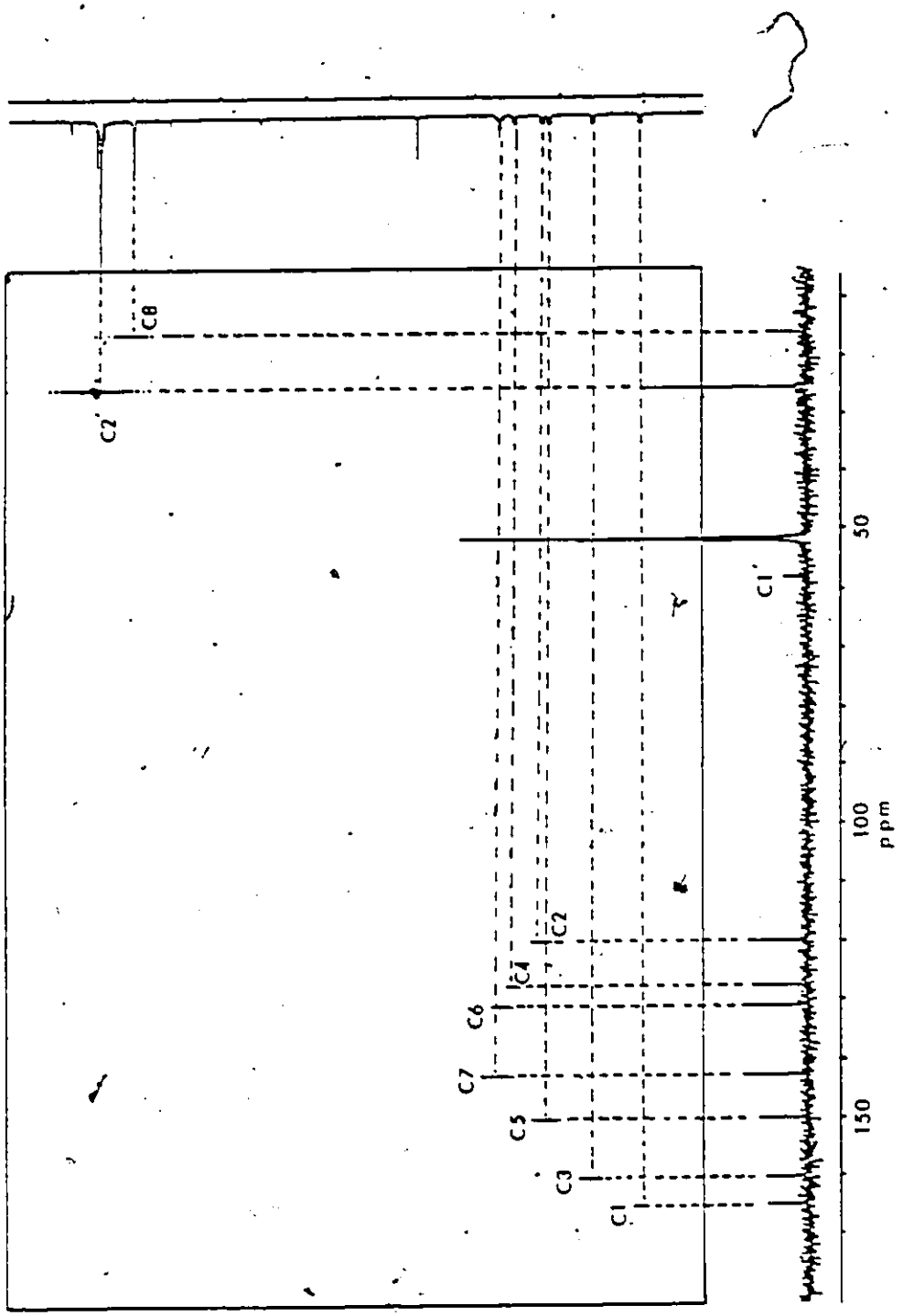

Figure 2-3: $^{13}C\{^{1}H\}$ shift correlation NMR spectrum for N-t-butyl-2,4,6-octatrienylidene iminium perchlorate, 31.

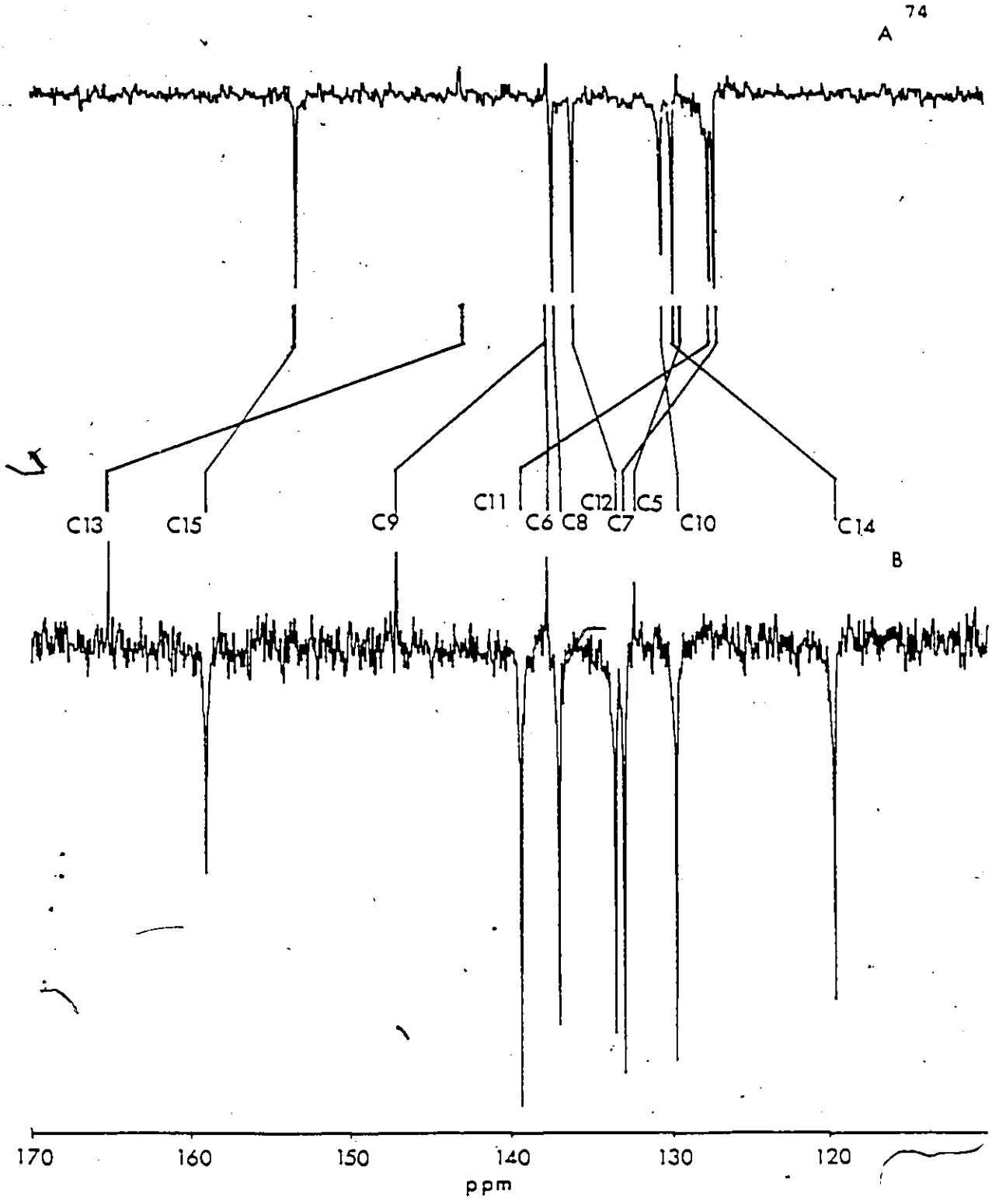

Figure 2-4: Vinyl region of ^{13}C NMR spectra of N-t-butyl-retinylidene imine, 47 (A), and its perchlorate salt, 52 (B).

IV. Solid State ^{13}C NMR Spectroscopy

The solid state ^{13}C NMR spectroscopy spectra of five simple conjugated iminium salts, 34 and 41-44, and four retinylidene iminium salts 48, 51, 52 and 54 were obtained using cross polarization magic angle spinning (CPMAS) methods. The chemical shifts of these compounds are listed in Tables 2-11 and 2-12. The spectra of all iminium salts except 34, 48 and 51 were provided by Dr. R.E. Wasylishen at Dalhousie University in Halifax. Identification of the quaternary and methyl carbons was made using a delay without decoupling pulse sequence (201), which suppresses CH and CH_2 resonances, Figure 2-5. The remainder of the resonances were assigned by comparison with solution spectra or literature values (48,76,128,202,203).

All of the iminium salts studied, with the exception of 54 showed the presence of one isomer in accordance with solution ^{1}H and ^{13}C NMR spectroscopy findings. It is clear from the spectrum of 54 that two different compounds are present and that at least one of these is a dimethyl all-trans retinylidene iminium salt. The solution ^{1}H NMR spectrum of 54 indicated that the 13-cis isomer of this iminium salt, 55, was present to the extent of approximately 13% at 21°C. In order to determine if the second component in the solid state ^{13}C spectrum of 54 was 55, the salt was dissolved in CD_2Cl_2 at -60°C; conditions under which 55 would be kinetically stable. However, the ^{1}H NMR spectroscopy spectrum obtained at -60°C showed that only the all-trans isomer was present. Upon warming of this solution the 13-cis isomer, 55, became more abundant. Since 55 is not present at -60°C, it is concluded that it

Table 2-11

Solid State ^{13}C NMR Chemical Shift[a,b] Data For Some Iminium Salts

	Compound				
Position	34	41	42	43	44
C1	171.35	164.3	172.2	162.8	170.8
C2	118.94	117.1	118.9	116.9	118.5
C3	159.78	164.3	163.5	162.8	163.0
C4	131.15	135.1	134.6	133.2	131.5
C5, C9	150.86	133.9	132.6	133.2	131.5
C6, C8	20.88	128.3	126.9	129.9	131.5
C7	-	138.3	136.3	140.9	138.8
C10	-	141.9	146.2	140.9	143.7
C11, C15	-	122.6	124.1	121.7	123.8
C12, C14	-	130.8	130.8	130.5	131.5
C13	-	133.9	132.6	132.5	131.5
CH_3	-	40.5	44.9	39.4	41.4

a in ppm. Numbering of carbons as in text.
b referenced to adamantane, 29.5 and 38.57 ppm. Measured at 21°C.

Table 2-12

Solid State ^{13}C NMR Data[a,b] For Retinylidene Iminium Salts

	Compound			
Position	48	51	52	54
C1	35.47	34.47	36.69	34.74
C2	40.43	38.77	45.15	44.11
C3	20.84	19.34	19.92	19.42
C4	35.47	33.62	34.78	36.22
C5	131.69	128.99	136.76	137.40
C6	140.03	139.06	140.11	138.57
C7	131.69	132.42	134.29	130.56
C8	136.84	138.68	136.76	137.40
C9	143.99	149.51	147.60	149.22
C10	130.37	130.26	129.66	127.81
C11	140.03	138.68	140.11	138.57
C12	132.37	132.42	133.41	133.25
C13	162.75	167.13	167.16	166.73
C14	122.54	118.92	120.34	117.52 118.95
C15	166.90	160.00[c]	160.98	162.09 162.77
C16	31.52	28.77	29.90	27.98 29.93
C17		29.51		31.50
C18	25.41	23.31	22.32	21.33 23.31
C19	13.43	12.94	12.84	13.42
C20	17.20	14.42	15.53	16.08 18.17
C1'	54.75	58.56	60.29	40.88
C1''	-	-	-	48.95 51.24
C2'	32.55	27.94	32.23	-
C3'	20.84	-	-	-
C4'	15.70	-	-	-

a chemical shift in ppm. Numbering of carbons as in text.

b referenced to adamantane, 29.50 and 38.57 ppm. Measured at 21°C.

c broad singlet

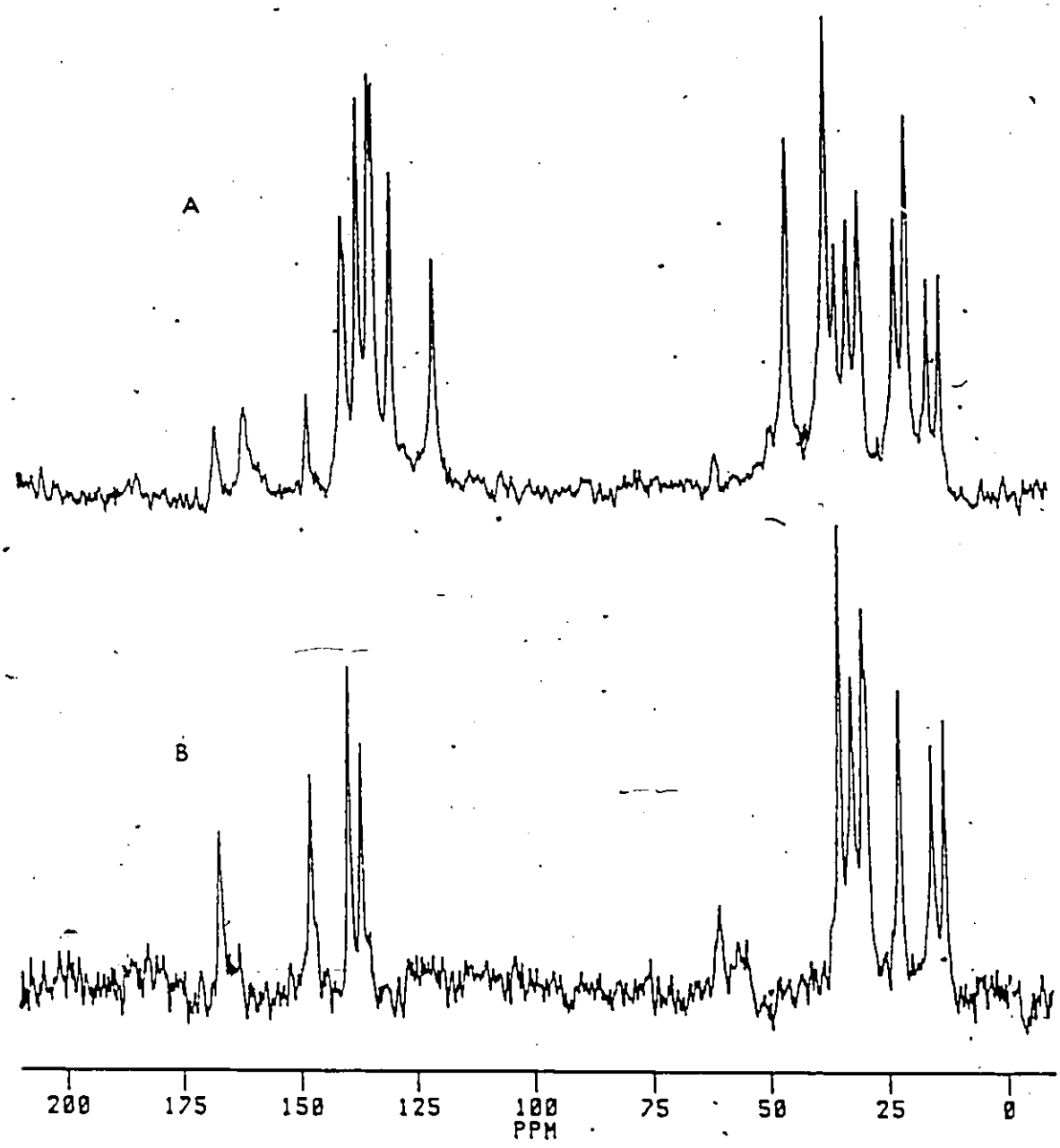

Figure 2-5: CPMAS ^{13}C NMR spectrum of N-t-butyl-retinylidene iminium perchlorate, 52 (A) and suppressed (B).

can not be the second compound in the solid state ^{13}C NMR spectrum of 54. This compound must be either a different conformational isomer about a C-C single bond, or a second symmetrically unrelated molecule of the all-trans retinylidene iminium salt, 54. resulting from crystal packing effects.

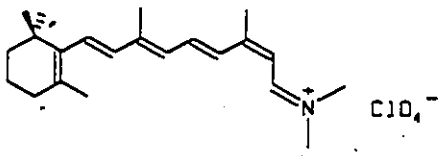

SS

The solid state spectrum of 34 contained three carbons which appeared as doublets. These result from residual coupling to the nitrogen quadrupole of the carbons adjacent to the iminium nitrogen (204). This phenomenon has previously been detected in similar compounds (202). In all other solid state spectra, coupling to the nitrogen quadrapole was eliminated by by the use of a stronger magnetic field.

V. Absorption Spectroscopy

i. Solution Spectra

The absorption spectra of iminium salts 30-33, 41-44 and 48-54 were measured at room temperature in CH_2Cl_2. Absorption maxima and extinction co-efficients are shown in Tables 2-13 and 2-14. All of the spectra exhibited a broad, intense featureless peak, characteristic of the π-π^* transition in iminium salts.

Table 2-13.

Absorption Spectra Data[a] (nm) for Iminium Salts

Compound	λ_{max}	ε_{max} ($\times 10^{-4}$)	λ_{max} (solid)
30	314	3.65	292
31	370	3.48	344
32	338[b]	2.35	-
33	378[b]	-	-
34	320	3.56	312
48	454	-	448
49	476	4.06	510
50	467	-	462
51	470	3.89	442
52	472	4.26	504
53	464	4.44	448
54	498	4.05	460

a in CH_2Cl_2 at 21°C.

b in MeOH.

Table 2-14

Absorption Spectra Data (nm) for Aromatic Iminium Salts

	λ max			
Compound	$CHCl_3$	C_6H_6	ETOH	Solid
41	348	350	350	394
42	356	352	350	348
43	-	356	356	382
44	360	362	358	370

ii. Solid State Spectra

Absorption spectra were measured for many of the iminium salts in the solid phase as listed in Tables 2-13 and 2-14. The use of solid state absorption spectra in organic chemistry has been quite limited and most examples in the literature of its use are found for inorganic compounds (205). The purpose of its use in this study of iminium salts was twofold. Firstly, a method was developed which was simple to use but also gave reproducible spectra. Secondly, solid state spectra should, in principle, yield valuable information about the overall structure of a molecule in the crystalline state. The most important structural features which were examined were those of cation/anion interactions and conformational changes which may have occurred on moving from the solution phase to the solid. Typically, solid state absorption peaks were broader than in solution but still gaussian in shape. Spectra were obtained using very thin layers of microcrystalline sample on either a glass or quartz slide (205,206). In some experiments where light scatter was particularily excessive a reference sample of KBr was used. Quantitative measurement of extinction coefficients was impossible using this technique. A reference sample of all-trans retinal was used to determine if either of the slides perturbed the position of the absorption maximum. This was found to absorb at 386 nm, very close to its value in methylene chloride of 382 nm. The error in the absorption maximum from each solid spectrum was approximately ± 5 nm.

VI. X-ray Crystallographic Studies

Single crystals of 44 and 45, suitable for x-ray crystallographic determination, were grown by the distillation of ethyl ether into acetonitrile solutions of the respective compound. The crystals were found to be stable at room temperature in the absence of moisture. Each structure existed in the same monoclinic space group, $P2_1/c$. Details of the collection of data and the solution of the structures can be found in the Experimental section and the Appendix.

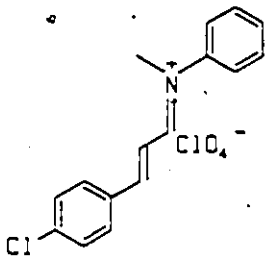

44

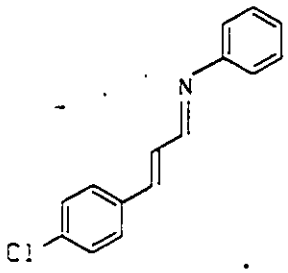

45

The structures of 44 and 45 are remarkably similar within the carbon skeleton of each molecule, Figures 2-6 and 2-7. Except for C(1)-N and C(1)-C(2), bond lengths and bond angles for non-hydrogen atoms, found in Tables 2-15 and 2-16, are all similar within experimental error for the two structures.

Each molecule is composed of three planar fragments which are twisted from each other to varying degrees. The atoms involved in each plane and the dihedral angles between planes are listed in Tables 2-17 and 2-18. In both structures, the dihedral angle between planes P1 and P2 is significantly smaller than the angle between planes P2 and P3.

The crystal packing arrangements of 44 and 45 are markedly diff-

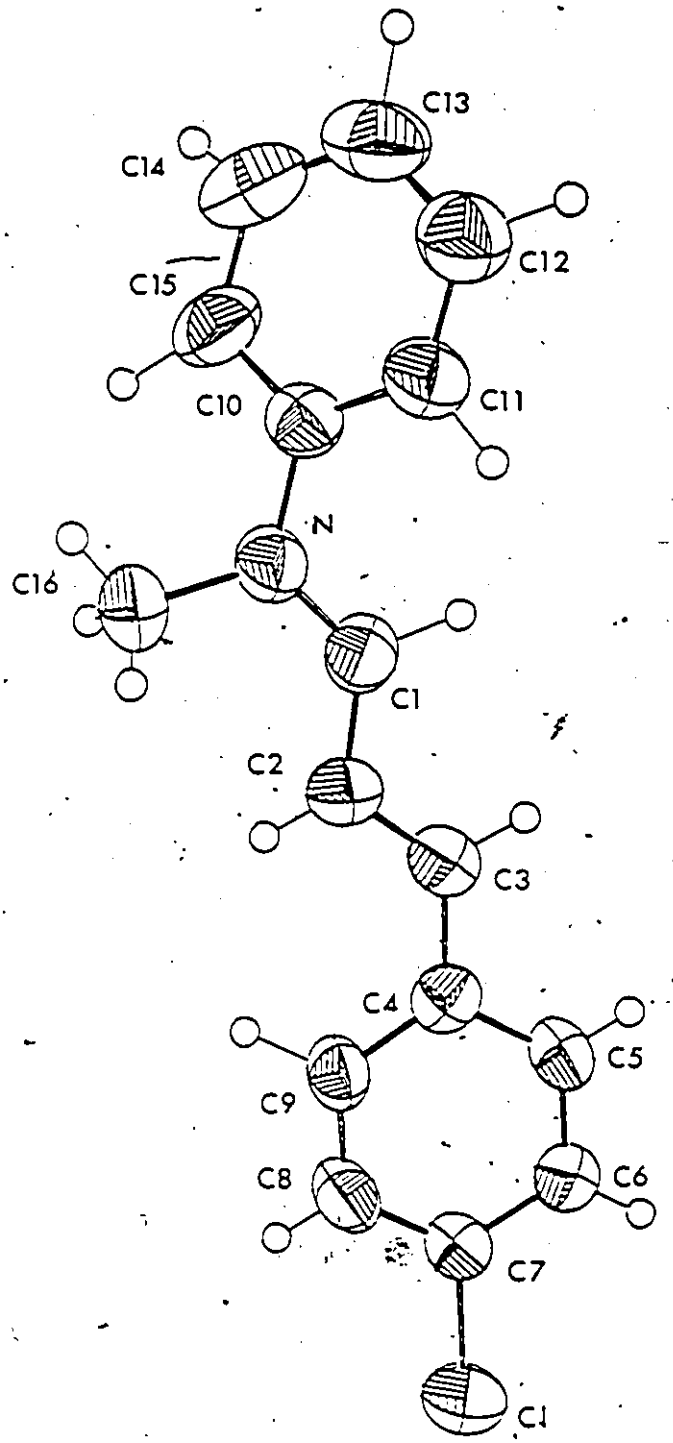

Figure 2-6: Ortep diagram for N-phenyl-N-methyl-3-(p-chlorophenyl)-2-propenylidene iminium perchlorate, 44.

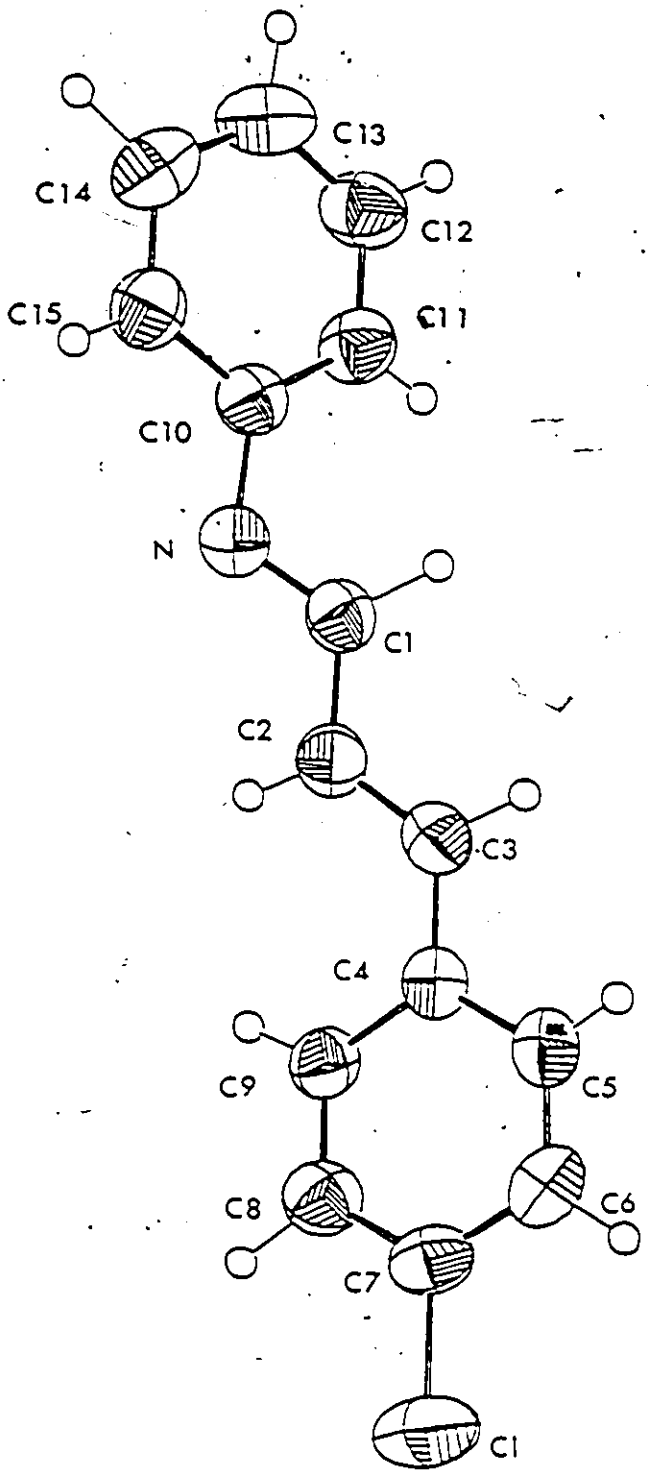

Figure 2-7: Ortep diagram for N-phenyl-3-(p-chlorophenyl)-2-propenylidene imine 45.

Table 2-15

Bond Lengths (Å) and angles (deg.) for N-phenyl-N-methyl-3-(p-chlorophenyl)-2-propenylidene iminium perchlorate, 44.

Bond Lengths:

Cl(1)-O(1)	1.351(7)	Cl(1)-O(2)	1.341(5)
Cl(1)-O(3)	1.411(4)	Cl(1)-O(4)	1.350(8)
C(1)-N	1.325(8)	C(1)-C(2)	1.410(8)
C(2)-C(3)	1.330(10)	C(3)-C(4)	1.448(8)
C(4)-C(5)	1.398(9)	C(4)-C(9)	1.377(7)
C(5)-C(6)	1.371(8)	C(6)-C(7)	1.369(7)
C(7)-C(8)	1.364(9)	C(7)-Cl(2)	1.739(6)
C(8)-C(9)	1.366(8)	C(10)-N	1.438(6)
C(10)-C(11)	1.374(8)	C(10)-C(15)	1.400(9)
C(11)-C(12)	1.368(9)	C(12)-C(13)	1.379(13)
C(13)-C(14)	1.376(12)	C(14)-C(15)	1.398(10)
C(16)-N	1.483(9)		

Bond Angles:

O(1)-Cl(1)-O(2)	108.5(4)	O(1)-Cl(1)-O(3)	107.8(3)
O(1)-Cl(1)-O(4)	104.2(5)	O(2)-Cl(1)-O(3)	114.4(3)
O(2)-Cl(1)-O(4)	110.4(4)	O(3)-Cl(1)-O(4)	111.0(4)
C(2)-C(1)-N	126.2(5)	C(1)-C(2)-C(3)	118.0(5)
C(2)-C(3)-C(4)	126.8(5)	C(3)-C(4)-C(5)	119.7(5)
C(3)-C(4)-C(9)	122.4(5)	C(4)-C(5)-C(6)	122.0(5)
C(5)-C(6)-C(7)	118.4(6)	C(6)-C(7)-C(8)	120.4(5)
C(6)-C(7)-Cl(2)	119.2(5)	C(8)-C(7)-Cl(2)	120.4(4)
C(7)-C(8)-C(9)	121.4(5)	C(4)-C(9)-C(8)	119.8(8)
C(11)-C(10)-N	119.2(5)	C(15)-C(10)-N	119.1(5)
C(10)-C(11)-C(12)	120.0(7)	C(11)-C(12)-C(13)	120.0(7)
C(12)-C(13)-C(14)	120.4(7)	C(13)-C(14)-C(15)	121.0(7)
C(10)-C(14)-C(15)	116.9(6)	C(1)-N-C(10)	119.6(5)
C(1)-N-C(16)	121.3(5)	C(10)-N-C(16)	119.1(5)

Table 2-16

Bond Lengths (Å) and angles (deg.) for N-phenyl-3-(p-chlorophenyl)-2-propenylidene imine, 45.

Bond Lengths:

C(1)-N	1.274(4)	C(1)-C(2)	1.444(4)
C(2)-C(3)	1.327(5)	C(3)-C(4)	1.461(4)
C(4)-C(5)	1.401(4)	C(4)-C(9)	1.388(4)
C(5)-C(6)	1.376(4)	C(6)-C(7)	1.380(4)
C(7)-C(8)	1.380(4)	C(7)-Cl	1.733(3)
C(8)-C(9)	1.378(5)	C(10)-N	1.415(3)
C(10)-C(11)	1.392(4)	C(10)-C(15)	1.385(4)
C(11)-C(12)	1.378(5)	C(12)-C(13)	1.377(5)
C(13)-C(14)	1.375(5)	C(14)-C(15)	1.375(5)

Bond Angles:

C(2)-C(1)-N	122.1(2)	C(1)-C(2)-C(3)	123.5(3)
C(2)-C(3)-C(4)	127.3(3)	C(3)-C(4)-C(5)	122.7(3)
C(3)-C(4)-C(9)	119.9(2)	C(4)-C(5)-C(6)	121.3(3)
C(5)-C(6)-C(7)	119.2(3)	C(6)-C(7)-C(8)	121.3(3)
C(6)-C(7)-Cl	119.8(2)	C(8)-C(7)-Cl	119.0(2)
C(7)-C(8)-C(9)	118.6(3)	C(4)-C(9)-C(8)	122.2(3)
C(11)-C(10)-N	117.8(2)	C(15)-C(10)-N	123.8(3)
C(10)-C(11)-C(12)	121.0(3)	C(11)-C(12)-C(13)	119.9(3)
C(12)-C(13)-C(14)	119.7(3)	C(13)-C(14)-C(15)	120.6(3)
C(10)-C(15)-C(14)	120.6(3)	C(1)-N-C(10)	119.1(2)

Table 2-17

Best Fit Planes and C-O contacts (Å) for N-phenyl-N-methyl-3-(p-chlorophenyl)-2-propenylidene iminium perchlorate, 44.

Plane		Distance of Atom From Plane (Å)
P1	C(3)-N, C(16)	C(1) 0.000(6), C(2) -0.000(7) C(3) -0.000(7), C(16) 0.005(9) N 0.000(5)
P2	C(4)-C(9)	C(4) -0.008(6), C(5) 0.000(6) C(6) 0.005(7), C(7) -0.002(6) C(8) -0.007(7), C(9) 0.012(7)
P3	C(10)-C(15)	C(10) -0.001(6), C(11) 0.004(8) C(12) -0.002(9), C(13) -0.006(9) C(14) 0.012(10), C(15) -0.004(8)

Dihedral Angles (deg.)

P1-P2	9.8
P1-P3	45.0
P2-P3	36.8

Shortest C-O Contacts

C(1)-O(1)	3.39	C(6)-O(4)	3.29
C(1)-O(3)	3.23	C(9)-O(3)	3.53
C(1)-O(4)	3.48	C(10)-O(3)	3.46
C(2)-O(2)	3.26	C(11)-O(3)	3.55
C(2)-O(4)	3.34	C(14)-O(1)	3.50
C(5)-O(4)	3.35	C(16)-O(2)	3.37

Table 2-18

Best Fit Planes for N-phenyl-3-(p-chlorophenyl)-2-propenylidene imine, 45.

Plane		Distance of Atom From Plane (Å)			
P1	C(3)-N	C(1)	0.042(3),	C(2)	0.050(3)
		C(3)	-0.042(3),	N	-0.026(2)
P2	C(4)-C(9)	C(4)	-0.013(2),	C(5)	0.009(3)
		C(6)	0.008(3),	C(7)	-0.014(3)
		C(8)	0.008(3),	C(9)	0.009(3)
P3	C(10)-C(15)	C(10)	0.004(3),	C(11)	-0.008(3)
		C(12)	0.002(3),	C(13)	0.008(4)
		C(14)	-0.010(3),	C(15)	0.002(3)

Dihedral Angles (deg.)

P1-P2	21.5
P1-P3	38.4
P2-P3	59.2

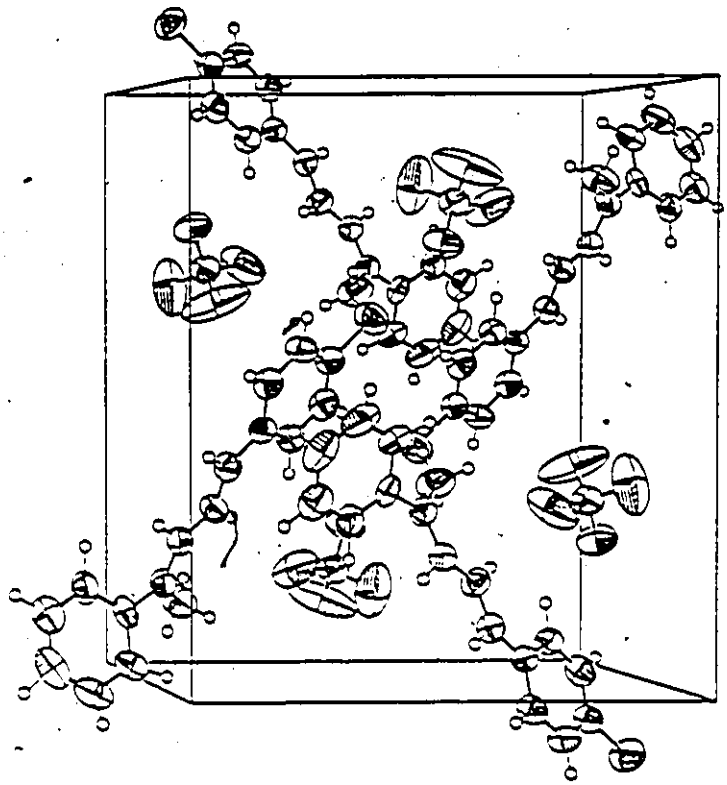

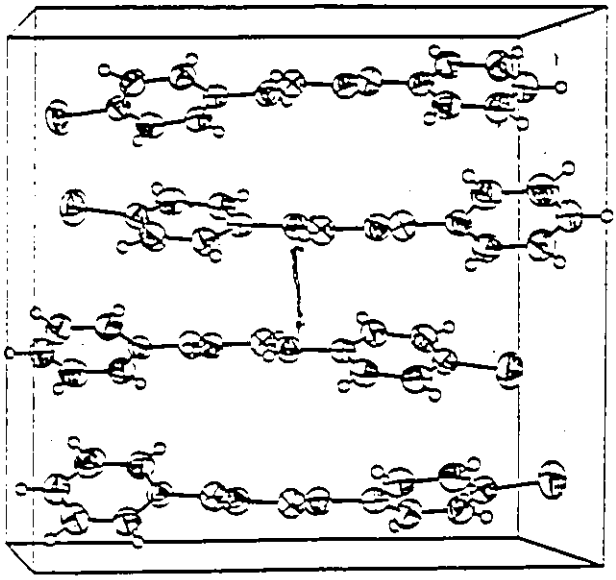

Figure 2-8: Crystal packing for N-phenyl-N-methyl-3-(p-chlorophenyl)-2-propenylidene iminium perchlorate, 44.
Figure 2-9: Crystal packing for N-phenyl-3-(p-chlorophenyl)-2-propenylidene imine 45.

erent, likely because of the presence of the perchlorate anions in 44. In the unit cell of 45, Figure 2-9, the four molecules are arranged in a layered fashion such that each molecule is aligned head to tail with the next.

The spatial arrangement of 44 is shown in Figure 2-8. In this structure the cations form a rough spiral perpendicular to the BC plane. The overlapping portions of the molecules alternate between the N-phenyl end and the p-chloro phenyl end near the centre of the unit cell. The perchlorate anions in this structure form tunnels which parallel the axis of the cationic spiral. The perchlorate anions are not in the same plane as the cations, but rather above and below this region. This gives rise to each cation being surrounded by four symmetrically related anions. In crystal structures of similar iminium salts (202) it was found that cations and anions were located in approximately the same plane and that cations overlapped head to tail, much like in 45.

The x-ray crystallographic structures of two other iminium salts 34 and 54 were also attempted. In 34, a unit cell was found for the space group Pnma however a suitable solution could not be determined. The retinylidene iminium salt, 54, was discovered to be a multiple crystal and thus only unit cell parameters could be obtained from precession photography.

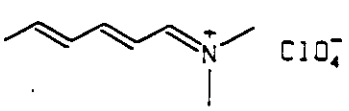

34

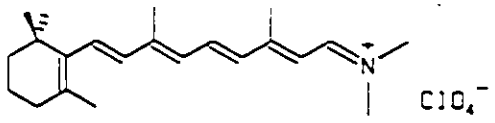

54

DISCUSSION

In the previous section, the results obtained from experiments on a variety of iminium salts and protonated aldehydes were presented. The relevance of these studies to the overall structure of iminium salts in terms of geometry, charge delocalization and cation/anion interactions are presented in this section.

It is useful before considering the structure of the retinylidene iminium salts to examine in detail some of the simpler conjugated systems. This will allow the basic principles of charge delocalization and cation/anion interactions to be developed.

A. Simple Conjugated Iminum Salts

The iminium salts 30-34 and 41-44 are related in that they possess one to three double bonds conjugated to the formal C=N bond. All of these compounds possess a trans (E) geometry about C=C and C=N bonds (except 34, which is symmetric about C=N) as found by either ^{1}H NMR spectroscopy or x-ray crystallography.

I. Charge Delocalization

Three different strategies were used to investigate charge delocalization in these simple iminium salts. The most direct method used was x-ray crystallography which also allowed for a detailed structural comparison between the iminium salt 44 and its corresponding imine 45, to be made. The second approach used was an empirical bond-valence

relationship which allowed for a "quantitative" assessment of charge delocalization. Parallelling this method was an analysis of ^{13}C NMR spectroscopy chemical shift data which has previously been suggested as a measure of charge delocalization.

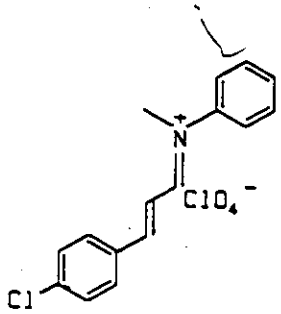

44

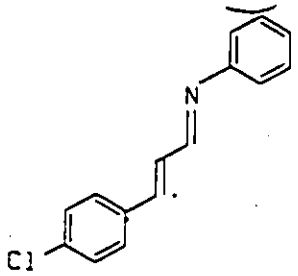

45

i. X-ray Crystallography

The structures of 44 and 45 are shown in Figures 2-9 and 2-10. These molecules differed only by the presence of the N-methyl group and the perchlorate anion in 44. It is immediately apparent that these structures are quite similar in geometry. Each molecule is divided into three best fit planes, Tables 2-17 and 2-18. In both cases, the dihedral angle between the N-C(3) plane and the 3-phenyl ring is substantially smaller than that between N-C(3) plane and the N-phenyl ring. In terms of conjugation, this orientation is expected in 44 since conjugation of the C(3) to phenyl with the iminium function 56, should be more important than involvement of the N-phenyl group, 57. As a result, better π orbital overlap is occurring in the N to C(9) portions of 44 and 45, as

compared to the C(3) to C(15) section.

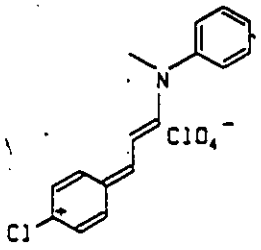

56

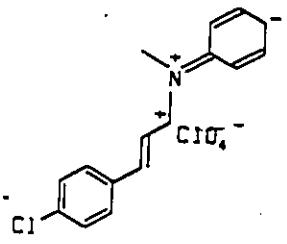

57

The bond lengths of these molecules should give some indication of positive charge delocalization in 44. In a localized system such as 58, where the positive charge is placed on nitrogen, "normal" single and double bonds exist. That is, they would be expected to alternate in internuclear distance such that single bonds are much longer than double bonds. As charge is delocalized through the system this alternation will decrease with former single bonds now possessing some double bond character, and vice versa, 59, equation 24. An intermediate C-C distance would be achieved near that of benzene, at 1.395 Å (207).

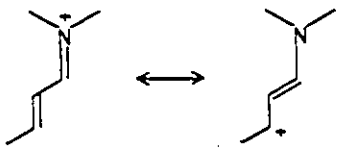

(24)

58 59

In the imine 45, the C(1)-N bond length is 1.274(4) Å. This is well within the range of 1.23-1.29 Å expected for the C=N bond in simple

conjugated imines (208). In 44, the corresponding bond is substantially lengthened at 1.325(8) Å. It is also longer than that found in the unconjugated tetramethylmethylene iminium ion, 1.30 Å, which has been suggested to represent a "pure" $C=N^+$ bond (209). Accompanying this change in the C=N bond length there is a decreased C=N stretching frequency in the infrared spectrum of 44, 1621.63 cm^{-1}, compared to 1628.01 cm^{-1} in 45. These findings are consistent with positive charge delocalization to C(1) in 44 resulting in bond elongation.

The α,β double bonds, C(2)-C(3), in 44 and 45 are 1.330(10) Å and 1.327(5) Å respectively. These are the same within experimental error and show that no large change in the C-C bond length occurs upon conversion of the imine to the iminium salt. This is substantiated by the C=C stretching frequencies of these bonds which are nearly identical for both compounds, Table 4-1. In contrast, cyanine dyes, which have extensive positive charge delocalization, exhibit an average C(2)-C(3) bond length of 1.381(14) Å (210,211). In the present cases, the C(2)-C(3) bond distance is more representative of the 1.342 Å found in ethylene (212), or 1.360 Å in 1,3 butadiene (213). This lack of lengthening of C(2)-C(3) suggests that a formal double bond is present and that positive charge is not extensively delocalized to C(3).

The C(1)-C(2) bond length in 44 is slightly shorter than that in 45. This is consistent with charge delocalization to C(1) in 44 and is a result of coulombic attraction between electron deficient C(1) and electron rich C(2), which tends to shorten the bond (214).

ii. Bond Valence Approach

The analysis of X-ray crystal structures using the bond-valence method (215-220) can, in principle, provide a detailed picture of the charges within a molecule. Essentially, the bonds surrounding each atom are represented in terms of their valence, s. This is calculated from the empirical expression shown below, where R is the bond length of interest, R_o is a standard bond length and B is a constant. The sum of the bond valences for an atom is the atomic valence, V. Thus, any deviation of V from the formal valence of an atom should give an

$$s = e^{\frac{(R_o - R)}{B}} \quad , \qquad V = S\Sigma s$$

indication of the charge residing on that atom. The sum of these deviations of all atoms in an ion should sum to +1 in cations and -1 in anions for the complete molecule assuming that no "strong" interactions between the anion and hydrogens of the cation occur. In perchloric acid hydrates and inorganic acetate salts, Brown has shown that these interactions are quite extensive (219,220). However, in the current work, hydrogen atom positions are not known accurately. Therefore the degree of interaction between the cation and the perchlorate anion was determined through internuclear distances between the oxygens of the anion and carbons (or nitrogen) of the cation.

Bond valences for 44 and 45 are shown in Figure 2-10 and the atomic valences in Table 2-19. The most obvious trend in these figures

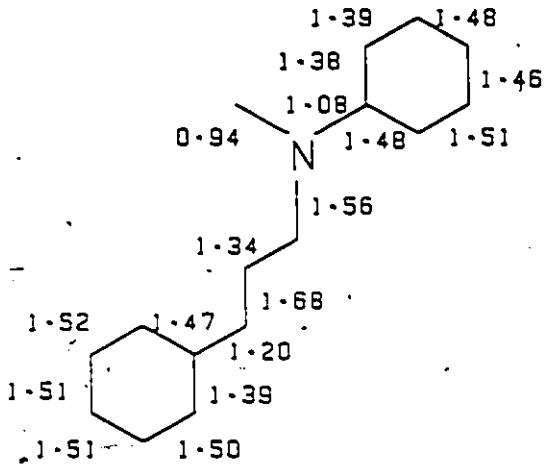

44

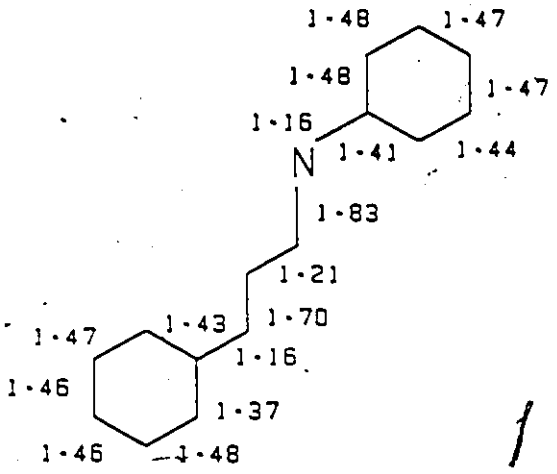

45

Figure 2-10: Calculated bond valences for 44 and 45.

Table 2-19

Atomic Valences and Charges for 44 and 45

	44		45	
Position	Valence	Charge	Valence	Charge
C(1)	3.90	+0.10	4.04	-0.04
C(2)	4.02	-0.02	3.91	+0.09
C(3)	3.88	+0.12	3.86	+0.14
C(4)	4.06	-0.06	3.96	+0.04
C(5)	3.89	+0.11	3.85	+0.15
C(6)	4.01	-0.01	3.92	+0.08
C(7)	-	-	-	-
C(8)	4.04	-0.04	3.93	+0.07
C(9)	3.99	+0.01	3.90	+0.10
C(10)	3.94	+0.06	4.05	-0.05
C(11)	3.99	+0.01	3.89	+0.11
C(12)	3.97	+0.03	3.91	+0.09
C(13)	3.94	+0.06	3.94	+0.06
C(14)	3.87	+0.13	3.95	+0.05
C(15)	3.77	+0.23	3.96	+0.04
C(16)	3.94	+0.06	-	-
N	3.58	+0.58	2.99	-0.01

is that the increased C(1)-N bond length in the iminium salt 44, compared to its imine 45, leads to a reduced bond valence. The calculated atomic valence for nitrogen is 3.58 in 44, 0.59 units higher than in 45. This places the calculated valence of nitrogen closer to tetravalent carbon, having a charge of +1, than neutral trivalent nitrogen. Thus the calculated charge for nitrogen in 44 of about +0.58 suggests that a large portion of the positive charge in 44 is residing on the nitrogen.

Bond-valence treatment of the allylic carbons in 44 and 45 also suggests that the bulk of positive charge is on the nitrogen. The atomic valences for C(1), C(2) and C(3) are all very close to four, the expected value for a neutral carbon atom. However, the greatest change exhibited on going from the imine to the iminium salt is found at C(1). Here, the valence decreases from 4.04 in 45 to 3.90 in 44, a difference of 0.14 units. This is substantially different from any of the other allylic carbons and represents a move towards a full positive charge on C(1) of 44 in which case the carbon valence would be three. This has been corroborated theoretically at the 6-31G** level (221) for the model compounds 60 and 61, where the greatest change in electron density occurs at C(1). These calculations also indicate that a slight increase in electron density occurs at nitrogen, which is in contrast to the bond valence results. However, previously reported calculations have shown that while the positive charge on C(1) is essentially the same as calculated from the bond valence method, a positive charge on nitrogen is also possible with values ranging up to +0.51 (56,127,142).

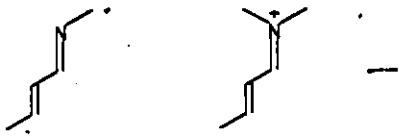

60 61

While the calculated charge for C(3) of 44 is quite close to that found for C(1), it should be noted that C(3) had a valence below 4.0 in the imine, and theif is little change in the valence of this atom upon protonation. This suggests that very little "extra" charge is filtering down to C(3) in 44.

Overall, it would appear that in 44 most of the positive charge is located on nitrogen and that a significant portion is delocalized to C(1). This corresponds to the ground state resonance structures shown in equation 25.

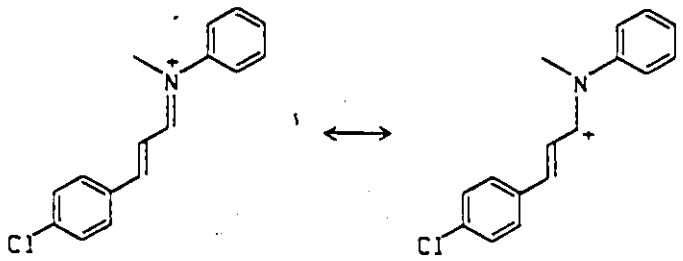

(25)

It is informative to compare these conclusions on the charge distribution in iminium salts with the corresponding oxolenium ions using X-ray crystallographic data. These oxolenium cations, which are closely related to iminium ions, are usually depicted as the resonance forms shown in equation 26, with 62 usually being regarded as the most impor-

tant resonance contributor. This would make oxygen trivalent, having a formal charge of +1, whereas resonance forms 63 and 64 would place oxygen as a neutral divalent atom. Analysis of crystal structure data of protonated carbonyl compounds and ethoxy substituted carbenium ions allows the relative importance of these resonance contributors to be assessed.

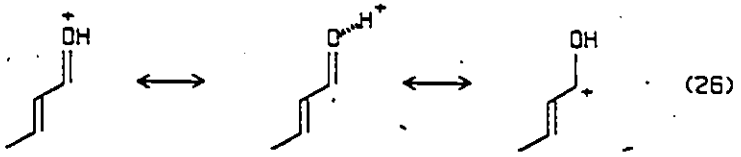

62 63 64 (26)

The crystallographic bond lengths of the ditropenyliumyl ether, 65, and ethoxyhomotropylium, 66, are shown in Figure 2-11 along with calculated bond valences (222,223). The atomic valences of both of these cations are shown in Table 2-20. It is evident from an analysis of bond lengths in these cations that a formal double bond (1.20 Å) to oxygen does not exist. In 65, a C_2 axis passes through the central oxygen making both C-O bond lengths an identical internuclear distance of 1.356(3) Å. This value is very close to a phenyl ether C-O bond length of 1.365(3)-1.370(1) Å (224) or that found in diaryl ethers, 1.353-1.412 Å (225). In terms of bond valences, these bonds are very nearly single bonds at 1.05 units each, and thus the atomic valence for oxygen, 2.10, suggests that very little participation by the oxygen lone pair is occurring in delocalization. Verification of this is found in the tropylium rings in which each C-C bond is intermediate between that of a C-C single bond, 1.54 Å, and a C-C double bond, 1.32 Å. The average bond valence is, as expected, slightly lower than the 1.50 in benzene and the

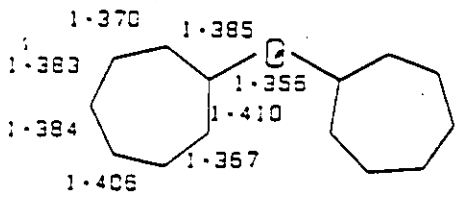

65

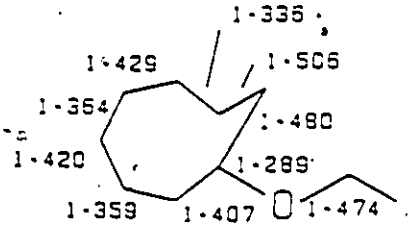

66

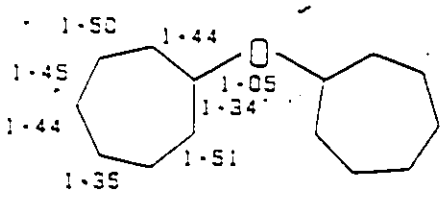

65

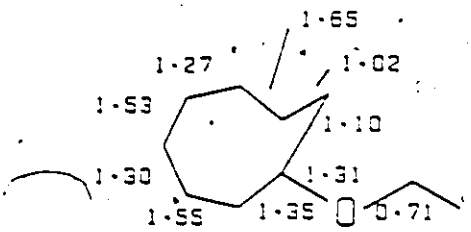

66

Figure 2-11: Crystallographic bond lengths (top) and calculated bond valences (bottom) for the ditropenyliummyl ether cation, 65, and the ethoxyhomotropylium cation, 66.

Table 2-20

Atomic Valences and Charges for 65 and 66

	65		66	
Position	Valence	Charge	Valence	Charge
C(1)	3.83	+0.17	3.76	+0.24
C(2)	3.85	+0.15	3.90	+0.10
C(3)	3.86	+0.14	3.85	+0.15
C(4)	3.79	+0.21	3.83	+0.17
C(5)	3.89	+0.11	3.80	+0.20
C(6)	3.95	+0.05	3.92	+0.08
C(7)	3.94	+0.06	3.67	+0.33
C(8)	-	-	4.12	-0.12
O	2.10	+0.10	2.02	+0.02

average atomic valence of 3.83 in 65, is extremely close to the theoretical value of 3.86 for a fully delocalized tropylium cation. This suggests that each carbon in the tropylium rings bears about +0.17 charge. Calculations by Bader and co-workers (226) have shown that while the bond orders in the tropylium cation are very close to those determined here, the charge on each carbon is somewhat lower at about +0.07. The remainder of the charge is dispersed evenly about the seven hydrogen atoms. In the present case, hydrogen atom positions were not accurately known and a bond-valence of one was assumed. Thus no charge is placed on the hydrogens. The results of Bader suggest that the C-H bond valence must be somewhat lower. Overall, on the basis of a bond-valence analysis, the ditropylium cation, 65, still seems to bear the bulk of its two positive charges in each of the seven membered rings and only a minimal amount on the oxygen.

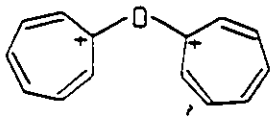

$2(SbCl_6^-)$

65

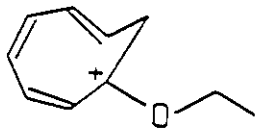

$SbCl_6^-$

66

Further evidence for the involvement of the oxygen atom in charge delocalization is found in the ethoxyhomotropylium cation, 66, This molecule possesses two very different C-O bonds. The shorter of the two, C(1)-O, has a bond valence of 1.39. However, the bond between C(9)-O is extremely long for a C-O bond and has a valence of only 0.70. It seems that the oxygen is compensating for a shortening of one C-O bond by the

lengthening of the second. As a result the atomic valence for oxygen in this case is only 2.09, very close to that in the ditropylium ether structure, 65.

Bond-valence analysis shows that there is an inherent difference in the behavior of conjugated cationic systems which involve oxygen and nitrogen. The above examples show that in iminium salts the majority of positive charge is on the nitrogen and that a smaller amount of charge is delocalized to the a carbon. The exact amount of charge on C(1) appears to be about 30% of the total positive charge, based on bond-valence considerations. Conversely, in oxolenium ions little or no charge resides on the oxygen atom and the positive charge becomes delocalized throughout the carbon framework, as was shown in 64, equation 26. The extent of this delocalization probably depends on the substituents on the oxygen. In crystal structures which have a protonated oxygen, there is always a very strong in-plane hydrogen bonding between the proton and the counteranion (227). Consequently, a resonance form such as 63 is probably important, reducing the amount of charge on the carbon framework.

iii. ^{13}C NMR Spectroscopic Analysis

The chemical shift of an atom is the summation of several contributions, equation 27. In conjugated π systems, the most dominant term is the paramagnetic factor δ_p^{λ}, which has been found to be related to the π electron density (δ^{λ}) and the π bond order of an atom. Hence the relationship of the change in a particular ^{13}C chemical shift between a

charged and a neutral organic molecule ($\Delta\delta^A$) and the change in carbon electron density (ρ^A) was developed by Karplus and Pople (228), equation 28. Data from a series of organic molecules including both cations and anions has provided values of α = 160 - 180 ppm/electron. For carbenium ions a value of α = 160 ppm/electron is generally accepted (229,230).

$$\delta^A = \delta_d{}^A + \delta_p{}^A + \Sigma_{B \neq A}[\delta^B + \delta_{ring}{}^A] \qquad (27)$$

$$\Delta\delta^A = \alpha(\rho^A - 1) \qquad (28)$$

An analysis of the $\Delta\delta$ values derived from the ^{13}C NMR spectroscopy data of 44 as compared to 45 shows that the largest change is about 21 ppm at C(3), Table 2-21. The $\Delta\delta$ for C(1) is much smaller (8.3 ppm) than this. Based on crystallographic and bond-valence analyses, which showed that more positive charge was found on C(1) than on C(3), the C(1) $\Delta\delta$ was expected to be much larger. However, previous NMR studies have generally found that the chemical shift of a carbon α to a heteroatom is a poor indicator of the charge distribution (229,231). In this respect, charge distribution to the α carbon is more accurately determined using x-ray crystallographic techniques as was shown in the previous section.

^{13}C chemical shift/charge density correlations were also examined in the iminium salts 30 and 31 and the analogous protonated aldehydes 38 and 39, as shown in Table 2-21. There are some substantial differences in the ^{13}C NMR spectra of these compounds as they are protonated. In all cases the odd numbered carbons are shifted to lower field compared to the

Table 2-21

Calculated Charge Density Based on ^{13}C NMR Chemical Shift[a] Data

	Compound				
Position	30	31	38	39	44
C1	0.06	0.00	0.03	-0.01	0.06
C2	-0.07	-0.07	-0.04	0.01	-0.05
C3	0.12	0.12	0.20	0.20	0.13
C4	0.00	-0.03	0.03	-0.03	-0.02
C5	0.11	0.08	0.21	0.18	0.02
C6	-	-0.01	-	0.02	0.01
C7	-	0.05	-	0.17	-
Total	+0.22	+0.14	+0.43	+0.54	+0.15

a charge density for each carbon = $\frac{\{\delta Ci(\text{iminium salt}) - \delta Ci(\text{imine})\}}{160}$

corresponding neutral imines 26 and 27 and aldehydes 36 and 37. However, the magnitudes of $\Delta\delta$ for the odd numbered carbons are much larger in the oxygen cations 38 and 39, consistent with an increased positive charge on these atoms.

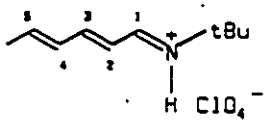

30

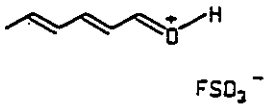

38

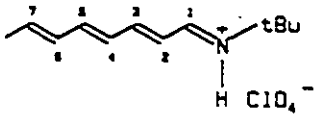

31

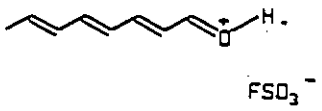

39

Chemical shift changes also occur in the even numbered carbons of these compounds. In the iminium salts, 30 and 31 these carbons undergo small shifts to higher field, compared to little change in the analogous carbons in the protonated aldehydes 38 and 39. Since these $\Delta\delta$ differences are significant for several carbons, a comparison of the extent of charge delocalization for these two types of cations should not be restricted to only the odd numbered carbons. In order to overcome this difficulty and assess the total positive charge on the carbon skeleton of these ions, the sum of the $\Delta\delta$ values for each cation was determined, Table 2-21. Two trends are clear from these values. First, the charge density totals for 38 and 39 are 2-4 times larger than those of 30 and 31 suggesting that a much larger amount of positive charge is delocalized in the protonated aldehydes than the iminium salts. The total charge on the carbons in the iminium salts 30 and 31 is only 0.14-

0.22 implying that the remainder of this charge (+0.78 to +0.86) must be on nitrogen or on the proton bonded to nitrogen. However, based on the findings for 44, the positive charge on C(1) may have been underestimated due to the heteroatom effect. If this is the case in 30 and 31, the total positive charge on the carbon skeleton of these molecules may be slightly higher.

A second important trend occurs in cations 38 and 39, which exhibit substantially different charge density sums. The addition of one double bond to the system (39 vs. 38) increases the $\Delta\delta$ on the carbon framework of the molecule by 25%. Thus in 39 the ability of the carbon framework to stabalize positive charge is enhanced. A similar effect has been previously reported for a series of conjugated cyclic ketones.

II. Cation Anion Interactions

To this point the structures of the cationic portion of iminium salts and protonated aldehydes have been discussed with little reference to the counteranion. As it has been shown that the anion can have immense effects on the absorption spectra of iminium salts and NMR chemical shifts, it is interesting to examine this question in more detail with the results available from this work.

i. Location of the Anion

In general, it has been found from x-ray crystallographic determinations of organic salts (227,232-234) that cations which have a

proton bonded to a heteroatom, either oxygen or nitrogen, always have an anion located nearby such that a linear hydrogen bond exists between cation and anion, 67. For example, this has been found to be the case in every reported crystal structure of a protonated ketone (235-237).

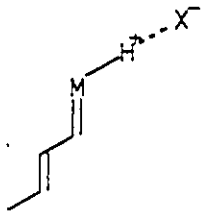

67

In crystal structures of ammonium salts an anion is always found hydrogen bonded to the acidic protons on nitrogen (232-234). The iminium salts 30-34 fall into this category and although crystal structures of these compounds could not be obtained, it is expected that in each case the anion will be located close to the proton on nitrogen. The iminium salts 27 and 41-44 lack a proton bonded to nitrogen and thus present intriguing cases as to where the anion is located. In one case 44, this was determined crystallographically.

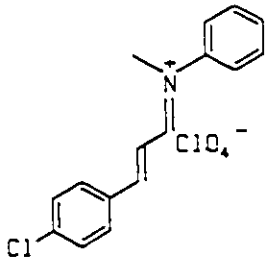

44

The shortest N-O contact in the crystal structure of 44, between

the nitrogen atom of the cation and an oxygen of the perchlorate counter-ion is 3.86 Å. This is well beyond the sum of the Van der Waals radii for these two atoms (2.90 Å). In the allylic chain, there are short C-O interactions at both C(1) and C(2), Table 2-17. The contact at C(1) is consistent with the expected apprpach of a negatively charged anion to a positively charged carbon. Analyses of the C(1)-N bond length and atomic valence of C(1) in the previous section showed that some positive charge is present at this position. A similar approach of the anion to C(1) has been previously found in crystal structure determinations of protonated benzophenones where a proximate anion is positioned at an angle of 70-100° from the carbonyl plane (237). This has been suggested to represent the lowest energy approach path for a nucleophilic attack of a protonated carbonyl. In the present case, the perchlorate anions in 44 can be considered to be formally acting as nucleophiles on C(1). In all of these cases, the C=O or C=N segment of the molecule is planar, which allows for an unhindered approach pathway of the anion from above or below this plane.

There is no interaction of an oxygen of the perchlorate anion with C(3) that is closer than 3.584(8) Å. If the positive charge in this molecule were delocalized, it would be expected that an approach of the anion at C(3) would occur much like that at C(1). The lack of this interaction reinforces the previous conclusions that very little charge is delocalized to C(3) in 44. It is also interesting that the lack of a perchlorate anion near nitrogen in 44 may indicate that a much lower positive charge resides there than was calculated by the bond-valence

approach.

ii. Effects on ^{13}C NMR and Absorption Spectra

The effects that an anion can have on the ^{13}C NMR and absorption spectra of an iminium salt were analysed by increasing the number of C=C bonds conjugated to the iminium function, and varying the anion and in both the solution and solid states.

In solution, the effect of chain length on the absorption maximum is clearly evident in the iminium salts 30-34, and 52, Table 2-13. Despite minor changes in the carbon skeleton a very good linear correlation was found as shown in Figure 2-12, in which the λ_{max} of the salts is plotted against the number of double bonds. An approximate relationship of $\lambda_{max} = 211 + 54n$ was determined where n is the number of C=C bonds. The 54 nm increment for each C=C bond was significantly lower than that found in cyanine dyes (107 nm) (238) and slightly lower than that found by Sorensen for polyenylic systems (65 nm) (239). It is however, higher than the 30 nm value in hydrocarbon polyenes (240).

Absorption spectra data for some of these iminium salts was also obtained in the solid state, Table 2-13. In most of these cases the λ_{max} was blue shifted from that measured in solution. The iminium salt 30, which had the shortest C=C chain, exhibited the greatest blue shift (2400 cm^{-1}), whereas 34, which was dialkylated at nitrogen had a much smaller blue shift (801 cm^{-1}).

The iminium salts 41-44 showed different trends in the solution and solid states. In solution the perchlorate salts 42 and 44 absorbed

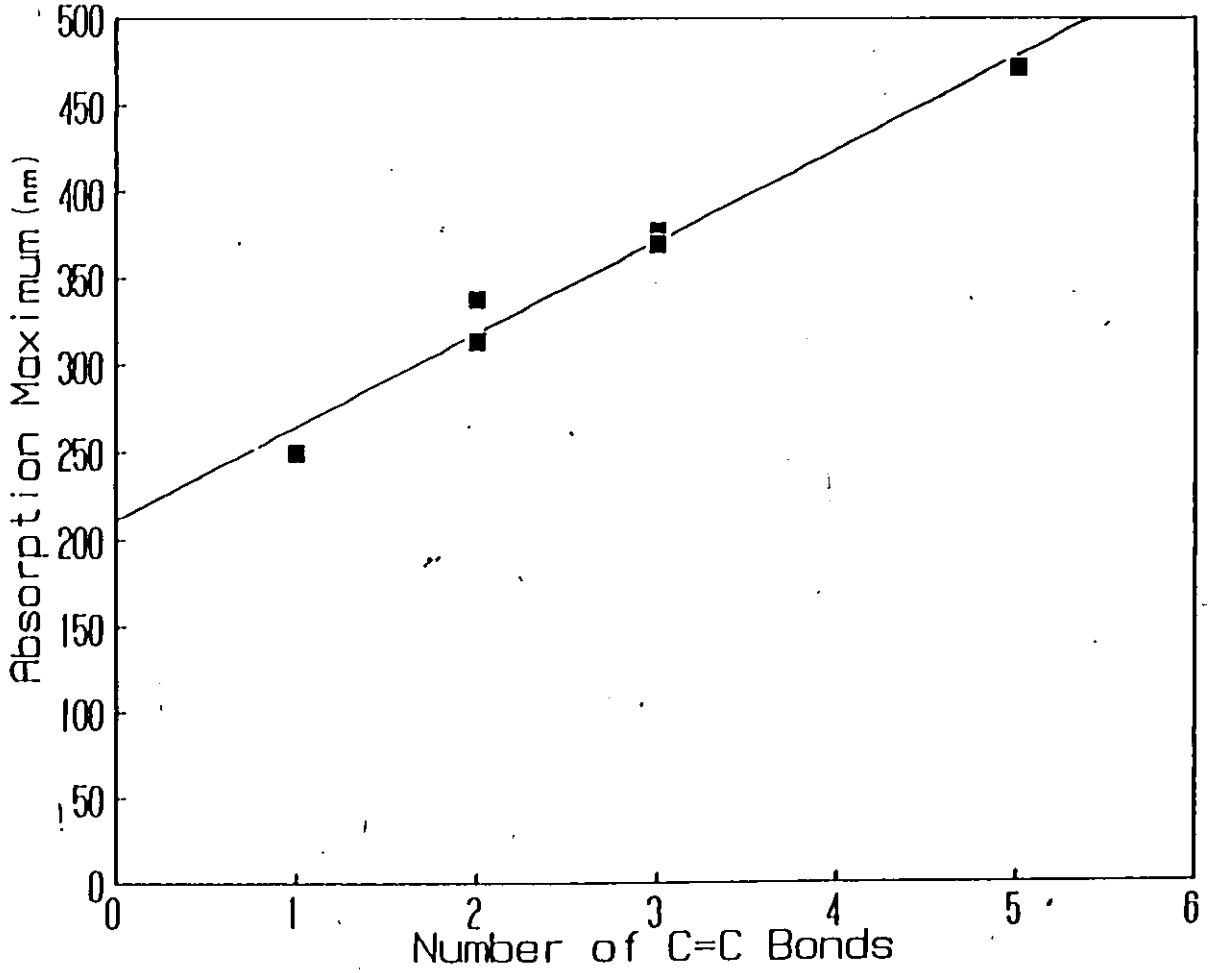

Figure 2-12: Plot of number of C=C bonds vs. the absoption maximum for several iminium salts having perchlorate anions.

at a longer wavelength than their corresponding trichloroacetate salts, 41 and 43. However in the solid state this ordering was reversed and the trichloroacetate salts absorbed at a substantially longer wavelength than in solution. These iminium salts were also studied by solid state ^{13}C NMR spectroscopy where any specific cation/anion pairing should ideally be detectable. It was apparent that there was a significant difference in the chemical shifts within the vinyl regions of the molecules with the trichloroacetate anions 41 and 43 compared to the perchlorate anions 42 and 44, Table 2-11.

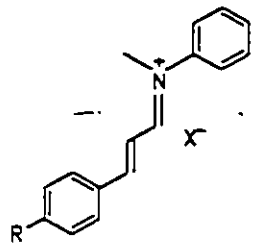

		Benzene	Solid
41	R=H, X=Cl_3COO	350	394
42	R=H, X=ClO_4	352	348
43	R=Cl, X=Cl_3COO	356	382
44	R=Cl, X=ClO_4	362	370

The changes in absorption maxima between solution and solid phases can best be rationalized by the changes in the cation/anion interaction in each state. It is important to note that two different relationships exist for the iminium salts described above. The first of these involves a cation which is hydrogen bonded to the anion. This occurs for the salts 30 and 31 which have a perchlorate anion. The second possible association is one where the iminium nitrogen is dis-

ubstituted. This occurs in the iminium ions 34 and 41-44. For this type of interaction a hydrogen bond between the nitrogen and the anion does not exist, and the anion must interact with some other portion of the cation.

In solution, the minimum distance between cation and anion is attained when the two exist as a contact ion pair. This distance is close to the sum of the Van der Waal's radii for each ion and has been previously studied (241-246) in carbanions having an alkali cation, 68. In 68, the distance between cation and anion can be increased by increasing the polarity of the solvent or decreasing the temperature (241-243). This results in solvent-separated ion pairs. The absorption spectra of these two types of ion pairs are quite different. The contact ion pair spectrum is blue shifted from that of the solvent-separated ion pair by as much as 2100 cm^{-1}. Furthermore, an excellent correlation exists between the anion distance and the absorption maximum for a series of cations (241). It has been suggested that a closer interaction of the ion pair stabalizes the complex, resulting in a decreased ground state energy and thus a blue shift in the absorption spectrum. This applies when changing from a solvent-separated ion pair to a contact ion pair or on moving from a large cation to a smaller one. This theory has been corroborated by ^{13}C NMR spectroscopy which showed that π electron density was most strongly polarized towards C(α) in a contact ion pair or with a small cation and resulted in an upfield shift of this carbon resonance.

In iminium salts possessing a protonated nitrogen (as opposed to a dialkyl substituted nitrogen), similar trends to those above have been

noted by Blatz (32) and by Vocelle (132). A blue shift in the absorption spectrum is found in non-protic solvents as the polarity decreases and a good linear relationship was found between the anion radius, and thus the cation/anion distance, and the absorption maximum.

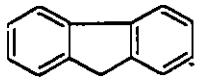

X^-

X=Na, K, Rb, Cs

68

The blue shifts in the absorption maxima of iminium salts 30 and 31 in the solid state as compared to the solution state are excellent examples of the trends discussed above. In methylene chloride, which has a dielectric constant of 9.08, the perchlorate anion is partially solvated and thus can not attain a minimum distance from the cation. However, in the solid state the cation/anion interaction is maximized since no solvent is present and a minimum distance in the ion pair results. Corroborating this result is the previously calculated perchlorate-nitrogen distance in solution (3.5-4-0 A based on absorption maxima (32,143)) compared to the crystallographic distance (2.93 A) (247,248).

In the cases where the iminium salts are disubstituted on nitrogen a slightly different situation holds since the major anionic interaction does not occur with nitrogen. The iminium salt 44 has an important cation/anion interactions at C(1) as found crystallographi-

cally, Table 2-17. Curiously, the absorption spectrum of 44 in the solid state is approximately the same as that in benzene, as shown in Table 2-14, suggesting that the cation/anion interactions in 44 are very similar in both phases. A similar result is found for the iminium salt 42. Ideally a shorter absorption maximum in the solid state compared to that in solution should have resulted as was the case in the iminium salts 30 and 31. This may be the result of the much lower polarity of benzene (ε=2.28) which would favour a tighter ion pair for 42 and 44 compared to the more polar methylene chloride (ε=9.08) in which 30 and 31 were studied. Thus the change in the absorption maximum on going to the solid state in 42 and 44 is much smaller. A second factor is that a smaller blue shift between solution and solid states results when a hydrogen bond, as in 30 and 31, is not involved. This is shown ideally for the dimethyl substituted iminium salt 34, where the solid state spectrum is only slightly blue shifted from that in solution, Table 2-13. The magnitude of this shift (801 cm^{-1}) is only 30% of that observed for 30 (2400 cm^{-1}).

The iminium salts 41 and 43, which each have a trichloroacetate anion, absorbed at slightly lower wavelengths than their corresponding perchlorate salts in solution. Assuming the trichloroacetate anion occupies the same region of space as did the perchlorate anion in 44, this could result from the decreased size of the carboxylate group as compared to perchlorate.

In the solid state, iminium salts 41 and 43 were significantly red shifted, approximately 44 and 26 nm respectively from their solution

spectra. These shifts can not be rationalized based on a simple anion distance model, since the closer approach by the trichloroacetate anion to the C=N bond should result in a blue shift, as has been previously demonstrated (32,143).

Examination of solid state ^{13}C NMR data of 41 and 43 shows that the positions of most of the resonances are similar to those in the perchlorate salts 42 and 44, Table 2-11. However, in both cases C(1) is shifted significantly downfield in the perchlorate salts, compared to their respective trichloroacetate salts. Again, this is not consistent with a closer approach of the trichloroacetate anion in the solid. In the fluorenyl anions previously discussed 68, a closer contact between C(α) and the cation caused an increase of π electron density on C(α) and thus an upfield ^{13}C shift (243). In the present case a closer contact between the trichloroacetate anion and C(1) in 41 and 43 should remove π electron density from C(1) and shift its ^{13}C resonance to lower field, compared to C(1) of the perchlorate salts, 42 and 44. Calculations by Nakanishi and co-workers have corroborated this idea (133).

The solid state ^{13}C NMR spectrum of 43, Figure 2-13, again shows that this iminium salt is not a simple case of a cation/anion interaction. Two resonances for $CI_3\underline{C}OO^-$ are located near 167 ppm inferring that two acetate molecules existed per cation. Elemental analysis data, Table 4-1, verified this finding. It is clear that the interaction of the second acetate molecule is causing the red shift in the solid state. One explanation to account for this would be a complex between the trichloroacetate anion and the acid, 69. This homoconjugate ion can

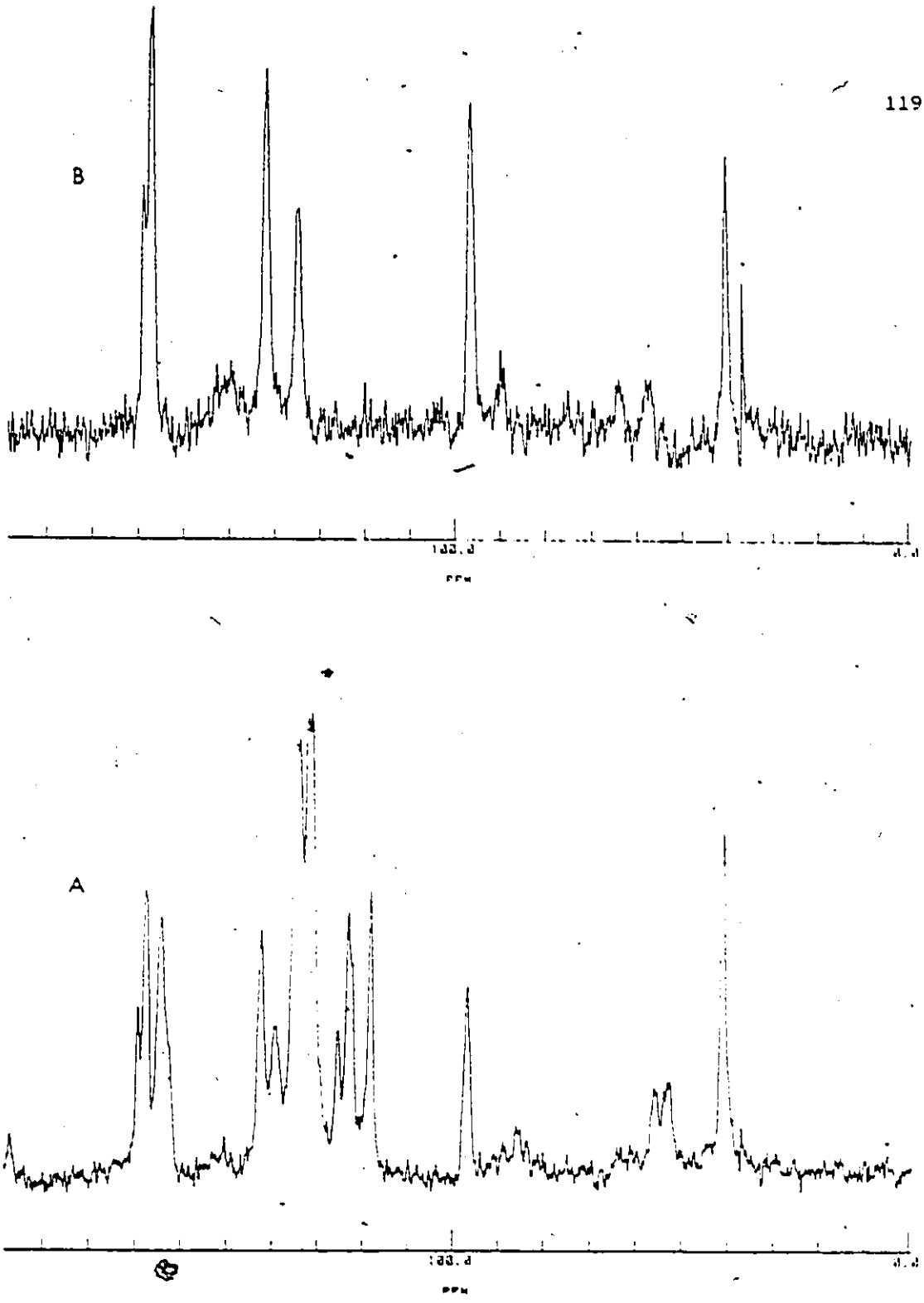

Figure 2-13: CPMAS ^{13}C NMR spectrum of N-phenyl-N-methyl-3-(p-chlorophenyl)-2-propenylidene iminium trichloracetate, 43 (A) and suppressed (B).

be envisioned as being a much larger anion than the perchorate in 44 and thus causes a red shift.

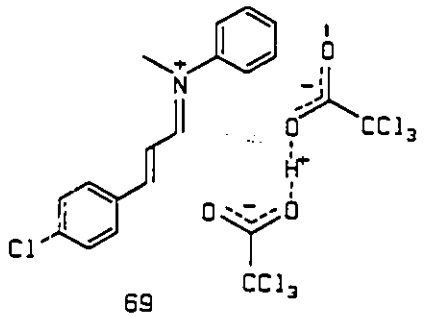

69

The fact that in solution a bathochromic shift was not observed for 41 and 43 compared to 42 and 44 may be a result of the second molecule of acid being dispersed in the methylene chloride and having a small association with the anion. During the crystallization process, cations which become associated with homoconjugate pairs tended to precipitate from solution more readily. This type of homoconjugate acid pairing has previously been suggested to occur in N,N dialkylated retinylidene iminium salts giving rise to a red shift at higher trichloroacetic acid concentrations (31). In order to determine if homoconjugate pairing is occurring in 41 and 43, these salts should have their UV spectra measured in the presence of excess trichloroacetic acid. This would favor the formation of the homoconjugate pairs and should produce a substantial red shift in the spectrum.

III. Summary

This structural investigation of simple conjugated iminium salts revealed several important aspects of charge delocalization and cation-/anion interactions. In terms of charge delocalization, both x-ray crystallography and bond-valence approaches show that most of the positive charge in iminium salts is located at the nitrogen. However, a significant portion of the charge delocalizes to C(1). In contrast, positive charge delocalization in oxolenium cations is much more extensive and a substantial amount of charge delocalizes to the conjugated system of these cations.

Cation/anion interactions in iminium salts were studied directly using x-ray crystallography and a unique combination of absorption spectroscopy and ^{13}C NMR spectroscopy in both solid and solution states. In iminium salts, generally a blue shift is noted in the absorption spectra on moving from the solution to the solid phase. This is simply a result of a tighter cation/anion pairing in the solid state. The anomoly to this trend are iminium salts which are dialkylated on nitrogen and contain a trichloroacetate anion. It was found that these ions showed a significant red shift in the solid state as compared to in solution. Solid state ^{13}C NMR provided evidence that this is a result of a homoconjugate anion pair forming during crystallization.

B. Retinylidene Iminium Salts

I. Charge Delocalization

Charge delocalization in retinylidene iminium salts has been examined previously by a variety of methods. In solution, ^{1}H and ^{13} NMR spectroscopic methods and absorption spectroscopy have been used extensively to monitor electronic changes in retinylidene salts. Similar studies in the solid state are only now beginning to surface and are important because they exclude solvent from the structure and allow a closer cation/anion interaction to occur as is the case in the binding site of either bacteriorhodopsin or the visual pigment.

i. Absorption Spectroscopy

Most of the retinylidene iminium salts studied 48-53, contained both an alkyl group and a proton on nitrogen. The various anions employed in these salts were each assumed to lie in a linear arrangement with N-H, as has been found for protonated ketones (235-237). If all the anions used are considered as spheres and the anion sizes are estimated from the crystallographic radii, then plotting the reciprocal of anion size versus the absorption maximum yields a linear relationship, Figure 2-14. A similar correlation had been previously noted by Blatz et al. (32) in which only monoatomic halogen anions were employed. A correlation between acid strength and the absorption maximum of the retinylidene iminium salts 49-52 in solution was also attempted but did not result in any noticeable trend. This has been noted previously in a similar study using strong acids (32.132).

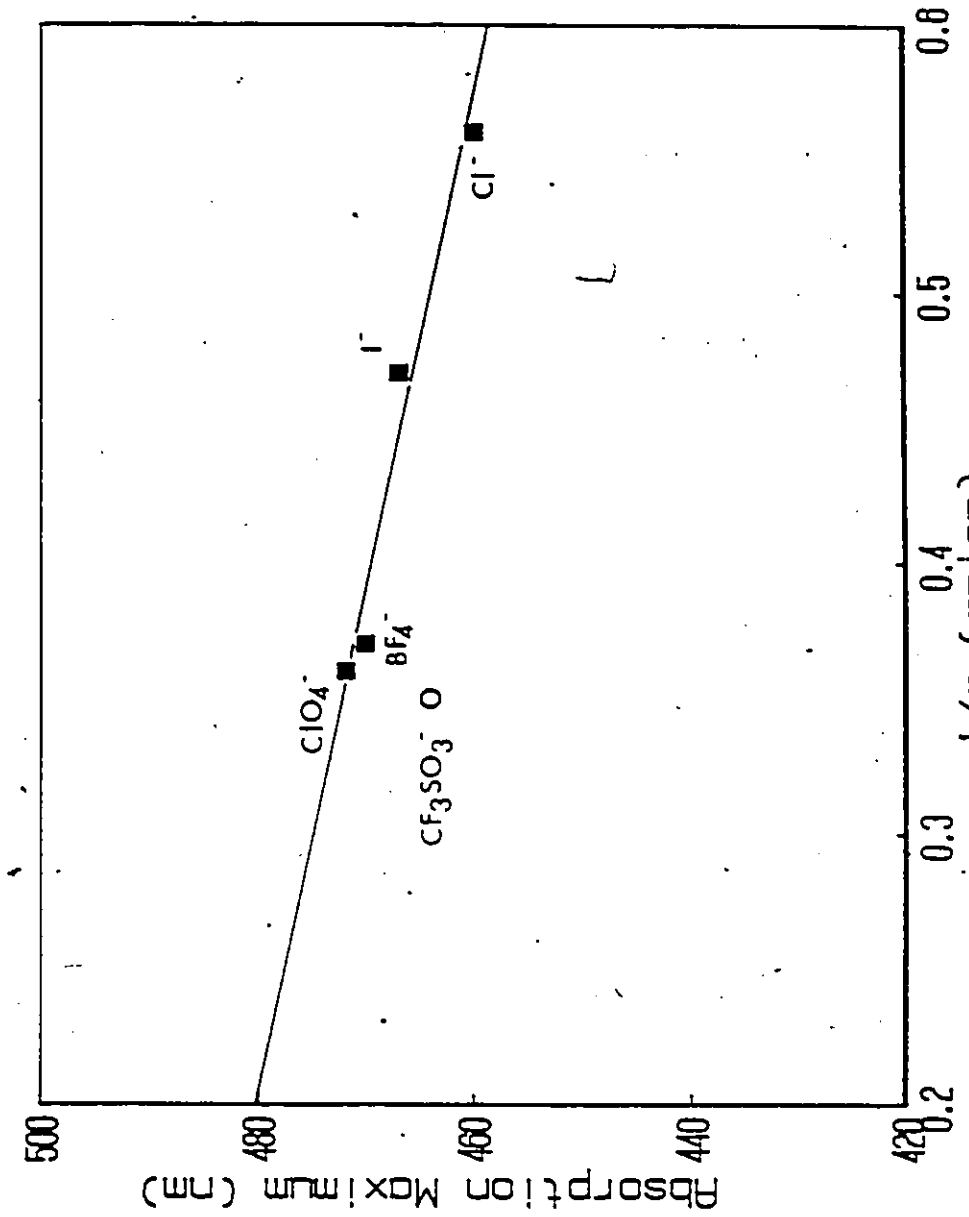

Figure 2-14: Plot of the reciprocal of the anion radius (1/r) vs. the absorption maximum for the retinylidene iminium salts, 50-53 and 70.

In solution the retinylidene iminium salt 52 had the longest wavelength absorption (472 nm) of any of the protonated species, Table 2-13. This would correspond to the lowest ground state energy species of the retinylidene series 49-53, and would suggest that 52 has the most positive charge delocalized through the polyene chain, based on earlier studies by Blatz (32).

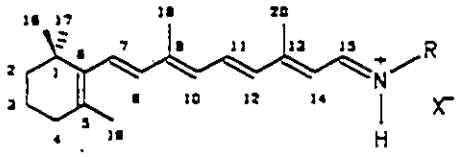

48 R=nBu, $X=Cl_3CCOO^-$
49 R=nBu, $X=ClO_4$
50 R=tBu, X=I
51 R=tBu, $X=BF_4$
52 R=tBu, $X=ClO_4$
53 R=tBu, $X=CF_3SO_3$

ii. Charge Density - NMR Spectroscopy Correlations

In the retinylidene iminium salts 50-53 the chemical shifts of the odd numbered carbons, C(15), C(13), C(11), C(9) and C(7) move to lower field as the anion radius increases, Figure 2-15. The greatest change in chemical shift occurs at C(13), where a 4 ppm difference was noted over this range of anion sizes. The changes observed with the other carbons are much smaller. These changes are consistent with an increase in positive charge, particularly at C(13), in the polyene chain as the cation/anion distance increases. There is only a small change in the chemical shift of C(15) with increasing anion size. However, in view of the insensitivity of the shifts of this carbon noted in the previous

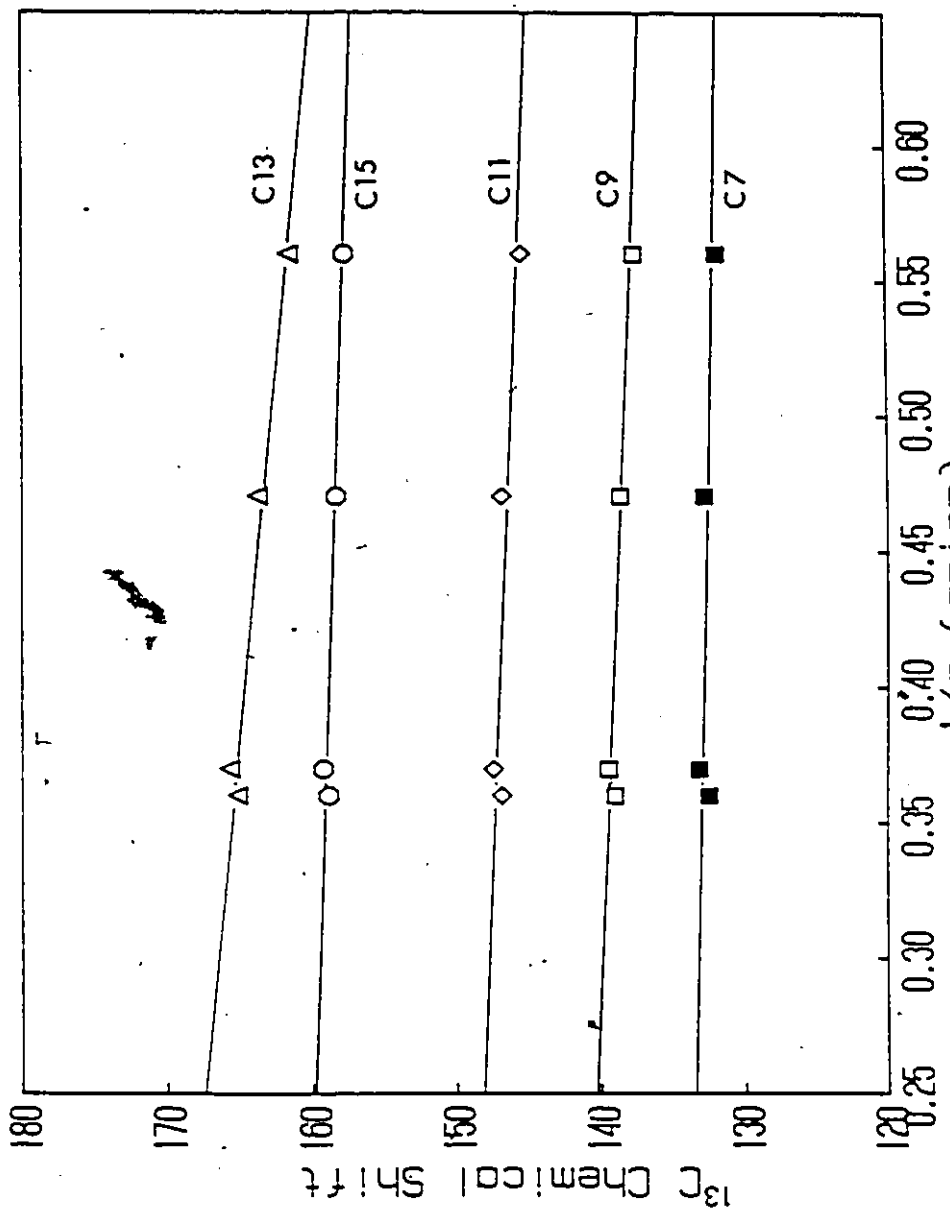

Figure 2-15: Plot of the reciprocal of the anion radius (1/r) vs. the ^{13}C chemical shift for the retinylidene iminium salts, 50-52 and 70.

section (229,231) and independently by others (249), this should not be taken to indicate that only a small increase in positive charge is occurring here as the anion size increases.

The corresponding changes in π electron density of each carbon can be obtained from the change in chemical shift of a specific carbon upon protonation, Table 2-22. In the case of the salt with the smallest anion, chloride 70, studied by Shriver et al. (52), a charge of +0.11 on C(13) is estimated. For the largest anion, perchlorate, a charge of +0.14 is found on C(13), a 25% increase. The amount of positive charge on C(11), C(9) and C(7) decreases in that order. The average charges for C(11), C(9) and C(7) are +0.07, +0.06 and +0.03 respectively.

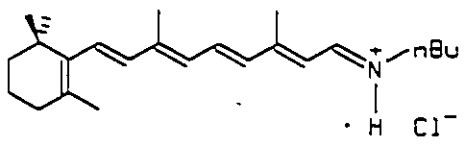

70

This charge density correlation shows quantitatively that increasing the nitrogen/anion distance has the largest influence on C(13) in retinylidene iminium salts. This represents the expected agreement with the trend based solely on the chemical shift/anion relationship, Figure 2-15, and corresponds to the major resonance contributor, 71. Similarily, a much smaller portion of the positive charge is delocalized to the more remote carbons C(9) and C(7). These changes in charge density are also consistent with the slopes for the various carbons in

Table 2-22

Calculated Charge Density Based on ^{13}C NMR Chemical Shift[a] Data

	Compound				
Position	50	51	52	53	70[b]
C7	0.03	0.04	0.03	0.03	0.02
C8	0.00	0.00	0.00	0.00	-0.01
C9	0.06	0.06	0.06	0.06	0.04
C10	-0.01	0.00	-0.01	-0.01	-0.01
C11	0.07	0.07	0.07	0.07	0.06
C12	-0.02	-0.02	-0.02	-0.02	-0.02
C13	0.13	0.14	0.14	0.13	0.11
C14	-0.07	0.04	-0.07	-0.06	-0.06
C15	0.03	0.04	0.03	0.03	0.03
Total	+0.22	+0.27	+0.23	+0.23	+0.16

a charge density for each carbon = $\frac{\{\delta Ci(\text{iminium salt}) - \delta Ci(47)\}}{160}$

b calculated and normalized from reference 43.

Figure 2-15. The steepest slope is for C(13), which undergoes the largest increase in positive charge as the anion size increases and the shallowest slope is that of C(7), which is relatively unaffected.

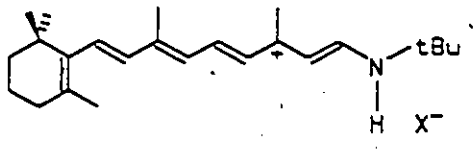

71

The total charges in the retinylidene salts 50-52, Table 2-22, are very close to those found for the simple conjugated iminium salts 30 and 31, Table 2-21, suggesting that an increase in polyene chain length does not result in increased charge delocalization. This provides strong evidence that the bulk of the charge in retinylidene iminium salts, about +0.75 units, must reside on the nitrogen or its proton. This is in good agreement with ^{15}N NMR spectroscopy studies by Mateescu and co-workers (200), which suggested that increasing chain length affected the chemical shift of the nitrogen by relatively small amounts, thus reflecting very little difference in the charge density on this atom.

II. The Structure of the Retinal Chromophore

This section on the overall structure of retinylidene iminium salts is subdivided into two sections - cation/anion interactions, and conformation. Variations of these two factors have been shown to influence both the absorption and NMR spectra of several retinylidene

iminium salts, and presumable will have the same effects in the natural pigments, rhodopsin and bacteriorhodopsin.

i. Cation/Anion Interactions

The differences in the absorption spectra of the retinylidene iminium salts in the solution and the solid state were similar to those found in the simple iminium salts. That is, a blue shift in the absorption maximum of most of the iminium salts 48-54 is noted on going from the solution to the solid state, Table 2-13. This would seem to result from a tighter cation/anion pair in the solid state than in methylene chloride.

The transition from solution to the solid state can have several effects on the relationship between the cation and anion in iminium salts, in addition to the cation/anion distance which has been previously discussed. When different anions are involved, such as those in the retinylidene iminium salts 50-53, the nature of the anion should be very important. The "hardness" of the anion should affect the degree of the cation/anion interaction in the solid state more than in solution because the cation and anion will not be solvated. A "soft" anion should show relatively little change in its association with the cation in solution and the solid state, whereas a "hard" anion will tend to pair very tightly with a "hard" cation such as a retinylidene ion (250).

The trend in the magnitude of the blue shift in the retinylidene iminium salts 50-53 conforms quite well to the "hard acid/hard base" principle upon moving from the solution to the solid state. The smallest

blue shift was found for the iodide salt 50 (200 cm^{-1}) which falls into the "soft" anion category. The largest blue shifts were found for the BF_4^- (1350 cm^{-1}) and triflate salts (770 cm^{-1}). Both of these anions are classified as "hard" anions and thus bind strongly in the solid state.

The magnitude of the largest blue shift in the retinylidene series, 1350 cm^{-1} in 51, is much smaller than that in the iminium salts 30 (2400 cm^{-1}) and 31 (2040 cm^{-1}). The sequential decrease in the magnitudes of these blue shifts in these iminium salts would seem to arise from a dependency of the shift on the chain length. However, more extensive studies are required to corroborate and provide an explanation for this trend.

The retinylidene iminium salt 54, in which there will be no N-H bonding, showed a red shifted spectrum in solution from that in the solid state. However, an assessment of the magnitude of this change is difficult since 54 exhibits a dependence of the absorption maximum with concentration. In dilute solution ($6x10^{-6}$ M), the λ_{max} is 506 nm whereas at more concentrated levels ($7x10^{-5}$) the absorption maximum is blue shifted to about 488 nm. Irving and Leermakers (31) have previously shown that a similar retinylidene ion, 72, exhibits this same broad range of absorption maxima, depending on the concentration of the salt in solution. This was rationalized in terms of the perchlorate anion being greatly dispersed in dilute solution, having a large cation/anion distance and therefore a long wavelength absorption. As the concentration increases, the perchlorate anion becomes more closely associated with the iminium ion and thus stabilizes the ground state energy of the

molecule, shifting the absorption maximum hypsochromically.

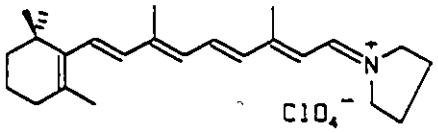

72

One further type of cation/anion relationship that was considered was that involving a second interaction much like that in Nakanishi's "point charge" model (133). In the iminium salt 53, the electron rich trifluoromethyl group of the triflate anion can act as the second negative source by interacting with the polyene chain of the cation.

With the exception of C(14)H, the ^1H NMR spectrum of 53 is very similar to that of other retinylidene iminium salts which lacked this extra perturbation, Table 2-5. This proton is deshielded by 0.53 ppm, compared to the imine 47, the largest of any of the protons on the polyene chain. Vocelle and co-workers (195-197) have studied these types of interactions extensively and have interpreted a large deshielding value such as that for C(14)H to be a result of the interaction of this proton with a second "charged" group in an anion. Using molecular modelling, the CF_3 group of the triflate anion was found to be positioned near C(14)H and towards C(13), 73. In is important to note that the interaction here is with the proton on C(14) and not the carbon itself, unlike Nakanishi's point charge model. Thus a blue shift should result in 53 compared to a chromophore with a similar anion without this second perturbation.

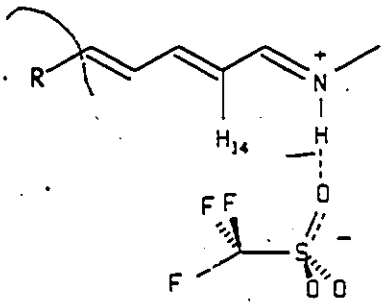

73

Examination of Figure 2-14 shows that the absorption maximum for 53 lies below (blue shifted) the linear correlation between anion size and absorption maximum, in excellent agreement with the predicted shift from the "point charge" model.

ii. Conformation of the Chromophore

The retinylidene iminium salts 49 and 52 showed a markedly different shift in their absorption maxima than the other retinylidene iminium salts studied on going from the solution to the solid state, Figure 2-16. The absorption spectra of 49 and 52 showed maxima which were red shifted 34 nm and 32 nm respectively in the solid state, Table 2-13. These red shifts are not characteristic of a simple cation/anion interaction and have been interpreted to result from a conformational change about the C(6),C(7) bond of the retinylidene chromophore in the solid state, from that in solution.

The ground state energy difference between a twisted 6-s-cis and a planar 6-s-trans retinylidene ion conformer, 74, is small (251). In retinal itself, the 6-s-cis conformer is favoured, but only by about 2.5

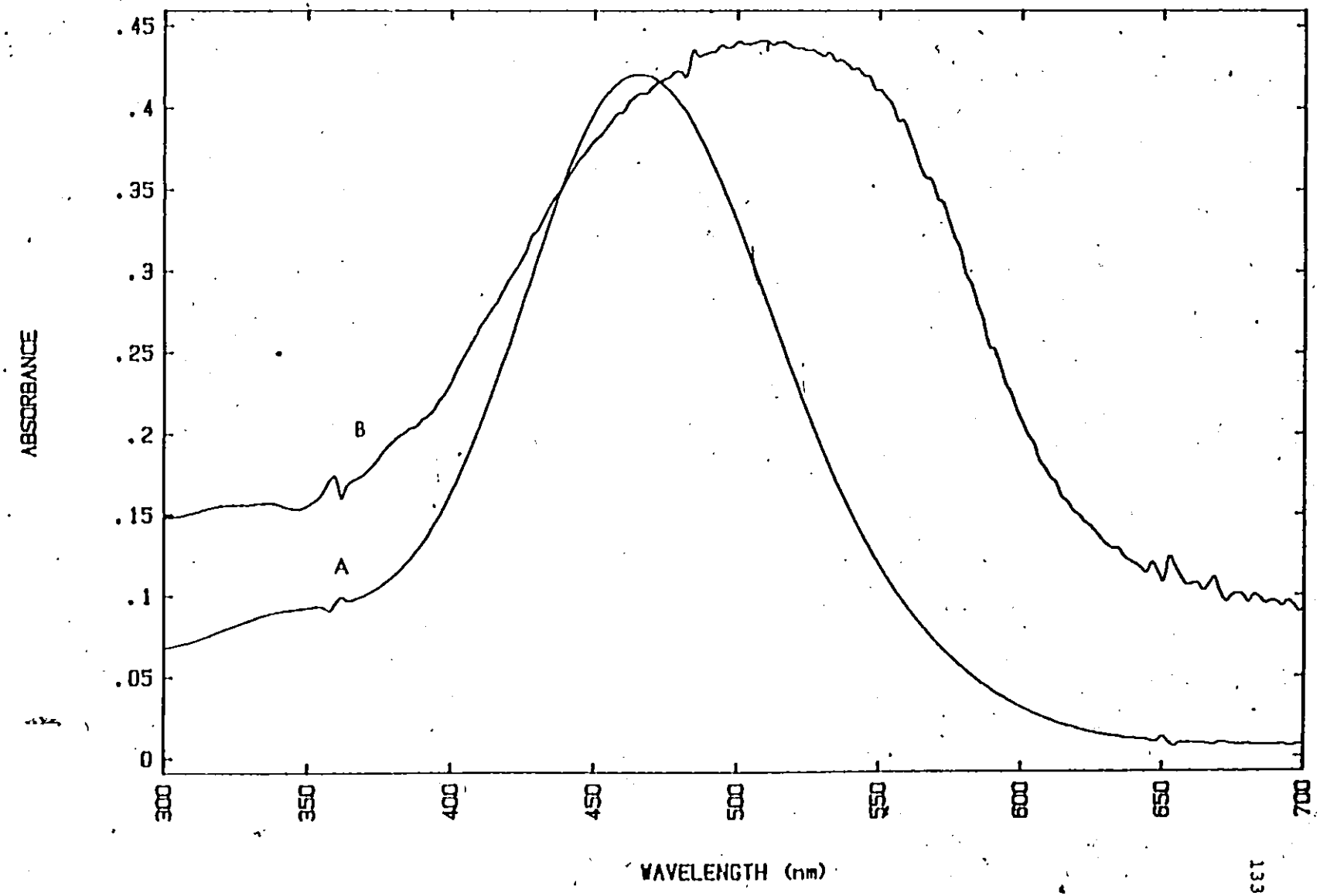

Figure 2-16: Absortion spectra of N-t-butyl-retinylidene iminium perchlorate, 52, in solution (A) and the solid state (B).

kcal/mol. Indeed, most crystal structures of retinal derivatives (252-255) and their related compounds show that the C(6),C(7) bond is in the twisted s-cis conformation and that the dihedral angle ranges from 40° to 62°. However, there are a small number of structures which have been found to exist in the planar 6-s-trans conformation (254,256,257). The conformation about the C(6),C(7) bond in bacteriorhodopsin has recently been found to be 6-s-trans using solid state ^{13}C NMR spectroscopy techniques (128).

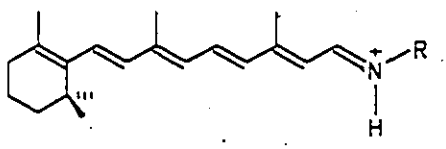

74

It was suggested some years ago (143) that twisting about the C(6),C(7) bond in retinylidene iminium salts could alter the absorption maximium by up to about 50 nm. The longest wavelength absorption that was expected was about 500 nm for the planar 6-s-trans all-trans isomer conformer, while shorter absorption maxima were predicted for various twisted 6-s-cis forms. The absorption maximum for a 6-s-cis all-trans retinylidene iminium salt with a dihedral angle of 60° about the C(6),C(7) bond is expected to be about 460 nm.

In solution the absorption maximum for 52 is 472 nm. The conformation of this retinylidene iminium salt about the C(6),C(7) bond was probed in solution by a nuclear overhauser experiment at -60°C in

which the C(18) methyl group was irradiated. A 15% observed enhancement was noted for C(8)H, suggesting that the major conformer in solution is 6-s-cis.

The absorption maximum for 52 (504 nm) in the solid state is very close to the predicted absorption maximum of 500 nm for the 6-s-trans conformer (143) and hints that this chromophore may exist in a planar 6-s-trans conformation in this phase. It is important to note that in this spectrum a small blue shift will occur due to a tighter cation/anion interaction in the solid state as compared to solution. However, the red shift which accompanies the proposed 6-s-cis to 6-s-trans conformation change on going from the solution to the solid state must predominate.

In 52, the magnitude of the blue shift due to the tighter cation-/anion interaction in the solid state was approximated from the absorption spectra of 51, which underwent a "normal" shift to shorter wavelength on moving from the solution to the solid state (28 nm). The contribution from the conformational change in 52 from twisted 6-s-cis to 6-s-trans was estimated as being the equivalent of adding one double bond to the twisted 6-s-cis conformer. From Figure 2-12, this was found to be about 54 nm. Thus the expected red shift for the conformational change of 52 from 6-s-cis in solution to 6-s-trans in the solid is the difference between these two values, about 26 nm. This would suggest that the absorption maximum of 6-s-trans 52 in the solid state should be at 498 nm. This is in excellent agreement with the observed value of 504 nm for 52 in the solid state. On the basis of this, it is also expected that the conformation of the n-butyl retinylidene iminium salt 49, is 6-

s-trans in the solid state since it shows a similar trend in its absorption maxima as 52. In both of these cases, the observed solid state absorption maxima are in close agreement with that calculated by Honig for a 6-s-trans retinylidene chromophore (143).

Further evidence for the presence of the 6-s-trans conformer in the solid state and the 6-s-cis conformer in solution comes from a detailed ^{13}C NMR spectroscopic study by Harbison (48) which indicated that the C(5) chemical shift varies with the conformation of the C(6),C(7) bond. In the 6-s-trans conformer this resonance is located near 136 ppm and in the 6-s-cis conformer a chemical shift of about 128 ppm has been noted, Table 2-23.

In solution, the C(5) chemical shifts of the retinylidene iminium salts 48-54 are close to the middle of the values noted by Harbison and suggest that both conformations exist in a dynamic equilibrium with approximately equal amounts of each being present. Harbison conservatively estimated that about 75% of the retinylidene ion composition in solution was 6-s-cis, and 25% was 6-s-trans. In this work, an attempt was made here to freeze out only the more stable 6-s-cis conformer of 52 at -60^{o}C, and monitor the 6-s-cis composition by the chemical shift of C(5). However, no carbon chemical shift changed by more than 0.52 ppm and the shift of C(5) did not approach that the 6-s-cis conformer at 128 ppm. This was expected, since the barrier for the interconversion of the 6-s-trans to 6-s-cis conformers was expected to be only about 8 kcal (251).

The solid state ^{13}C spectrum of 52 shows notable differences from its solution spectrum at C(2), C(5), C(6), C(13) and C(15). As is the

case with the other iminium salts studied by solid state ^{13}C NMR spectroscopy, the changes at C(13) and C(15) are probably a result of enhanced cation/anion interactions in the solid state. However, much larger changes are evident at C(2) and C(5), which both shift over 4.5 ppm downfield in the solid state. Both of these changes are consistent with the conformation of 52 being 6-s-trans in the solid state 75, Tables 2-23 and 2-24. The shift of C(5) is nearly identical with that determined by Harbison for the 6-s-trans conformation of several retinal compounds.

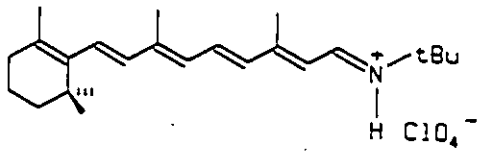

75

The chemical shift change of C(2) in the solid state from that in solution can also denote a 6-s-cis to 6-s-trans conformational change, although it does not seem to be as good of a marker as the C(5) resonance. In this study, the chemical shift of C(2) in the solid state is at significantly lower field than in solution, Table 2-24. This is in consensus with the ^{13}C NMR studies by Harbison, where the chemical shift of C(2) was always further downfield in the 6-s-trans conformer, although it fell within no defined range.

The iminium salt 51 has a similar ^{13}C spectrum in the solid state and in solution, again with the notable exception of the resonances for C(5) and C(13). The lower field resonance for C(13) is most likely a result of the closer anion/cation packing in solid state versus the

Table 2-23

^{13}C Chemical Shifts for C-5 Position of Retinal Derivatives

	6-s-cis	6-s-trans
All-trans retinal[a]	128.5	-
13-cis retinal[a]	126.7	136.8
All-trans retinoic acid[a]	127.8	135.9
51	128.99	-
52	-	136.8

a reference 48.

Table 2-24

^{13}C Chemical Shifts for C-2 Position of Retinal Derivatives

	6-s-cis	6-s-trans
13-cis retinal[a]	39.5	43.5
All-trans retinoic acid[a]	40.5	41.4
51	38.77	-
52	-	45.15

a reference 48.

solution. This is not expected to affect a remote carbon such as C(5) which has moved about 3.6 ppm upfield in the solid from its location in solution. In the solid state, this resonance has the expected chemical shift of the 6-s-cis conformation, Table 2-23, which is also present in solution. These conclusions are consistent with the absorption spectra of 51 in the solution and solid state which showed only a blue shift. A further note on the conformations of retinylidene iminium salts 51 and 52 in the solid state concerns the methyl resonances C(16) and C(17). In a planar 6-s-trans conformation these two carbons should be magnetically equivalent since a mirror plane would pass through the entire molecule down the length of the polyene chain. Only one resonance for both carbons should be present in the ^{13}C NMR spectrum. In the 6-s-cis conformation, these two carbons should be magnetically inequivalent since the C(6),C(7) bond is twisted by some 60°. This would place one methyl group above the polyene chain of the chromophore, while the second methyl group would be roughly in this plane, as has been found in the crystal structure of all-trans retinal. Equilibration between these two groups would not be expected in the solid state since this would require the C(18) methyl group to pass through the same plane as the polyene chain in the planar 6-s-cis conformer, and undergo a severe interaction with C(8)H. The planar 6-s-cis conformer has been found to be the highest energy conformer and the calculated energy barrier for this process is about 10 kcal/mol (251). Therefore, two resonances should result for C(16) and C(17) from the chromophore being in the twisted 6-s-cis conformation.

The retinylidene iminium salts 51 and 52 show exactly the predicted pattern above, Table 2-12. In 51, there are two resonances at 28.77 and 29.51 ppm for C(16) and C(17), while in 52 there is only one resonance for these carbons at 29.90 ppm. This confirms that these two retinylidene iminium salts exist in different conformations about the C(6),C(7) bond in the solid state. As suggested from the C(5) and C(2) chemical shift data, 51 is in the 6-s-cis form and 52 is in the 6-s-trans form, 75.

The retinylidene iminium salt 54 can not be classified conclusively as 6-s-cis or 6-s-trans in the solid state. The solid state ^{13}C NMR spectrum of 54 clearly shows that two conformational isomers are present. The number of resonances in this spectrum made it difficult to unequivocally analyze but it is clear that several of the resonances corresponded to the 6-s-cis conformer, while others were similar to that of the 6-s-trans iminium salt. The variation of absorption maximum of 54 with concentration eliminates this method as a probe for the 6-s-trans conformer in the solid state since a base solution absorption maximum could not be obtained. However, it is intriguing that the solid absorption spectrum of 54 possesses an asymmetrical shape with a tail in the curve at higher wavelengths. This is consistent with the presence of two conformational isomers as observed in the solid state ^{13}C spectrum.

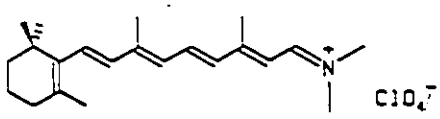

54

III. Summary

Charge delocalization in retinylidene iminium salts was assessed using ^{13}C NMR spectroscopy. It was found that most of the positive charge in these ions is located on the nitrogen or its proton and that about 10% of the charge resides on C(13). The total amount of positive charge which is delocalized in the conjugated system of these salts was similar to that found for the simple iminium salts discussed earlier.

The structure of retinylidene iminium salts was also studied by ^{13}C NMR and absorption spectroscopy in solution and in the solid state. Similar to the simple conjugated iminium salts, a blue shift was generally observed on moving from the solution to the solid phase. In two cases, the N-n-butyl and N-t-butyl retinylidene iminium perchlorate salts, 49 and 52 respectively, a red shift occurred in the absorption spectrum during this same phase change. This was probed by solid state ^{13}C NMR and concluded to be a result of a conformational change. In solution these ions exist in the 6-s-cis conformation, while in the solid state a 6-s-trans conformation predominates, similar to that in bacteriorhodopsin. This discovery of the 6-s-trans conformer in a natural pigment model system marks the first of its kind, and reaffirms the iminium salts 49 and 52 as prime candidates for further model system studies of bacteriorhodopsin.

Chapter 3

Photochemical and Thermal Studies of Conjugated Iminium Salts

The purpose of the experiments presented in this section is to determine the various photochemical and thermal isomerization pathways that conjugated iminium salts follow. These have previously been studied for several α,β unsaturated iminium ions in strongly acidic and neutral media using high field ^1H NMR techniques (186,188). The photochemistry of retinylidene iminium ions has also been studied earlier (173-175). However, in previous experiments the photoisomers were detected indirectly as their corresponding aldehydes using either HPLC or absorption spectroscopy. In this work, the direct observation, characterization and quantitation of the photoproducts from retinylidene iminium salt isomerizations is investigated using high field ^1H NMR spectroscopy. This technique also allows the thermal stabilities of the various retinylidene isomers to be determined.

Extensive photochemical studies of rhodopsin and bacteriorhodopsin have been previously reported. However, no conclusive evidence has been offered for the large differences in quantum yields between these two pigments and their model retinylidene iminium ions. One of the goals of this work is to examine the photochemistry of several retinylidene and other iminium salts, determining the quantum yields and/or regioselectivity in each case. The results obtained can then be

compared to those found in nature and discussed in terms of the organization and effect of the binding sites on the photochemistry in these two pigments.

RESULTS

A. Simple Conjugated Iminium Salts

I. Selection

Three simple conjugated iminium salts, 30, 31 and 34 were selected for photochemical study. These salts were selected because they possessed different substitution at nitrogen, different degrees of unsaturation, and all had non-nucleophilic counterions.

II. Preparation

The all-trans iminium salts 30, 31 and 34 were prepared as described in the previous chapter. Each of these iminium salts possessed small amounts of isomeric impurities, Table 3-1, which for the purpose of quantitative photochemical and thermal experiments, had to be accurately identified. Minor isomers were prepared in appreciable amounts, from the photolysis of the iminium salts 30, 31 and 34, equations 29-30, and identified and quantitated from an analysis of each ^{1}H NMR spectrum.

III. Characterization

The all-trans isomers 30, 31 and 34 were characterized by ^{1}H and ^{13}C NMR and absorption spectroscopy in the previous chapter, Tables 2-1,

Table 3-1

Isomeric Purity of Iminium Salts by ^1H NMR as Prepared

	Relative Percentage of Isomer			
Compound	Trans	2-cis	4-cis	6-cis
30	91.19	0.93	7.96	-
31	90.81	2.34	4.35	2.50
34	86.24	nd	13.76	-

nd. isomer not detected. Methylene chloride solvent, 22°C.

2-2 and 2-13. The characterization of the minor isomers present in each case was made by 250 or 500 MHz ^{1}H NMR analysis of each irradiated solution. This allowed for the identification of each geometric isomer based on coupling constant measurement or previously reported chemical shift information. Chemical shift and coupling constant data for all identified isomers are reported in Tables 3-2 and 3-3.

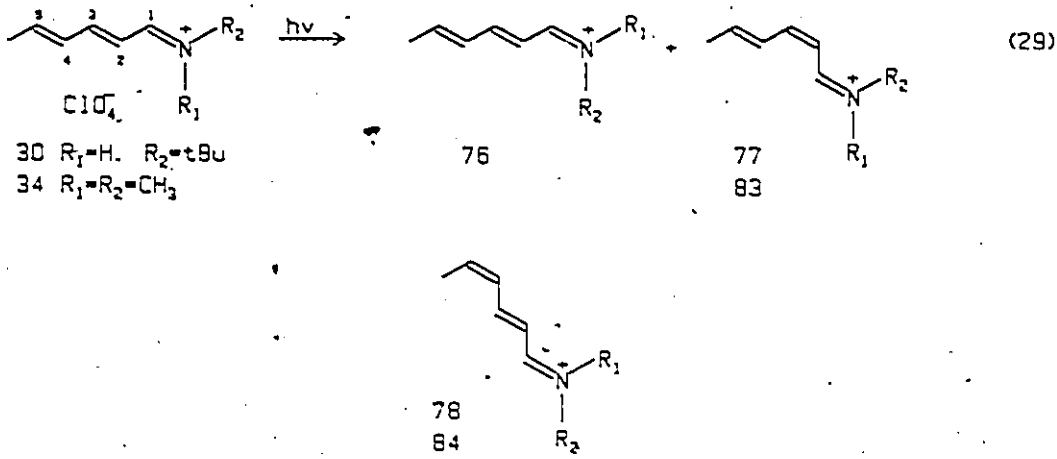

(29)

30 R_1=H, R_2=tBu
34 R_1=R_2=CH_3

76 77 83 78 84

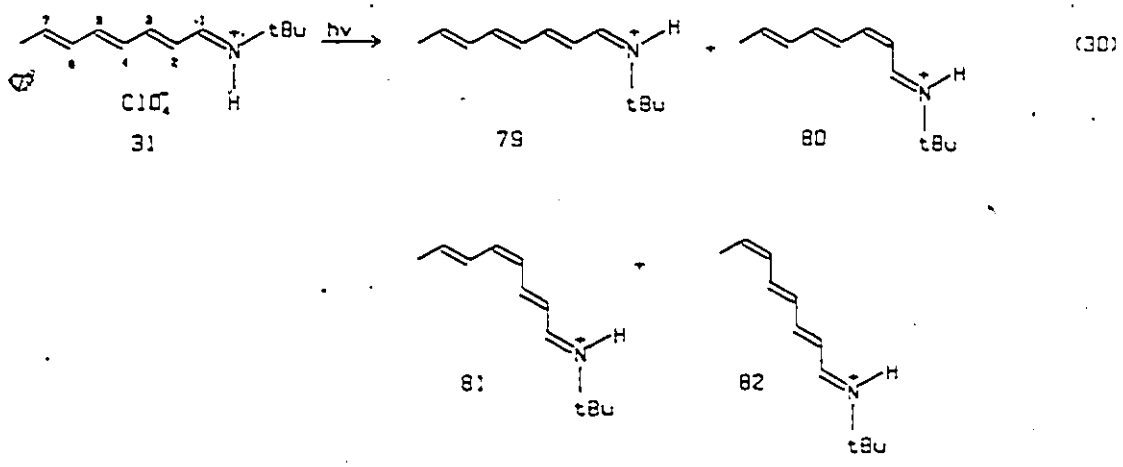

(30)

31 79 80 81 82

The identification of each iminium salt isomer was based either on comparison with literature values for ^{1}H NMR chemical shifts and/or

Table 3-2

^1H NMR Chemical Shift[a,b,c] Data For Aliphatic Iminium Salts and Their Primary Photoproducts.

	Compound					
Position	30	77	31	80	34	83
C(1)H	8.13dd	8.46dd	7.96dd	8.41dd	8.38d	8.82d
C(2)H	6.74dd	6.49t	6.84dd	6.58t	6.55dd	6.20t
C(3)H	7.49dd	7.26t	7.40dd	7.29t	7.63dd	7.37t
C(4)H	6.48dd	6.84bt	6.50dd	6.78bt	6.49dd	7.11bt
C(5)H	6.65dq	6.65dq	6.90dd	6.90dd	6.70dq	6.70dq
C(6)H	-	-	6.31dd	6.31dd	-	-
C(7)H	-	-	6.32dq	6.32dq	-	-
CH_3	1.99d	2.04d	1.92d	1.92d	2.02d	2.04d
C(1')H	-	-	-	-	3.49s	3.50s
C(1'')H	-	-	-	-	3.68s	3.77s
C(2')H	1.51s	1.54s	1.51s	1.54s	-	-

a s = singlet, d = doublet, t = triplet, dd = doublet of doublets, dq = doublet of quartets, bt = broad triplet.
b in ppm. Numbering of carbons as in text.
c referenced to CD_2Cl_2, 5.32 ppm. Measured at 21°C.

Table 3-3

^1H, ^1H Coupling Constant Data[a] For Iminium Salts

	Compound					
	30	77	31	80	34	83
$J_{1,N}$	16.64	16.60	16.47	16.45	-	-
$J_{1,2}$	10.39	10.97	10.43	11.01	10.54	10.86
$J_{2,3}$	14.71	11.20	14.60	10.63	14.43	10.86
$J_{3,4}$	10.65	11.20	11.34	10.63	10.87	11.27
$J_{4,5}$	15.07	13.04	15.11	15.11	14.93	13.52
$J_{5,6}$	6.64	6.64	12.03	12.03	6.87	6.87
$J_{6,7}$	-	-	17.65	17.65	-	-
$J_{7,8}$	-	-	5.43	5.43	-	-

a. in Hz. Numbering of carbons as in text.

coupling constants, or by utilization of ^1H NMR chemical shift trends that arise upon isomerization of the all-trans compounds. These trends are well documented in the literature for conjugated aldehydes and iminium salts (52,185,186,188,258). The chemical shift changes expected for 76-78, potential isomers of 30, equation 29, are depicted in Scheme 3-1. In each case, the largest changes in chemical shift from that of the all-trans isomer, 30, occur near the site of isomerization. The coupling constants across C(1)H,NH, C(2)H,C(3)H and C(4)H,C(5)H, being about 3-4 Hz smaller than those in the corresponding trans isomer 30 were also indicative of a cis geometry in 76-78.

The t-butyl iminium ion, 30 displayed characteristic doublets of doublets for C(1)H at δ 8.13, C(3)H at 7.49 and C(4)H at 6.48 ppm. These resonances were indicative of the all-trans configuration of 30. Upon irradiation of 30 at 300 nm, the ^1H NMR spectrum shown in Figure 3-1 was obtained. This spectrum showed that a second major isomer, not present in the starting material, had been formed in addition to the trans isomer 30. An examination of the aldiminium region of the ^1H NMR spectrum, 8.0-8.5 ppm, revealed that the new isomer had a similar doublet of doublets (AM_2) coupling pattern as 30, at 8.46 ppm. The magnitude of the larger coupling constant in this multiplet, 16.6 Hz, corresponded to $J_{1,N}$. A coupling of this magnitude is well within the range of coupling constants found for an anti C=N bond arrangement, typically 14-17 Hz (184), and indicated that the new isomer was not the syn isomer 76.

The resonance which occurred at 7.26 ppm in the ^1H NMR spectrum shown in Figure 3-1 was assigned to C(3)H. This apparent triplet was

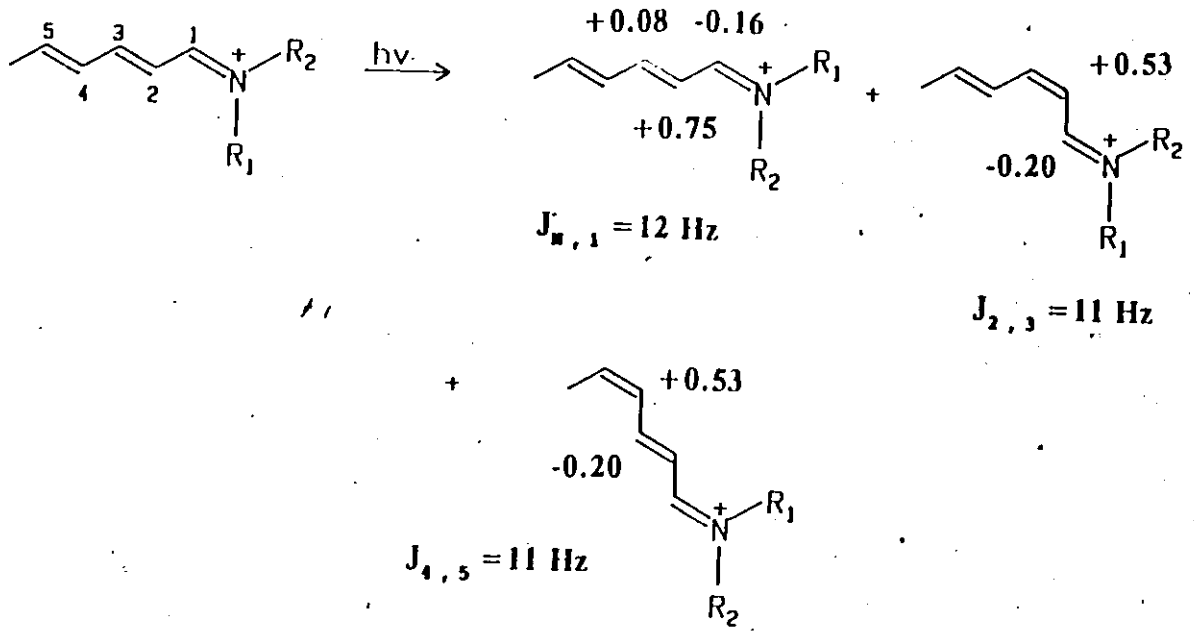

Scheme 3-1: Typical changes in ^{1}H NMR spectra for chemical shift (-ve denotes downfield, +ve upfield) and coupling constants for cis iminium salts as compared to their trans derivatives.

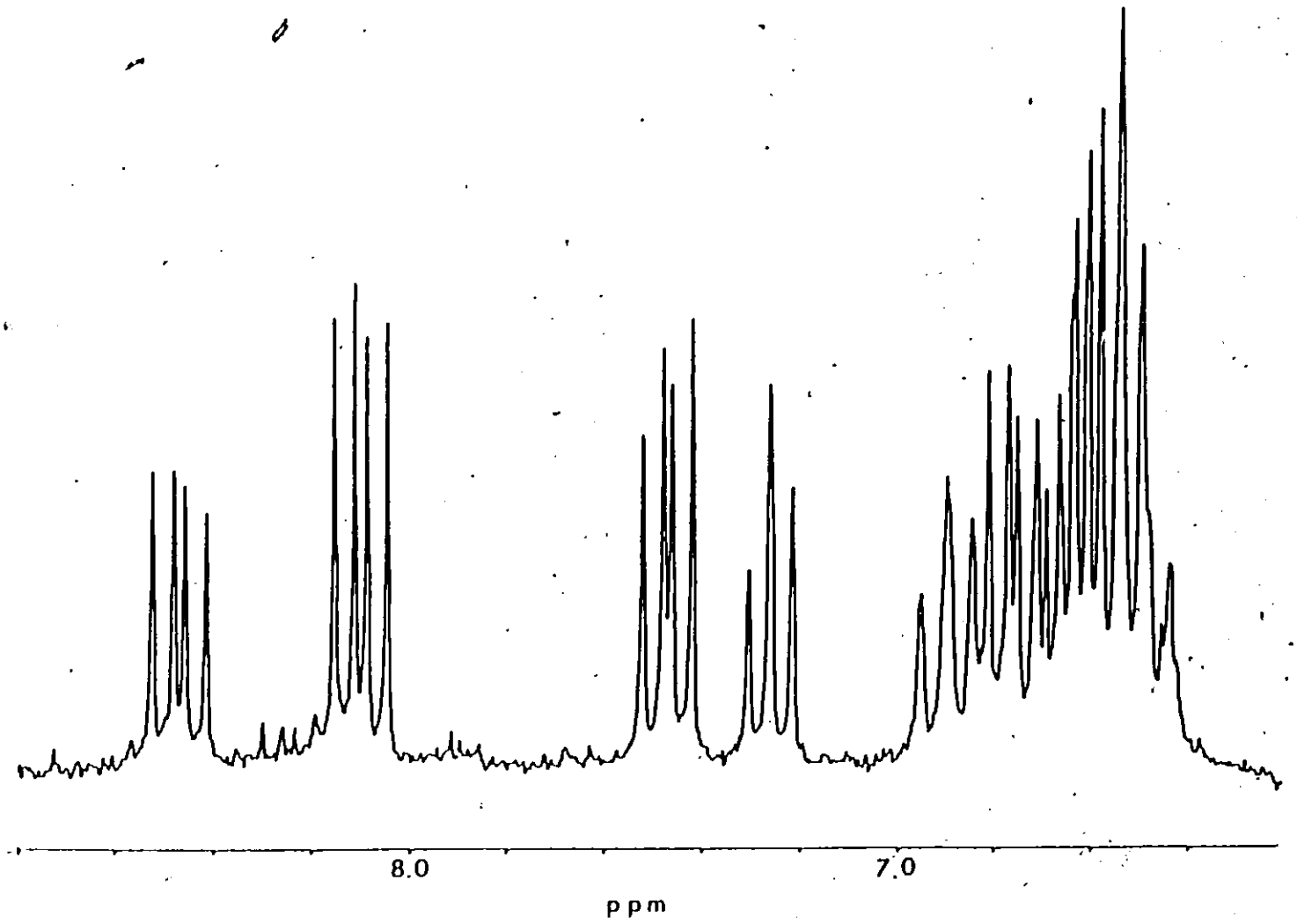

Figure 3-1: 250 MHz ^{1}H NMR spectrum of the vinyl region of 30 after irradiation at 300 nm.

formed from coupling of C(3)H to two magnetically equivalent protons with similar coupling constants of about 11.2 Hz. This value is consistent with a 2-s-trans configuration as found in the starting material, Table 3-3. However, the remaining coupling constant could not be attributed to a coupling of C(3)H with C(2)H across a trans double bond, typically about 14-16 Hz. The observed value of about 11.2 Hz for the coupling of C(2)H,C(3)H corresponded well with a cis C=C bond coupling constant of 9-12 Hz (258). This indicated that this isomer was the 2-cis iminium salt, 77.

The 4-cis isomer, 78, was also present in the spectrum shown in Figure 3-1, in a much smaller quantity than either 30 or 77. This material was also present in the starting material before irradiation. This isomer was identified by its characteristic C(1)H resonance which was located midway between those for C(1)H of 30 and 77. According to Scheme 3-1, this is exactly as expected. Isomerization about the C(4),C(5) bond should give rise to a smaller downfield shift of C(1)H in 78 than in 77 because C(1)H in 78 is farther removed from the isomerization site. The remaining resonances for the 4-cis isomer, 78, could not be identified due to the complexity of the spectrum, Figure 3-1.

The photoisomerization of 31 at 350 nm was more complex than that of 30, due to its additional C=C bond. The reaction was followed by ^1H NMR spectroscopy, comparing spectra before and after irradiation. As found for 30, the lowest field resonances, in the spectrum of 31 and its photoproducts, originated from the C(1) proton. In the irradiated solution, these appeared as two doublets of doublets at 8.0-9.0 ppm with

$J_{1,N}$ of about 16.5 Hz. Like those in 30 and 77, the appearance of these two similar sets of resonances suggested the presence of 31 and a second isomer containing an anti configuration about the C=N bond. The syn isomer 79 could not be detected.

The resonance corresponding to C(3)H in the new isomer was a triplet at 7.29 ppm, Tables 3-2 and 3-3. This resonance was much like that in 77. The coupling constants resulting from coupling of C(3)H to C(2)H and C(4)H were both about 10.6 Hz. This value was substantially smaller than the $J_{2,3}$ = 14.6 Hz in the all-trans isomer 31, suggesting that the primary photoisomer of 31 was the 2-cis iminium salt, 80.

The ^{1}H NMR spectra for 4-cis isomer 81, and the 6-cis isomer, 82, could not be unambiguously assigned since these isomers did not appreciably increase in concentrations upon irradiation. The identity of these two isomers was based solely on the proximity of the C(1)H resonance to that of the all-trans isomer, 31 or the 2-cis isomer 80.

The photoisomerization of 34 followed a similar course to that of 30 with isomerization about the C(2),C(3) bond occurring to form the 2-cis isomer, 83. This isomer was identified in an analogous manner to 77. Again, an upfield chemical shift of C(3)H and smaller C(2)H,C(3)H coupling constant of about 10.9 Hz was observed, Tables 3-2 and 3-3. It should also be noted that photoisomerization about the C=N bond of 34 could not be detected in this sample due to the symmetrical substitution about the nitrogen.

IV. Stability

Methylene chloride solutions of the trans iminium salts 30 and 34 were shown to be stable by ^{1}H NMR spectroscopy when kept at 22°C for up to periods of 24 hrs. These were the solvent and temperature conditions at which all photochemical experiments were carried out. Furthermore, the symetrically substituted compound 34 was shown to be stable, in methylene chloride solution, up to a temperature of 80°C for up to 24 hours. Extended heating of 34 yielded only decomposition products. These were not identified.

V. Photochemistry

i. Absorption Spectra

The absorption maxima of the trans iminium salts 30, 31 and 34 are reported in Table 3-4. The long wavelength absorption of each of these strongly absorbing compounds was a broad gaussian curve, characteristic of the π-π^* transitions of iminium salts.

ii. Quantitative Experiments

The iminium salts 30 and 34 were irradiated at 313 nm using a high pressure mercury arc lamp as a light source in a quantum yield apparatus. Wavelength selection was regulated using a monochromator with a bandwidth of 11.4 nm. Photon flux was determined using the decomposition of potassium ferrioxalate at this wavelength. The method chosen for quantifying the photoisomerization reactions of these iminium salts involved the measurement of apparent quantum yields, at a different time

Table 3-4

Absorption Spectra Data[a] (nm) for Iminium Salts

Compound	λ_{max}	ε_{max} ($\times 10^{-4}$)
30	314	3.65
31	370	3.48
34	320	3.56
49	476	4.06
52	472	4.26
54	498	4.05

a in CH_2Cl_2 at 21°C.

intervals by ^{1}H NMR spectroscopy (170). Photon flux over the duration of the experiment was shown to be constant from measurements made before and after the irradiation of iminium salts, and was used to determine each time interval of irradiation, recorded in Einsteins. This method was selected because accurate photostationary state concentrations, usually used to correct for light absorption by the new isomeric species, could not be obtained as the ^{1}H NMR spectrum became too complicated to analyse. Conversions to the primary photoproducts 77 and 83 were kept below 10% in all experiments.

The relative amounts of the trans isomers, 30 and 34 and the 2-cis isomers, 77 and 83, for each photoreaction were assayed directly from the irradiated solution using 250 MHz ^{1}H NMR spectroscopy (186,188). In the isomerization of 30 to 77, the relative amounts of the isomers were obtained by comparison of the areas of resonances associated with the t-butyl groups. In 34 to 83, the C(1)H resonances were employed. In each case four measurements were obtained at different degrees of conversion. The apparent quantum yield, Φ_{app} for each sample, was calculated from integration of the various resonances in the ^{1}H NMR spectrum. The resulting plots of Φ_{app} versus Einsteins for each photoisomerization, Figures 3-2 and 3-3, showed an excellent linear correlation ($r>0.90$). Each line was extrapolated to t=0 to give the initial quantum yield for the reaction.

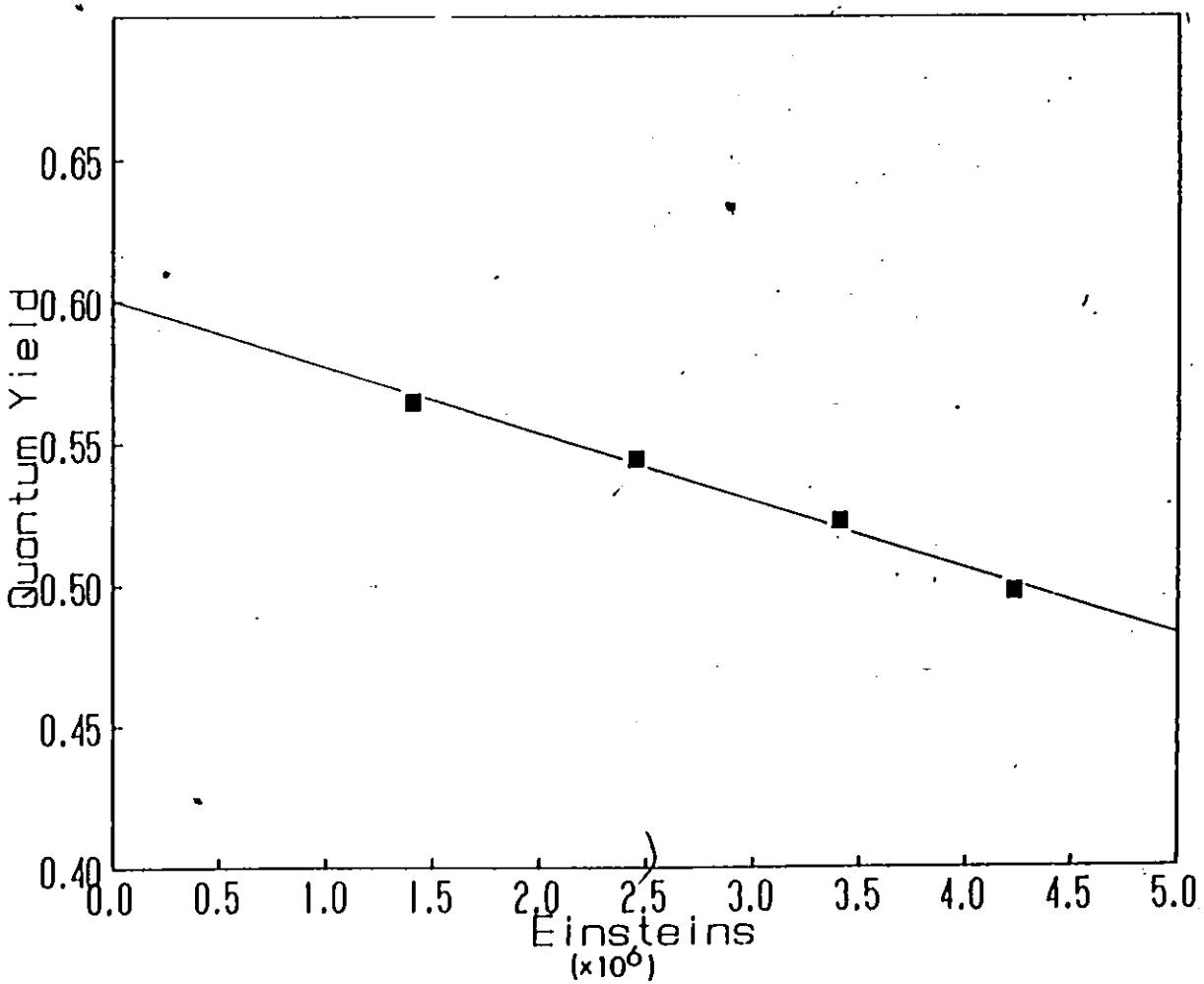

Figure 3-2: Plot of Einsteins vs. quantum yield for the conversion of 30 to 77 at 313 nm.

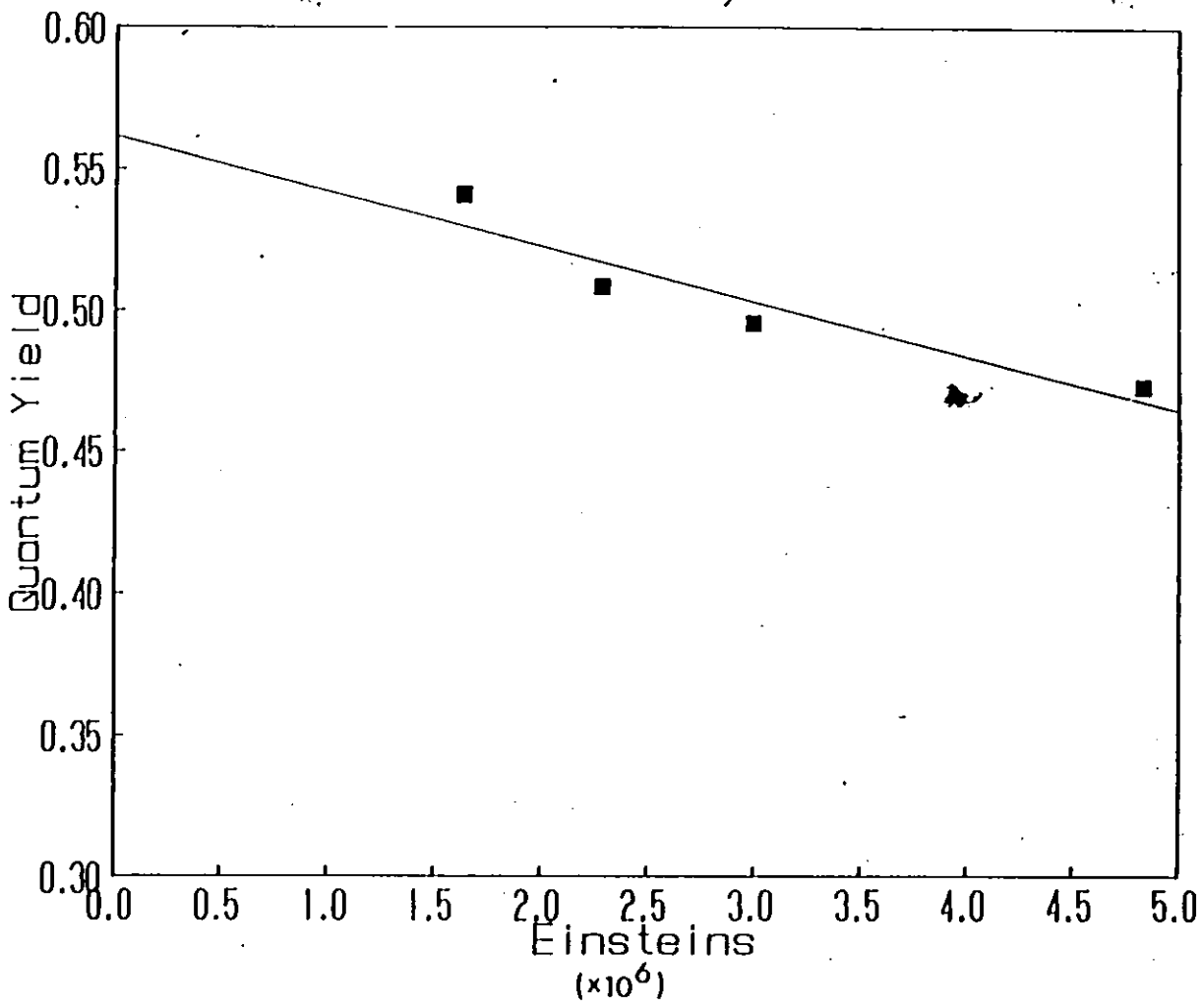

Figure 3-3: Plot of Einsteins vs. quantum yield for the conversion of 34 to 83 at 313 nm.

iii. Thermal Stability of Photoproducts

Solutions of the t-butyl 2-cis iminium salt 77 were thermally stable when kept at 22°C, the temperature of all photochemical experiments, Table 3-5. However, a catalysed isomerization was observed upon addition of a nucleophilic catalyst such as chloride to the solution, equation 31. The reaction of 77 to 30 was studied quantitatively by ^1H NMR spectroscopy using various quantities of dimethyl ammonium chloride to catalyse the process. Good, pseudo first order kinetics (r=0.99) were observed for four independent measurements in which the chloride ion concentration was in considerable excess of the iminium salt, Figure 3-4. The second order rate constant for this reaction was 4.4×10^{-4} $sec^{-1}{}_M{}^{-1}$.

The dimethyl 2-cis iminium salt, 83, completely isomerized to the starting trans material, 34, equation 32, without the addition of chloride at 22 C. The half-life for the isomerization of 83 to 34 was 16.7 hr, with $k=1.15 \times 10^{-5}$ sec^{-1} (r=0.99), Figure 3-5. This isomerization is sufficiently slow that it would have a minimal influence on photochemical experiments, which tended to last only about one hour.

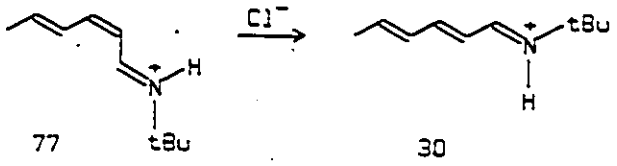

77 30 (31)

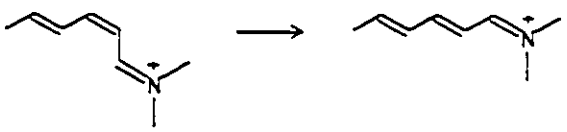

83 34 (32)

Table 3-5

Thermal Stabilities of Primary Iminium Salt Photoproducts[a] at 22°C

		Relative Percentage by ^{1}H NMR	
	Isomer	After irradiation	2 hr later
30	(Trans)	59	59
77	(2-Cis)	41	41
31	(Trans)	58	58
80	(2-Cis)	39	39
34	(Trans)	53	58
83	(2-Cis)	47	42
52	(All-trans)	45	47
90	(11-Cis)	20	18
54	(All-trans)	40	41
93	(11-Cis)	27	25

a. using relative peak heights of various ^{1}H NMR resonances. Estimated error in retinylidene series was about 10% due to some peak overlapping.

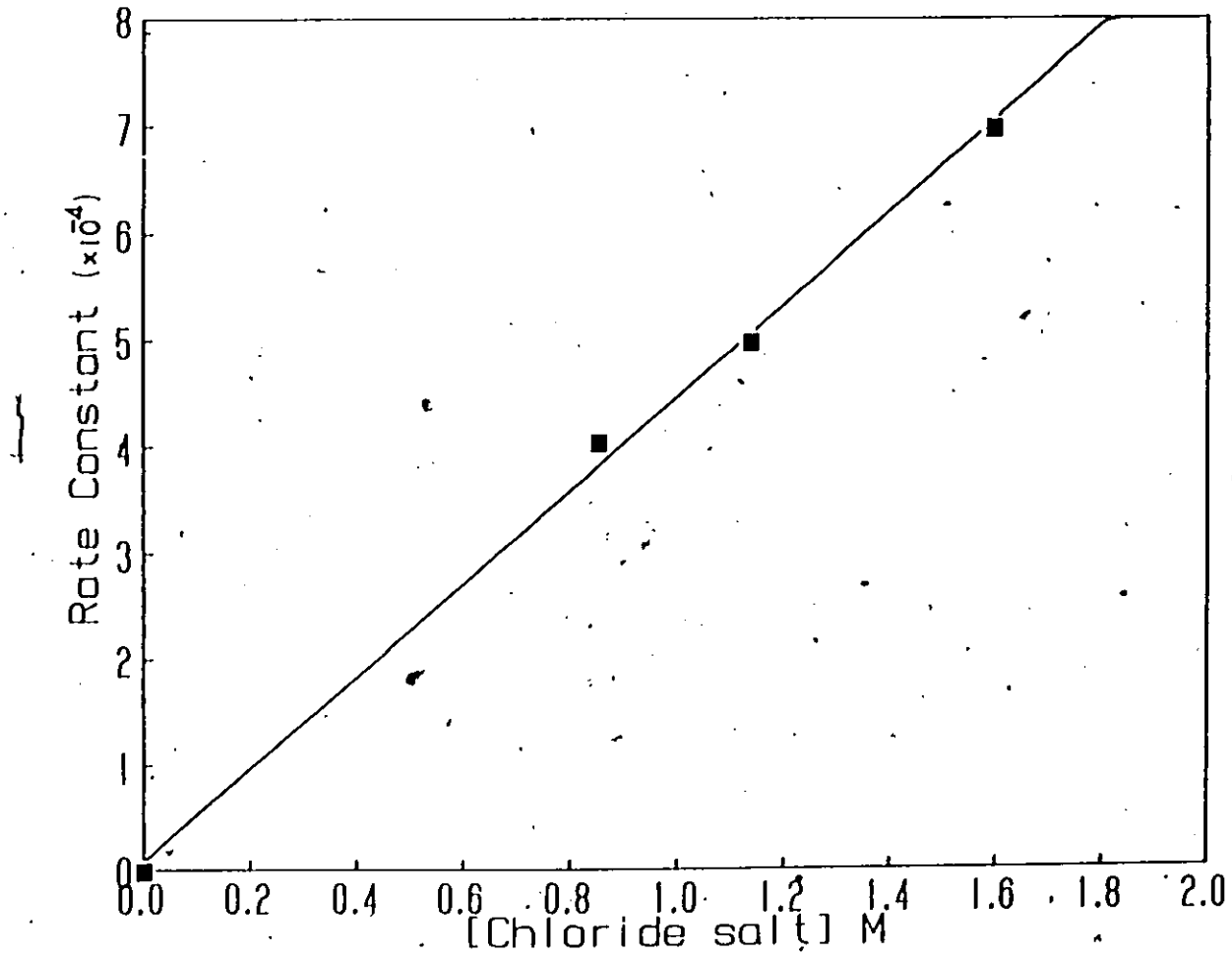

Figure 3-4: Plot of chloride concentration vs. rate constant for the catalysed isomerization of of 77.

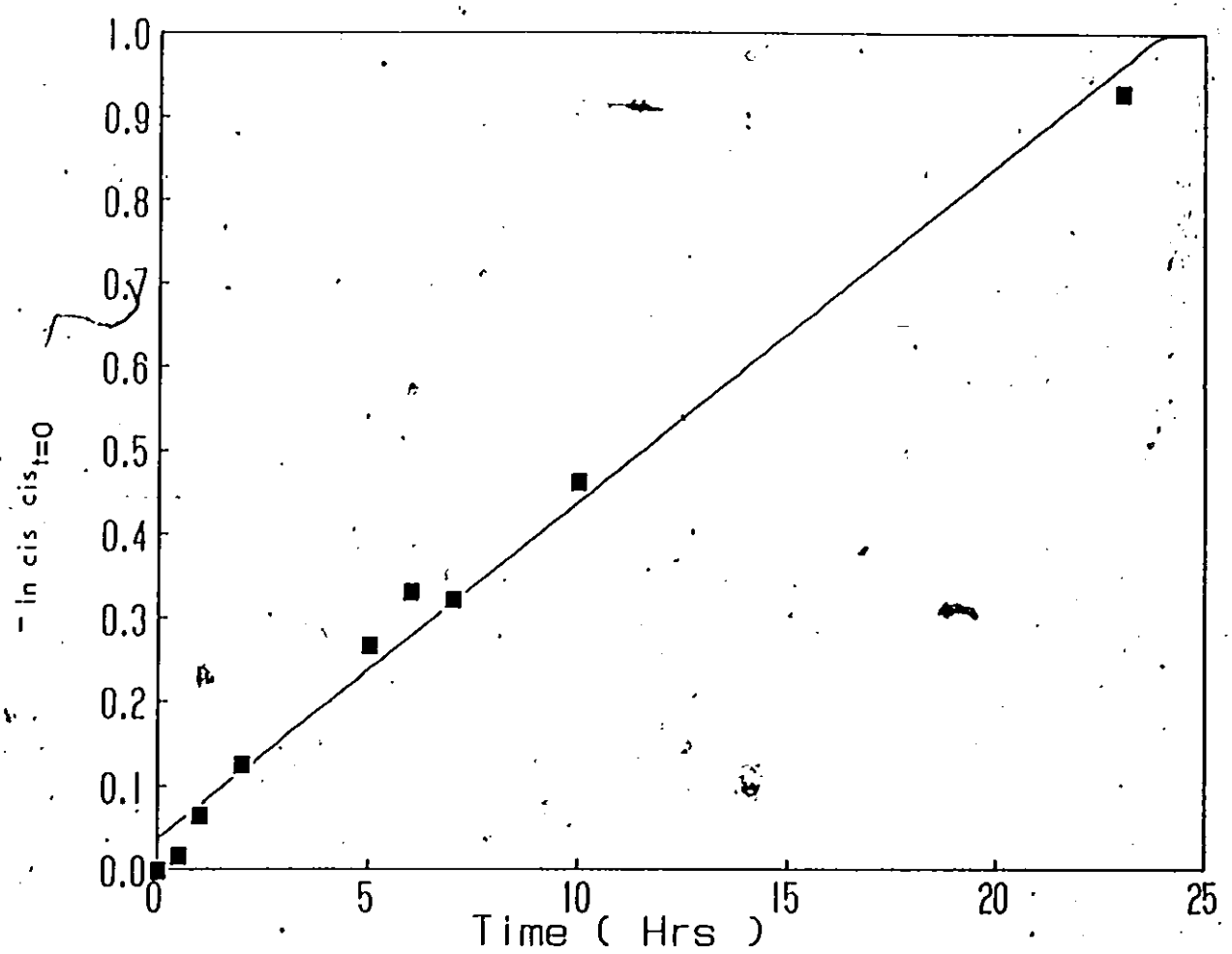

Figure 3-5: Plot of time vs. ln ratio 83/34 for the cis to trans thermal isomerization of 83.

B. Retinylidene Iminium Salts

I. Selection

The retinylidene iminium ions 49, 52 and 54 were chosen for photochemical studies. These compounds were selected because they possessed different substitutions at nitrogen and they contained a non-nucleophilic perchlorate counterion.

II. Preparation and Characterization

The all-trans retinylidene iminium salts 49, 52 and 54 were prepared as described in the previous chapter. Each iminium salt contained small amounts of isomeric impurities, formed on preparation of the ions, Table 3-6. The salts 49, 52 and 54 were characterized by ^{1}H and ^{13}C NMR, and absorption spectroscopy in the previous chapter, Tables 2-5, 2-6, 2-9 and 2-13. The characterization of the isomers of 49, 52 and 54 was made by examination, by high field ^{1}H NMR spectroscopy, of irradiated solutions of each compound which contained appreciable amounts of most of the mono-cis isomers, equation 33. Comparison of chemical shifts and coupling constants with previously reported data (52,185,186,188,259) was used to unequivocally identify each isomer. As was the case with the simple iminium salts 30, 31 and 34, trends in chemical shifts, Scheme 3-1, arising from the isomerization of salts 49, 52 and 54 were also used to aid identification, Scheme 3-2. Chemical shift and coupling constant data for all identified isomers are reported in Tables 3-7 to 3-9.

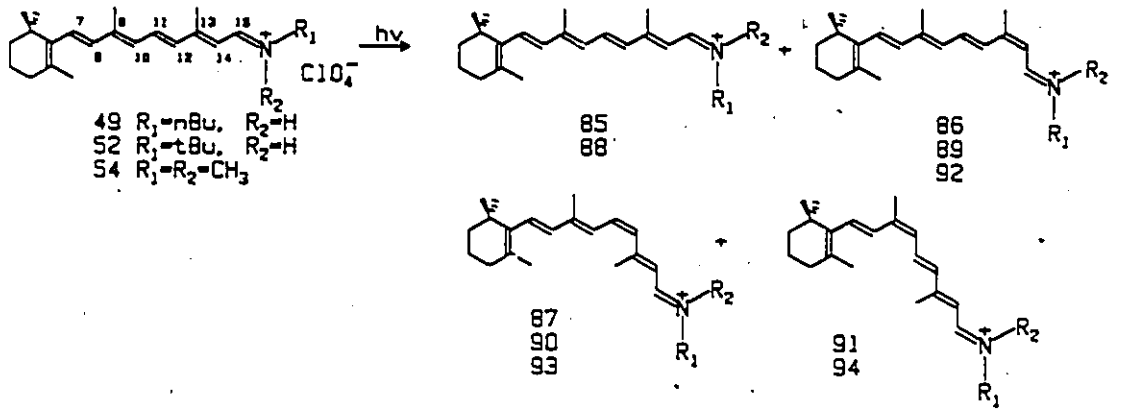

(33)

The least complicated ^{1}H NMR example to examine is that of 54. This all-trans isomer exhibited a doublet at 8.56 ppm, C(15)H, a doublet of doublets at 7.59 ppm, C(11)H, and several resonances between 6.2 and 6.6 ppm for the remaining vinylic protons, Tables 2-6 and 3-9. The ^{1}H NMR spectrum shown in Figure 3-6 was obtained upon irradiation of 54 at 350 nm in methylene chloride. This spectrum showed that a second major isomer, not present in the starting material, had been formed. In this spectrum, the resonances of C(15)H for both major isomers were located at 8.56 ppm and appeared as a broadened doublet. This suggests that the second isomer in this spectrum had a cis bond which is quite remote from C(15)H, Scheme 3-2. It should be noted that a syn C=N isomer of 54 could not be detected in this sample because of symmetrical substitution about nitrogen.

Analysis of the multiplets occurring between 7.1 and 7.7 ppm was critical in determining the structure of the photoproduct formed from the

Table 3-6

Isomeric Purity of Retinylidene Iminium Salts by ^1H NMR as Prepared

	Relative Percentage of Isomer			
Compound	All-trans	13-cis	11-cis	9-cis
49	90.50	9.50	nd	nd
52	96.50	3.50	nd	nd
54	87.30	12.70	nd	nd

nd. isomer not detected. Methylene chloride solvent, 22°C.

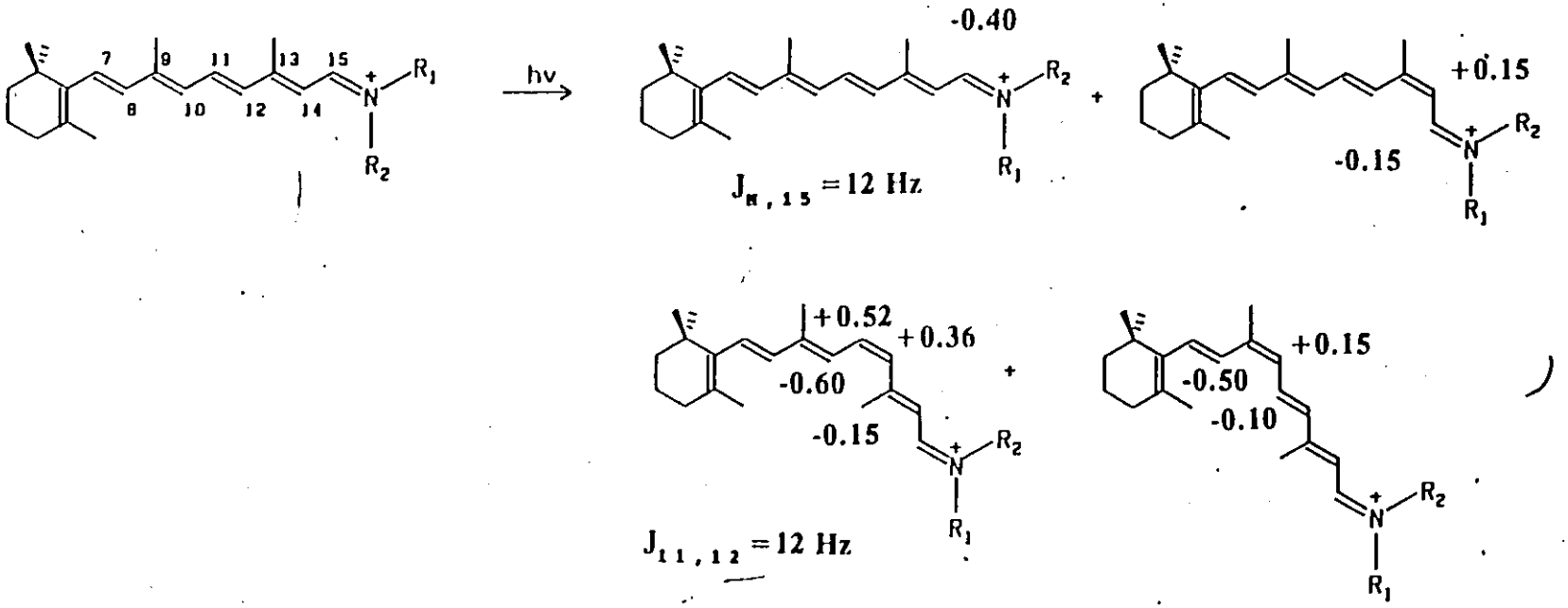

Scheme 3-2: Typical changes in ^{1}H NMR spectra for chemical shift (-ve denotes downfield, +ve upfield) and coupling constants for cis retinylidene iminium salts as compared to their trans derivatives.

Table 3-7

^1H NMR Chemical Shift[a,b,c] Data For Retinylidene Iminium Salts and Their Primary Photoproducts

	Compound					
Position	49	87	52	90	54	93
C(2)H	1.53t	1.53t	1.50t	1.50t	1.51t	1.51t
C(3)H	1.65m	1.65m	1.61m	1.61m	1.61m	1.61m
C(4)H	2.09t	2.09t	2.06t	2.06t	2.09t	2.09t
C(7)H	6.56d	6.56d	6.47d	6.47d	6.59d	6.59d
C(8)H	6.27d	6.27d	6.21d	6.21d	6.31d	6.36d
C(10)H	6.33d	6.75d	6.29d	6.74d	6.36d	6.75d
C(11)H	7.51dd	7.04dd	7.43dd	7.03t	7.59dd	7.08t
C(12)H	6.56d	6.18d	6.58d	6.23d	6.64d	6.23d
C(14)H	6.72d	6.30d	6.65d	6.73d	6.62d	6.41d
C(15)H	8.34dd	8.25dd	8.19dd	8.20dd	8.56d	8.58d
C(16)H C(17)H	1.08s	1.08s	1.05s	1.05s	1.08s	1.08s
C(18)H	1.77s	1.77s	1.74s	1.77s	1.78s	1.78s
C(19)H	2.13s	2.10s	2.10s	2.07s	2.16s	2.09s
C(20)H	2.36s	2.45s	2.32s	2.46s	2.46s	2.56s
C(1')H	3.74dt	3.74dt	-	-	3.74s	3.76s
C(1")H	-	-	-	-	3.47s	3.47s
C(2')H	1.81m	1.81m	1.51m	1.51s	-	-
C(3')H	1.43m	1.43m	-	-	-	-
C(4')H	0.99t	0.96t	-	-	-	-

a s = singlet, d = doublet, t = triplet, dd = doublet of doublets, dt = doublet of triplets, m = multiplet.
b in ppm. Numbering of carbons as in text.
c referenced to CD_2Cl_2, 5.32 ppm. Measured at 21°C.

Table 3-8

^1H, ^1H Coupling Constant Data[a] For Retinylidene Iminium Salts and Their Primary Photoproducts

	Compound					
	49	87	52	90	54	93
$J_{7,8}$	15.95	15.95	15.90	15.90	15.96	15.96
$J_{10,11}$	11.81	12.96	11.89	12.43	11.77	11.59
$J_{11,12}$	14.70	11.77	14.90	11.80	14.68	11.65
$J_{14,15}$	11.28	10.64	11.32	11.32	11.79	11.49
$J_{15,N}$	15.71	15.85	15.41	15.41	-	-

a in Hz. Numbering of carbons as in text.

Table 3-9

^1H NMR[a,b,c] Data For All-trans and 13-cis Retinylidene Iminium Salts

	Compound			
Position	54		92	
C(2)H	1.51t		1.50t	
C(3)H	1.61m		1.61m	
C(4)H	2.09t		2.06t	
C(7)H	6.59d	$J_{7,8}$=15.96	6.59d	$J_{7,8}$=15.96
C(8)H	6.31d		6.31d	
C(10)H	6.36d	$J_{10,11}$=11.77	6.33d	$J_{10,11}$=11.77
C(11)H	7.59dd	$J_{11,12}$=14.68	7.48dd	$J_{11,12}$=14.60
C(12)H	6.64d		7.22d	
C(14)H	6.62d	$J_{14,15}$=11.79	6.13d	$J_{14,15}$=11.98
C(15)H	8.56d		8.76d	
C(16)H C(17)H	1.08s		1.07s	
C(18)H	1.78s		1.78s	
C(19)H	2.16s		2.14s	
C(20)H	2.46s		2.43s	
C(1')H	3.74s		3.75s	
C(1")H	3.47s		3.47s	

a s = singlet, d = doublet, t = triplet, dd = doublet of doublets, m = multiplet.

b chemical shift in ppm, coupling constants in Hz. Numbering of carbons as in text.

c referenced to CD_2Cl_2, 5.32 ppm. Measured at 21°C.

Figure 3-6: Vinyl region of ^{1}H NMR spectrum of 54 before (A) and after (B) irradiation at 350 nm.

irradiation of 54. The triplet centred at 7.08 ppm was assigned to C(11)H of the isomeric iminium salt, coupled to C(10)H and C(12)H. This resonance is similar to the ones found for the 2-cis isomers 77, 80 and 83. In the present example, the triplet pattern of C(11)H corresponds to that expected for the 11-cis isomer, 93, with the characteristic cis coupling constant for $J_{10,11}$ of 11.59 Hz. This resonance occurs at higher field than C(11)H in 54. Accompanying this were the expected shifts to lower field of C(10)H, and to higher field of C(12)H and C(14)H, as suggested from Scheme 3-2.

The chemical shifts of several of the aliphatic protons are quite different in the 11-cis isomer, 93 as compared to its parent compound, 54. The largest of these differences occurred for C(20)H which was shifted from 2.46 ppm in the all-trans isomer 54, to 2.57 ppm in 119. This is consistent with previous ^{1}H NMR studies of retinylidene iminium salts, where resonances of C(20)H are shifted by 0.15 ppm to lower field in the 11-cis compared to the all-trans isomer.

The 13-cis isomer, 92, present in appreciable amounts in the starting material before irradiation, Table 3-6, was identified by an independent synthesis and ^{1}H NMR analysis of the 13-cis iminium salt, 92. Treatment of 13-cis retinal with dimethyl ammonium perchlorate at 0 C led to the formation of a mixture of the 13-cis, 92 (40%), and all-trans, 54 (60%), iminium salt isomers which allowed for the unequivocal identification of the 13-cis isomer by ^{1}H NMR spectroscopy, Table 3-9. The small multiplets at 8.76 and 7.48 ppm in the irradiated spectrum of 54, Figure 3-6, correspond to the C(15)H and C(11)H protons of the 13-cis

retinylidene iminium salt, 92.

The identifications of the cis isomers derived from the irradiations of 49 and 52 were more difficult than in 54, due to the additional coupling of C(15)H to N-H, and smaller changes in the chemical shifts between the cis isomers and the parent all-trans iminium salts, Figure 3-7. Nevertheless, confirmation that the 11-cis isomers, 87 and 90 were the primary photoproducts was made using the same methods as described above for 93. Comparison of ^{1}H NMR data for 112 and 116 with those of a previously reported 11-cis iminium salt (52) showed the same trends in chemical shift, especially for C(10)H, C(11)H, C(12)H, C(15)H and C(20)H. However, a direct comparison could not be made because of the large difference in solvent used in this and the previous report. Solvent changes have been shown previously to have a large effect on the ^{1}H chemical shifts of iminium salts.

III. Stability

The all-trans retinylidene iminium salts 49, 52 and 54 formed no other isomeric products, when kept at 22°C over periods of up to 24 hrs. This was monitored using high field ^{1}H NMR spectroscopy.

IV. Photochemistry

i. Absorption Spectra

The absorption maxima of the all-trans retinylidene iminium salts 49, 52 and 54 are reported in Table 3-4. The spectra of these compounds were broad gaussian curves typical of those found in conjugated iminium salts.

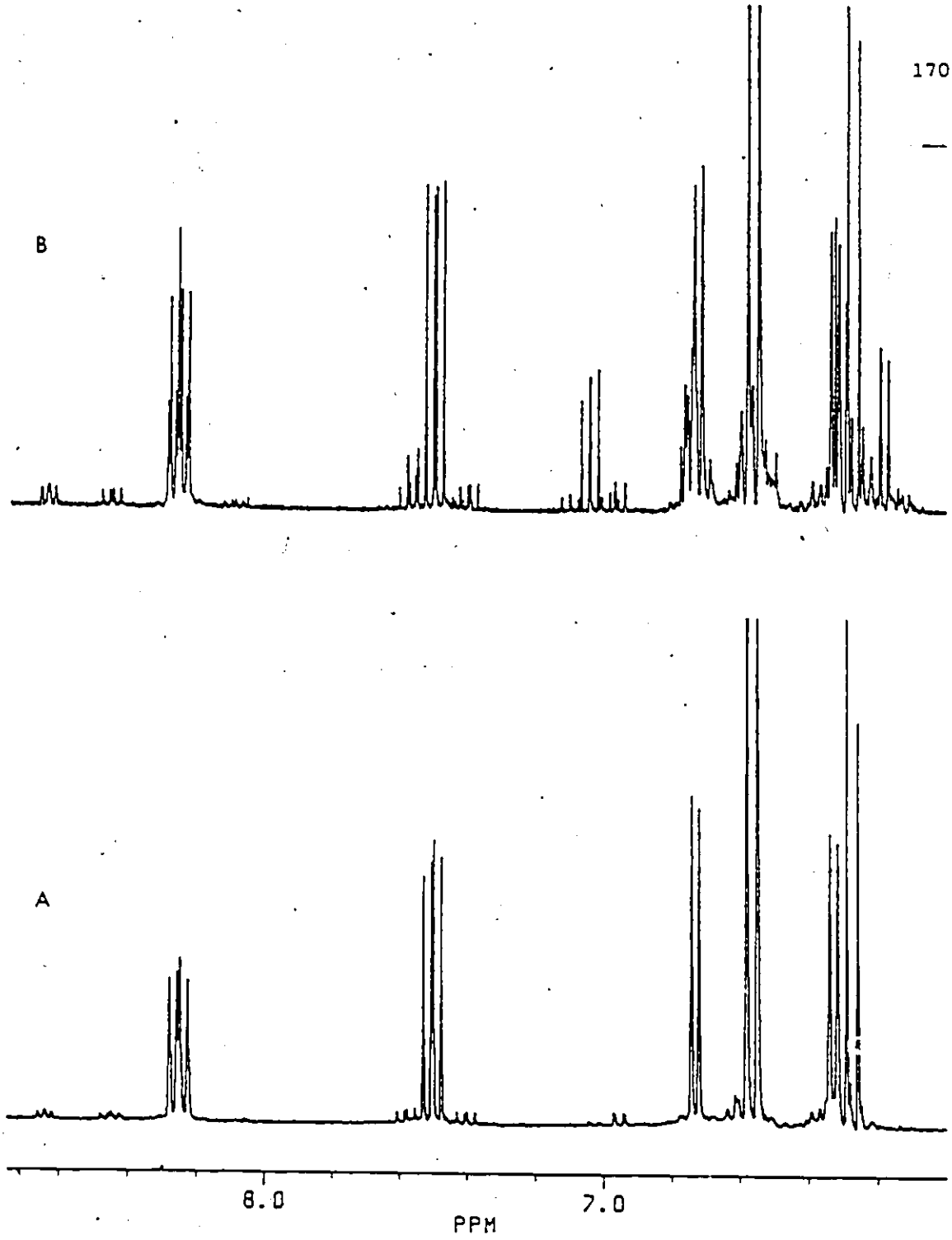

Figure 3-7: Vinyl region of 500 MHz ^{1}H NMR spectrum of 49 before (A) and after (B) irradiation at 350 nm.

ii. Qualitative Experiments

Irradiation of methylene chloride solutions of the all-trans isomers 49, 52 and 54 with light of λ 350, 436 or 468 nm led to the production of predominately the 11-cis isomers, 87, 90 and 93 respectively, equation 34. Typically, a conversion of the all-trans isomer to approximately 20% of the 11-cis isomer was found, as measured by ^{1}H NMR spectroscopy. This occurred regardless of the wavelength used when solutions of 49, 52 or 54 were irradiated for about one-half hour, Figure 3-7. During these early stages of photoisomerization, it was clear that only the 11-cis isomer was being formed, within the detection limits of 500 MHz ^{1}H NMR spectroscopy, about 1.0%. The 13-cis isomers, 86, 89 and 92, which were present in the starting material, did not appear to change in concentration as shown by ^{1}H NMR spectroscopy, Figure 3-7. Further irradiation for periods of up to two hours yielded three of the four possible mono-cis isomers in appreciable amounts. At this point the ^{1}H NMR spectra became extremely complex and complete assignment of all resonances was not possible. As a result, irradiations were not carried out for a sufficient length of time for the reaction to reach a photostationary state.

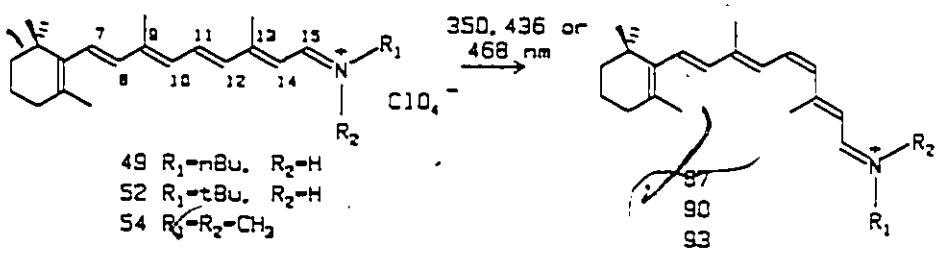

(34)

It was evident from the ^1H NMR spectra of irradiated solutions of 49 and 52 that no C=N syn isomers were being formed photochemically at 22°C. It was possible that this reaction was occurring, but went undetected because the syn isomers, 85 and 88, were isomerizing back to their anti forms, 49 and 52, thermally. To determine if this was occurring, both 49 and 52 were irradiated and assayed at -60°C by ^1H NMR spectroscopy at the same temperature. In both cases, it was found that the syn isomers, 85 and 88 were not being formed photochemically.

iii. Quantitative Experiments

The quantum yields for the photoisomerizations of the all-trans iminium salts 49 and 52 to their corresponding 11-cis isomers, 87 and 90 were measured using light of 468 nm and potassium ferrioxalate actinometry. A monochromator with a 20 nm bandwidth, and a 425 nm cut-off filter were employed. The quantum yield for the photoisomerization of 54 to 93 was determined by a relative method using 49 as the actinometer. Quantum yields were calculated using the procedure described previously for the hexadienyl iminium salts, 30 and 34. The relative amounts of the 11-cis and all-trans isomers were determined directly from the irradiated solution using ^1H NMR spectroscopy at either 250 or 500 MHz. The resonances corresponding to C(20)H in each isomer were integrated at various irradiation times, Figure 3-8. Conversions of the starting materials were kept below 5%.

The apparent quantum yields were plotted against Einsteins of light absorbed for the isomerizations 49 to 87 and 52 to 90, Figures 3-9

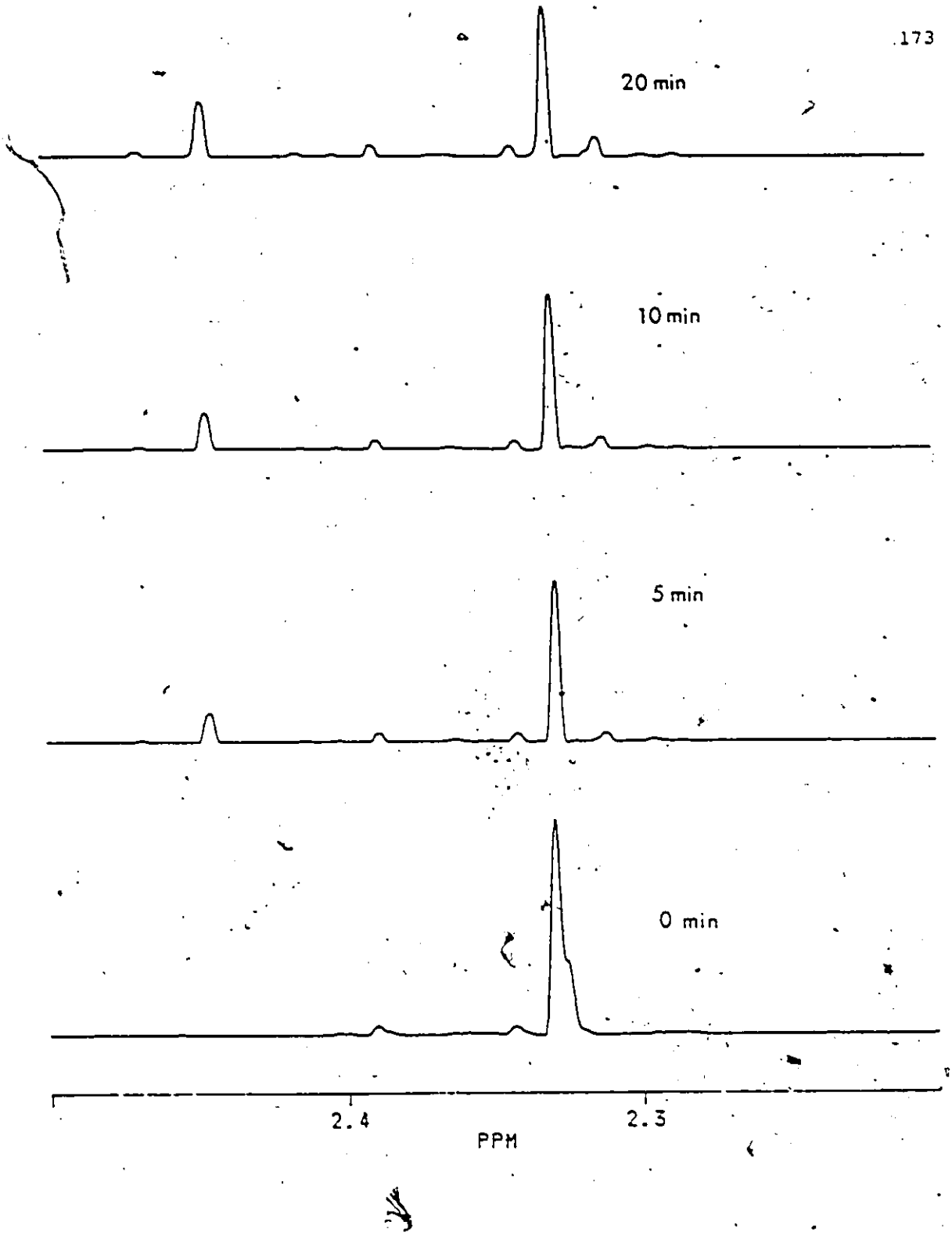

Figure 3-8: 500 MHz ^{1}H NMR spectrum of C(20)H resonance of 49 at different irradiation times.

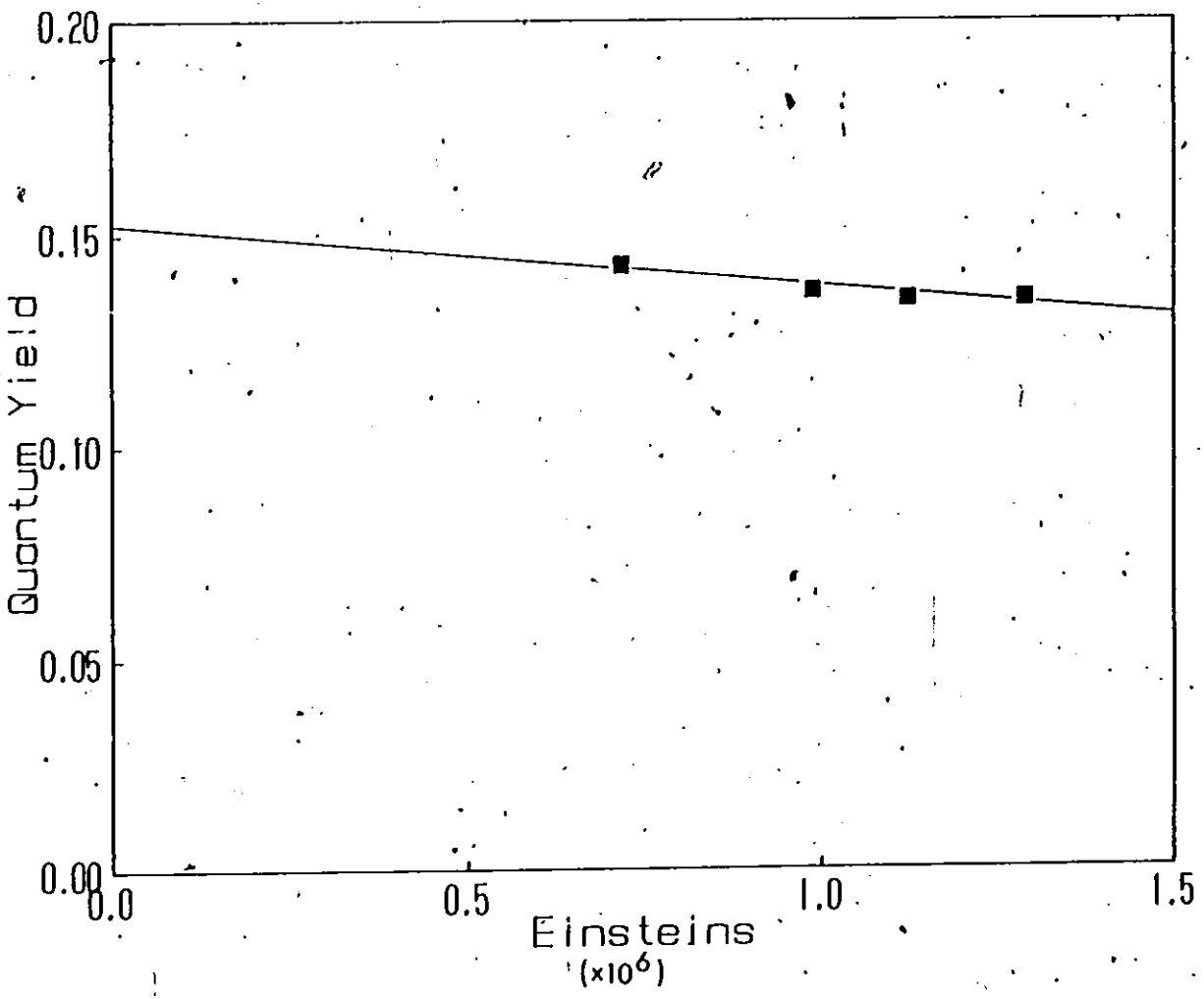

Figure 3-9: Plot of Einsteins vs. quantum yield for the conversion of 49 to 87 at 468 nm.

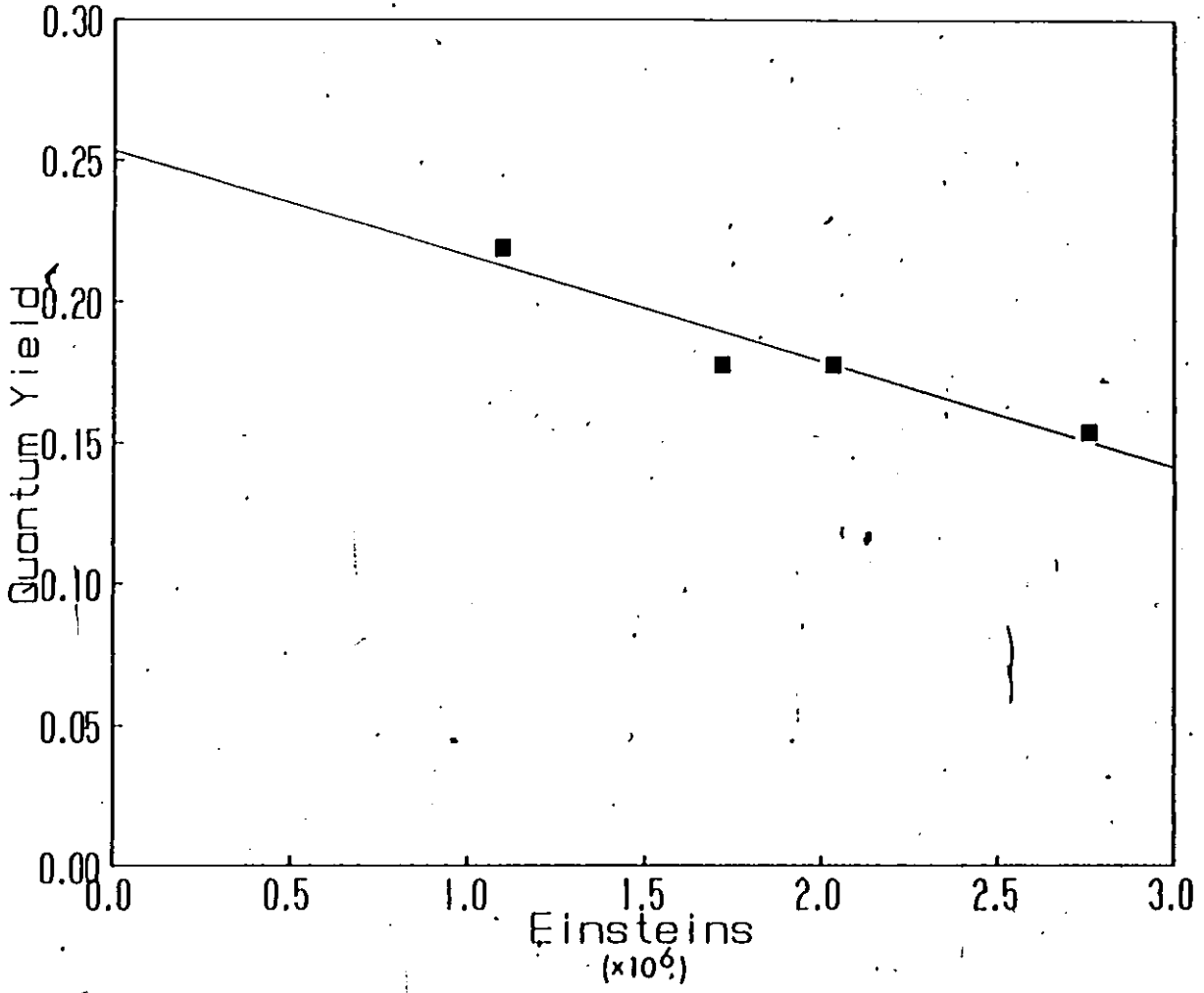

Figure 3-10: Plot of Einsteins vs. quantum yield for the conversion of 52 to 90 at 468 nm.

and 3-10. In each case, a good linear relationship ($r>0.90$) was found. From these plots, the initial quantum yields (at t=0) of 0.15 and 0.25 for 49 to 87 and 52 to 90 respectively were obtained. The quantum yield obtained for the photoisomerization of 49 → 87 was corrected for the 13-cis isomeric impurity found in the starting material (9.5%). This was done by assuming that the 13-cis isomer absorbed 9.5% of the light entering the sample. The corrected quantum yield for this reaction was 0.17. The quantum yield for the t-butyl retinylidene iminium salt isomerization was not corrected since the isomeric impurity in this starting material was only 3.5%. This was below the experimental error of the integration technique used for measuring the ^1H NMR resonances, which was approximately 5%. The calculated quantum yield of 54 to 93, 0.18, was nearly identical with that of 49 to 87.

iv. Thermal Stability of Photoproducts

The 11-cis retinylidene iminium salts 90 and 93 were shown to be thermally stable, by ^1H NMR spectroscopy, when kept at 22°C for a period of 2 hours, Table 3-5. This time period was much longer than the duration of the average photochemical experiment.

DISCUSSION

^1H NMR spectoscopy is a very powerful analytical method which can be used not only to identify but also to quantitatively analyse complex organic and inorganic compounds. The use of ^1H NMR spectroscopy with respect to retinylidene iminium salts and related compounds has been quite extensive and has produced a wealth of information on such topics as coupling constants, long range through space interactions and kinetics. However, an area which has received a large part of attention, namely the photochemistry of retinylidene iminium ions, has not been investigated using ^1H NMR spectroscopy. High field ^1H NMR spectroscopy allows for a photochemical or thermal reaction to be followed by assessing the reaction products directly. In previous photochemical studies of retinylidene iminium salts, this has not been attempted. However, in thermal kinetic studies of retinylidene ions and similar compounds, ^1H NMR has been shown not only to be informative but also to provide important quantitative information.

I. Thermal Chemistry

Methylene chloride was the least polar medium that dissolved sufficient amounts of the iminium salts studied here to permit accurate ^1H NMR spectra to be obtained. This solvent, when deuterated, does not interfere with proton resonances of any of the iminium salts. Methylene chloride also has the added advantage in that it is non-nucleophilic.

This is a desirable property of the solvent since it has been previously shown that C=C thermal isomerization is greatly accelerated by nucleophilic catalysis by the solvent or other nucleophiles in solution (186,188-190). In previous studies highly polar solvents such as methanol and acetonitrile have been used to study the photoisomerization of retinylidene iminium salts (173-177). However, these solvents do not mimic the hydrophobicity of the binding sites of rhodopsin and bacteriorhodopsin, and thus may not represent an accurate picture of the photoisomerization processes. These solvents are also nucleophilic (186,260).

A key feature of the iminium salts studied here is that they were isolated as solids and thus possess a single anion for each cation. In addition, the perchlorate anions used are substantially less nucleophilic than ions such as chloride or trichloroacetate, which have traditionally been used.

i. Simple Conjugated Iminium Salts

The trans iminium salts 30 and 34 are thermally stable in methylene chloride at 22°C, the temperature at which photochemical experiments were performed. Solutions of the 2-cis iminium salt 77 are also stable at room temperature, in methylene chloride. However, upon addition of chloride ion, 77 isomerized to the all-trans product, 30, equation 35. The 2-cis iminium salt 83 was found to isomerize to its trans isomer, 34, without the addition of chloride to the solution, equation 36.

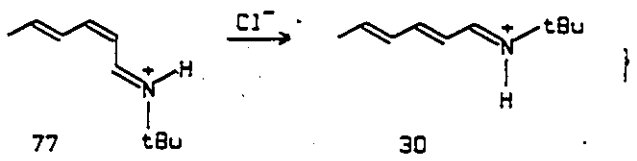

(35)

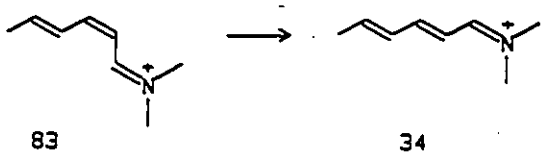

(36)

Since the 2-cis iminium salt 77 is stable in the absence of chloride ion, the thermal isomerization which occurs on addition of chloride to the solution must be mediated by the chloride ion itself. This is shown in Figure 3-4, where a plot of [chloride] vs. the rate of isomerization of 77 to 30 yields a straight line, suggesting that the reaction is second order, equation 37.

$$d[30]/dt = -k[77][(CH_3)_2NH_2Cl] \qquad (37)$$

The mechanism for the thermal isomerizations of cis iminium salts has been previously studied by Childs et al. (186,188,260) and by Rando and co-workers (189,190). Their work has presented strong evidence that, in the presence of a good nucleophile such as chloride, the cis/trans isomerization in iminium salts occurs via a nucleophilic pathway. Such a mechanism is suggested for the isomerization of 77 to 30 and is shown in

equation 38.

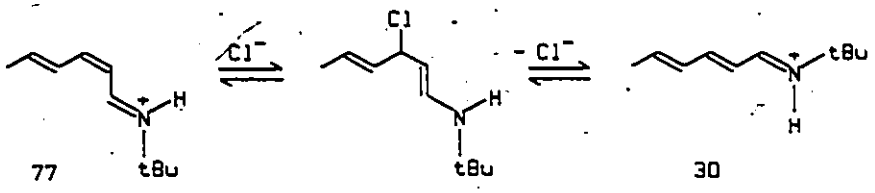

(38)

The thermal isomerization of 83 to 34 can be considered to occur through two possible mechanisms. The first involves simple C=C bond rotation. The second possibility is similar to that for 77, whereby a nucleophile catalyses the reaction.

Simple isomerization about the C=C bond in a 2-propenylidene iminium salt, 95, via a rotation mechanism, equation 39, has a calculated activation energy of about 40 kcal/mol (249). In conjugated iminium salts, it has been suggested that this barrier to rotation can be lowered by the presence of charge stabalizing groups at C(3) such as an additional double bond (185). This has the effect of potentially increasing the positive charge at C(3) through delocalization, and thus lowering the C(2),C(3) bond order. The results from the previous chapter suggest that the amount of positive charge on C(3) in the all-trans isomer 34 is minimal, and is essentially the same as that for the iminium salt 30, for which a hydrogen bond exists between cation and anion. Assuming that this electronic distribution is similar for the 2-cis isomers 77 and 83, the C(2),C(3) bond order and the activation energy for rotation of C(2),C(3) should also be similar. Thus, isomerization to the

all-trans compounds, 30 and 34, should not occur. This was the case for 77 in the absence of a good nucleophile. Along this same argument it is expected that the activation energy for rotation in 83 should fit somewhere between that of 95, 40 kcal/mol, and more conjugated systems such as the retinylidene iminium ions, about 22 kcal/mol (127). In 83, the measured activation energy for this reaction, 23.8 kcal/mol, is some 15 kcal/mol lower than the calculated energy for 95, and very near that calculated in more conjugated systems. It is therefore difficult to imagine that a simple rotational mechanism can be occurring during the isomerization of 83 to 34.

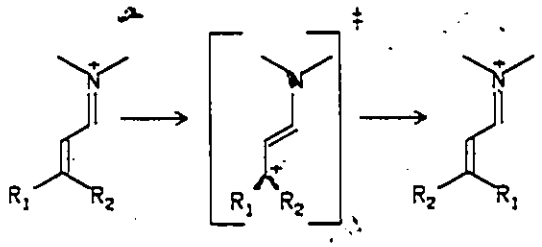

(39)

Cis/trans isomerization of 83 to 34 by a nucleophilic addition mechanism may involve one or several nucleophiles, present in the reaction medium. The possible nucleophiles may be methylene chloride, water, the perchlorate anion or other trace contaminants present. However, since this study was done using the same solvent as in 77, any influence that trace contaminants or water would have, should have been observable in 77 also. In addition, the presence of water would give rise to hydrolysis products, equation 40. No hydrolysis products were noted in either 77 or 83. Similarily, if methylene chloride acted as a

nucleophilic catalyst, this too would have been observed in 77. This too did not occur.

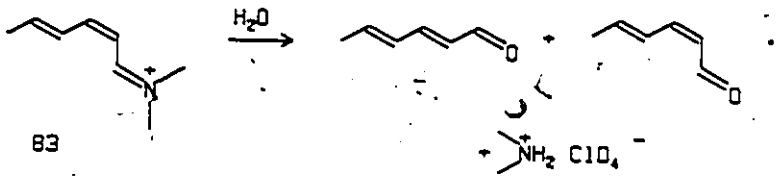

83 (40)

In the iminium salt 83, there is a significant difference in cation/anion pairing from that in 77. It was shown, in the previous chapter, that the perchlorate anion in 77 is hydrogen bonded to the nitrogen and thus is relatively fixed in position. However, in 83 the perchlorate anion can not hydrogen bond to the cation because the nitrogen is dialkylated. Thus the anion is "free" to move about the cation. Conceivably, the perchlorate could also act as a nucleophile, although a much poorer one than chloride in 77.

Isomerization of 83 to 34 by a nucleophilic mechanism would involve approach of the perchlorate anion to either C(3) or C(5), similar to nucleophilic attack by chloride in 77. Approach by the perchlorate to either C(3) or C(5) would increase positive charge at these carbons such that the bond alternation pattern in the molecules would be altered significantly. A tight ion pair could occur at this point. This would allow for facile bond rotation about C(2),C(3), leading to the trans isomer, 34, equation 41. The activation energy for this type of mechanism should be considerably lower than for a simple C=C bond

rotation. Indeed, recent calculations by Seltzer have shown that the activation energy for C=C isomerization can be decreased by about 50%, when such an interaction occurs (180).

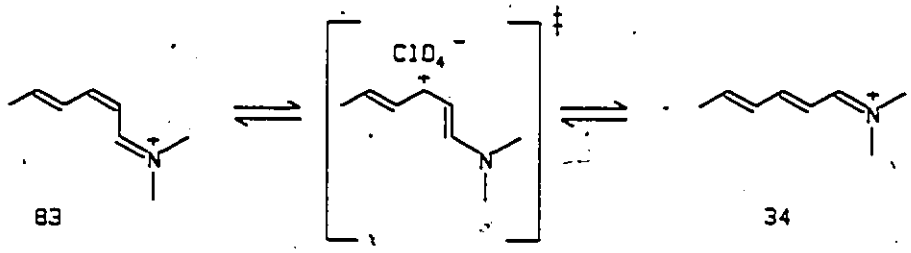

(41)

Further evidence for this type of isomerization can be derived from the relative nucleophilicities of perchlorate in 83 and chloride in 77. Since perchlorate is much less nucleophilic than chloride, the rate of the isomerization of 83 to 34 should be slower than that of 77 to 30 with only one equivalent of chloride (from Figure 3-4). In fact, the rate constant for nucleophilic catalyzed cis/trans isomerization by perchlorate anion (1.15×10^{-5} sec^{-1}) is about three times slower than with one equivalent of chloride (3.22×10^{-5} sec^{-1}). Although one might expect a larger difference between the magnitudes of these rate constants, they are still consistent with the order of nucleophilicity of these two anions. These observations suggest that the cis/trans isomerization of 83 to 34 must be occurring by the approach of the perchlorate anion to either C(3) or C(5) much like that in a nucleophilic catalysis mechanism.

ii. Retinylidene Iminium Salts

The starting compositions of the retinylidene iminium salts 49, 52 and 54, were found to contain small amounts of isomeric impurities, Table 3-6. These were identified and quantitated by ^1H NMR spectroscopy. In the retinylidene iminium salts, 49, 52 and 54, the 13-cis isomers 86, 89 and 92 are present in the amounts 9.5%, 3.5% and 12.7%, respectively. In previous studies of retinylidene iminium salts, these isomers have also been identified as the minor isomeric impurities (174,175,177). In the case of the n-butyl retinylidene iminium salt, 49, the amount of the 13-cis isomer, 86, found in the starting material is very similar to that previously reported (175). However, the amount of 13-cis isomer, 92, found in the starting material of the dimethyl substituted iminium salt, 54, is substantially lower in this study than has been previously found (177). The t-butyl retinylidene iminium salt, 52, has significantly less of the 13-cis isomer, 86, present in the starting material than either of the other two ions and represents one of the highest purity retinylidene iminium salts prepared to date. In terms of quantitative analysis for photochemical work, this made the retinylidene iminium salt, 52, the most desirable starting material.

The cis retinylidene iminium salts, generated upon irradiation, were stable at 22°C for the duration of the photochemical experiments. This was expected since the retinylidene iminium salts prepared in this study contained a non-nucleophilic perchlorate anion and were studied in a non-nucleophilic solvent, methylene chloride, similar to the simple conjugated iminium salts. This is an important finding for several

reasons. First, previous studies of retinylidene iminium salts have not shown conclusively that the cis isomers are thermally stable for long periods of time (174,175,177). These photochemical studies of all-trans retinylidene iminium salts have also utilized nucleophilic anions such as chloride (177) or trichloroacetate (174,175), which have been shown to catalyze cis to trans isomerizations (189,190). In terms of quantitative analysis of a trans to cis photoisomerization, any cis/trans thermal isomerization which occurs during a quantum yield measurement would undoubtedly be reflected in a lower quantum yield for the trans to cis process. Secondly, since the catalyzed rates of cis to trans thermal isomerization in retinylidene iminium ions are known to be different for each cis isomer (190), the isomer composition from the irradiation of these salts can also be effected.

In this work, the photoisomerizations of the retinylidene iminium salts 49, 52 and 54 show an extremely high regioselectivity for the C(11),C(12) bond. The combination of the thermal isomerization processes above, which have been shown to occur in simpler systems in this work and in the more complex retinylidene ions, may account for the apparent unselective nature of the retinylidene iminium salt photoisomerizations in previous studies (174,175,177).

Furthermore, the method of analysis previously used to the identify each retinylidene isomer also assumes that no isomerization of the cis retinylidene iminium salts occurs during the manipulations used (174,175,177). This method, involves the hydrolysis of the retinylidene iminium salts produced on irradiation of the all-trans isomer, and

subsequent HPLC analysis of the resulting retinal isomers. In this study, an identical analysis of irradiated iminium salt solutions (2 hrs) of 52 and 54, was compared with a ^{1}H NMR analysis, Table 3-10. The HPLC analysis confirmed the presence of the all-trans, 13-cis, 11-cis and 9-cis isomers for both 52 and 54, as determined by ^{1}H NMR spectroscopy. However, upon hydrolysis, there has been some significant changes in the isomer compositions, compared to those measured directly by ^{1}H NMR spectroscopy. In particular are the changes in the 13-cis isomer compositions, 89 and 93, which each increase approximately 90% upon hydrolysis. In fact, the relative amount of the 13-cis isomer in the HPLC analyses is approaching that of the equilibrium amount for retinal (22%) (261). This result is consistent with earlier work by Waddell and Donahue where it was reported that irradiation of a n-butyl all-trans retinylidene iminium ion yielded the 13-cis isomer at 468 nm as the major photoproduct (177).

It is quite clear from the examination of ^{1}H NMR spectra obtained in this study that very little, if any, of the 13-cis isomers are formed in the initial stages of the photoisomerization of 49, 52 or 54. The appearance of the 13-cis isomer in Waddell's earlier work must be incorrect, and most probably arises from hydrolysis/HPLC technique used to identify and quantitate the photoreactions. This comparison clearly shows the accuracy of ^{1}H NMR spectroscopy not only in the identification of each isomer but also in determining the relative amounts of each isomer.

Table 3-10

Comparative Analysis[a] of Retinylidene Iminium Salt Isomers by 250 MHz ^{1}H NMR and HPLC

		Relative Percentage by	
	Isomer	^{1}H NMR	HPLC
52	All-trans	44.6	37.3
89	13-cis	5.9	12.0
90	11-cis	20.3	19.5
91	9-cis	29.2	31.3
54	All-trans	37.6	40.8
92	13-cis	6.0	11.6
93	11-cis	27.1	21.8
94	9-cis	29.3	25.8

a. each value is the average of two identical experiments.

II. Photochemistry

i. Nature of the Excited State

The absorbance spectra of all of the iminium salts studied were characteristically broad and lacked any fine structure. This is in agreement with many other studies which document the absorbance spectra of conjugated iminium salts. The lack of fine structure in these spectra suggest that the S_1 excited states are composed of many vibrational levels, all very close in energy.

In the retinylidene iminium salts, the fact that the 11-cis isomer is formed as the primary photoproduct at three different wavelengths, suggests that isomerization is occurring from the S_1 excited state. This is in excellent agreement with previous studies by Honig et al. (143).

ii. Regioselectivity of Photoisomerizations

All of the iminium salt photoisomerizations studied have very high degrees of regioselectivity in the initial stages of photoisomerization. In the simple conjugated iminium salts 30 and 34, the primary photoproducts are the 2-cis iminium salts, 77 and 83 respectively. In the retinylidene iminium salts, 49, 52 and 54, the 11-cis photoisomers, 87, 90 and 93 are formed initially, equation 41. These regioselectivities are in agreement with calculations by Longlet and co-workers (262), which predict that the central bond is most susceptible to photoisomerization. The only compound which does not fit this trend is the 2,4,6-octatrienylidene iminium salt 31, which predominantly forms the

2-cis compound 80 upon irradiation. It was expected that an equal proportion of the 2-cis, 80, and 4-cis, 81, isomers should be produced in the early stages of the irradiation. This suggests that the regioselectivity of conjugated iminium salt photoisomerization may be governed by more than simply the central bond.

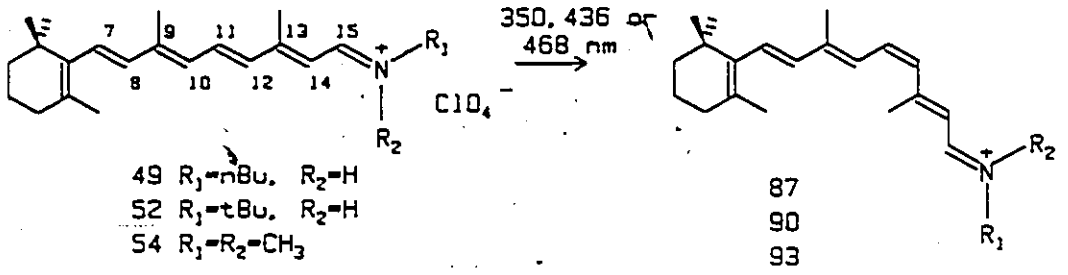

(42)

In the retinylidene iminium salts 49, 52 and 54, the selectivity for isomerization to the 11-cis isomers 87, 90 and 93 rather than the 13-cis isomers 86, 89 and 92 was large. This was noted from irradiations of each of the all-trans isomers to a point where the 11-cis isomers reached approximately 20%, Figure 3-7. In these cases there was no observable change in the 13-cis iminium salt composition from the starting material composition. Since the detection level of high field ^{1}H NMR spectroscopy in these experiments is about 1.0% this suggests that <1.0% 13-cis isomer was being formed photochemically in either 49, 52 or 54. In these cases the selectivity for the formation of the 11-cis isomers 87, 90 and 93 must be at least 20 times!

The identification of the 11-cis isomer as the primary photoproduct from the irradiation of all-trans retinylidene iminum salts was confirmed shortly after the completion of this work. Becker and

Freedman (175) used difference absorption spectroscopy/HPLC techniques to determine that the 11-cis isomer is the primary photoproduct from 350 nm irradiation of an all-trans retinylidene iminium salt. However, it should be noted that they reported appreciable amounts of the 13-cis photoisomer being formed. This is in contrast to the present study, and again may be a result of thermal formation of the 13-cis isomer during hydrolysis.

iii. Effects of Polyene Chain Length and Substituents on Quantum Yield

A comparison of the quantum yields for photoisomerization of the iminium salts 30 and 34 with those of the retinylidene iminium salts 49, 52 and 54 shows that there is a marked decrease in the quantum yield as the polyene chain length increases, Table 3-11. The quantum yields for the simple iminium salts 30 and 34 are two to three times larger than those of the retinylidene salts, but well within the range found for the C=C photoisomerization of other simple conjugated iminium salts (188, 249). This decrease in quantum yield with increasing chain length has been noted previously for C=N photoisomerization studies.

The iminium salts 30 and 34 also differ from the retinylidene iminium salts studies here in that the simple systems do not possess any methyl groups along the polyene chain. These may contribute to the quantum efficiency of a reaction through steric interaction in the excited state. This could influence the position of the critical geometry (energy minimum) in the excited state which is usually at 90°. In order to determine this, a study would require the measurement of cis

Table 3-11

Quantum Yield Data[a] for Isomerization of Some Iminium Salts

Compound	Product	λ_{ex}	Φ
30	77	313	0.56
34	83	313	0.60
49	87	468	0.15
52	90	468	0.25
54	93	350	0.17

a in CH_2Cl_2 at 21 C.

to trans quantum yields and a comparison with the quantum yields for the trans to cis isomers measured in this study. The sum of these should add to one if a common excited state energy minimum exists for these two processes. One approach to this would be to examine a series of polyenyl iminium salts such as 30 and 31, extend their conjugation and add methyl groups to various sites along the chain. The influence that the methyl groups have on the efficiencies of the forward and reverse photoisomerizations and on the position of the energy minimum in the excited state could then be determined.

In the previous chapter and other studies, it was shown that a hydrogen bond exists between the nitrogen and the perchlorate anion in 30, while in 34 the perchlorate is completely dissociated from the cation. However, these two compounds have similar quantum yields, 0.56 and 0.60 respectively, and form similar 2-cis primary photoproducts, 77 and 83. This suggests that the hydrogen bond in 30 does not reduce the efficiency or alter the regiospecificity of this reaction through its specific interaction with the perchlorate anion in solution. A similar result has been found by Childs and Dickie (188) in the photoisimerization of substituted 3-aryl-2-propenylidene iminium salts, equations 43 and 44. Interestingly, the quantum yields for these later reactions are nearly identical with those found in the present work.

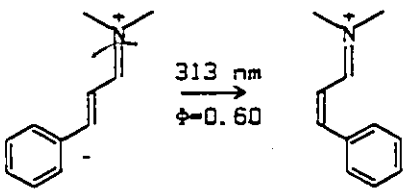

(43)

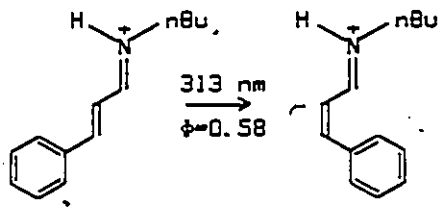

(44)

The retinylidene iminium salts 49, 52 and 54 form an 11-cis photoproduct upon irradiation, however the efficiencies of the transformations vary. The t-butyl substituted iminium salt 52, forms the 11-cis photoproduct 90, with an efficiency which is 50% larger than either the n-butyl salt, 49, or the dimethyl salt, 54. This is in contrast with findings in the simple iminium salts, where the t-butyl ion, 30, formed its 2-cis isomer with a similar efficiency as the dimethyl iminium salt, 34. A similar dependency of the quantum yield on the nitrogen substituent has been previously noted in photochemical studies of 11-cis retinylidene iminium salts (176), where quantum yields ranged from 0.05-0.34 and in aromatic iminium salts which had quantum yields of 0.27-0.75 (188). These results suggest that the quantum yields for these photoisomerizations may become more sensitive to the substituent on nitrogen as the conjugated chain increases in length.

iv. Comparison with the Natural Chromophores

The all-trans retinylidene iminium salts 49, 52 and 54 are analogous in structure to the chromophre in light adapted bacteriorhodopsin, BR_{568}. In terms of the structure and photoreactivity of bacteriorhodopsin, it appears that the best model is the iminium salt

52. As has been shown earlier, this molecule exists in the 6-s-trans conformation in the solid state, much like the natural chromophore, and has most of the positive charge localized nearest the nitrogen. In solution, 52 exists to some extent in the 6-s-trans conformation but the actual concentration of this conformer is difficult to assess. Bacteriorhodopsin presumably undergoes photoisomerization from the 6-s-trans state.

The quantum yield for the photoisomerization of 52 to 90 is 0.25, equation 45, very similar to that of bacteriorhodopsin, which has a quantum efficiency of 0.30 (80,81). This similarity in quantum efficiencies suggests that the protein in bacteriorhodopsin does not affect the efficiency of this reaction. However, the regioselectivities of the isomerizations for the retinylidene iminium salt 52 and for bacteriorhodopsin are different. In 52 the primary photoproduct is the 11-cis isomer while in bacteriorhodopsin the 13-cis isomer is formed, equation 46. This clearly indicates that the binding site in the bacterioopsin protein is influencing the regioselectivity of isomerization.

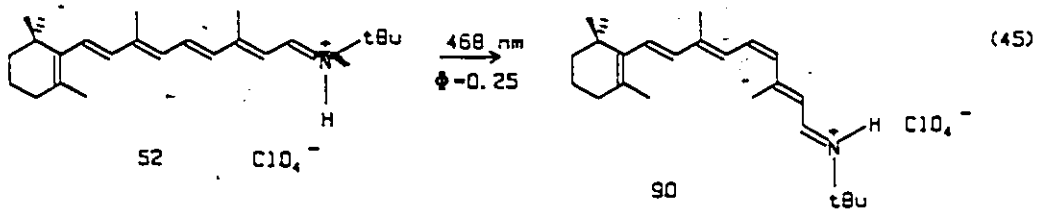

(45)

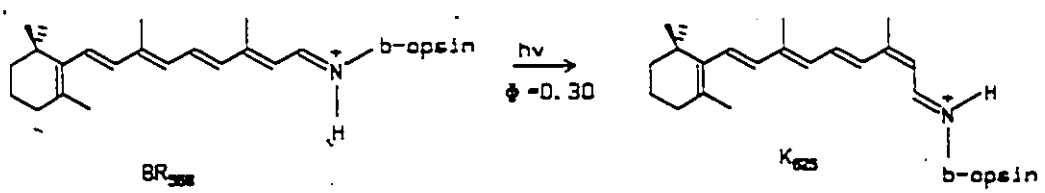

(46)

Structural studies on the intermediates in the bacteriorhodopsin photocycle (Scheme 1-2) have concluded that the first intermediate formed, K_{625}, is 13-cis (84,85). The only suggested modification in the protein cavity at this stage is an increase in the anion distance from the cation, resulting from the isomerization. This gives rise to the longer wavelength absorption of the K intermediate. Furthermore, binding site studies of various retinal isomers with bacterioopsin show that while the all-trans and 13-cis retinal isomers bind readily with bacterioopsin, the 11-cis retinal isomer does not (117). This has been previously rationalized on the longitudinal and latitudinal size limitations of the binding site cavity within the protein. Based on these results, it would seem likely that during the initial stages of the photochemical cycle of bacteriorhodopsin, the size restrictions in the binding site do not change considerably. Therefore, only the 13-cis photoisomer is exclusively formed in bacteriorhodopsin.

In solution where no environmental restrictions are present that may favour one cis isomer over the others, the retinylidene iminium salt 52 simply follows its energetically favoured path in the excited state which seems to be rotation about the central C(11),C(12) bond. Such a regioselectivity has not been shown previously in retinylidene iminium salts. Furthermore, the photoisomerization of 52 to 90 is the first example of a model all-trans retinylidene iminium salt which photoisomerizes, regioselectively, as efficiently as a natural pigment.

A comparison between 52 and the visual pigment rhodopsin can also be made. Both of these molecules undergo a photoisomerization to yield

an 11-cis product. In 52, this is a trans to cis process whereas in rhodopsin the reverse process occurs, equation 47. Similar to bacteriorhodopsin, the isomerization of the 11-cis chromophore in rhodopsin occurs in the well defined limits of its binding site. The first intermediate in the photoisomerization of rhodopsin, bathorhodopsin, has been suggested to be all-trans (62). However, since all-trans retinal does not bind with opsin, this suggests that a major change in the protein cavity of rhodopsin during the early stages of this isomerization must have occurred. This implies that in rhodopsin the opsin protein does not influence the regioselectivity of the isomerization, as in bacteriorhodopsin. This has been further verified in photochemical studies of 11-cis retinylidene imines and iminium salts which also form their all-trans isomers (175).

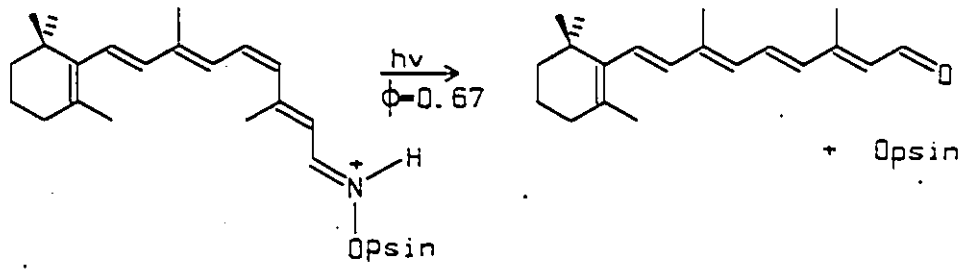

(47)

An estimate of the efficiency of the 11-cis to trans isomerization in 52 can be obtained from its photostationary state composition. This state was never fully reached in irradiations of 52. However, the composition of 52 after an extended irradiation of 2 hours, Table 3-10, which consists of the all-trans, 13-cis, 11-cis and 9-cis isomers may give an estimate of the photostationary state composition.

$$\Phi_{t\rightarrow c} C_t \varepsilon_t = \Phi_{c\rightarrow t} C_c \varepsilon_c \qquad (48)$$

The quantum yield for the photoisomerization of 90 to 52 is determined from equation 48, using known values for the extinction coefficients of the all-trans (ε_t) and 11-cis (ε_c) isomers (174), their concentrations at 2 hours and the quantum yield for the all-trans to 11-cis conversion ($\Phi_{t\rightarrow c}$). This yields a quantum yield of 0.59 for the conversion of the 11-cis retinylidene iminium salt 90 to its all-trans isomer 52, equation 49. This is in excellent agreement with the reported value of 0.67 for the similar reaction in rhodopsin. A similar calculation for the n-butyl retinylidene iminium salt, 87, yields a quantum yield of 0.40 for its photoisomerization to the all-trans isomer, 49. This is in good agreement with prevously reported values of 0.22-0.37 for this reaction.

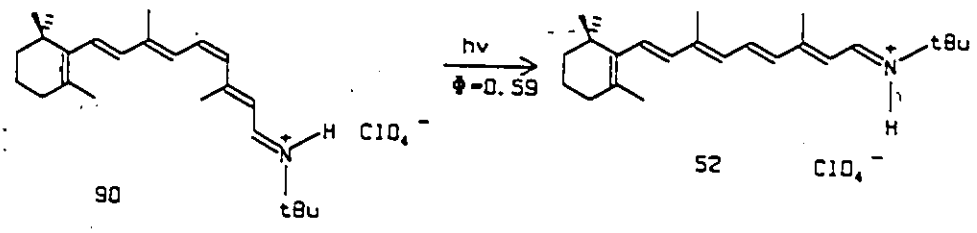

(49)

The calculated quantum yields for the cis to trans photoisomerizations of 87 and 90 assume that the cis/trans isomerization and trans/cis isomerization of these compounds occur from a common energy minimum in the excited state. If this is not the case then these

calculated values may be far from correct. Nevertheless, these approximations show that in all cases studied, cis/trans photoisomerization in retinylidene iminium salts is much more efficient than the corresponding trans/cis isomerization. This can be ascertained from the negative slopes of Figures 3-9 and 3-10, which indicate that light absorption and presumably isomerization by the cis isomers 87 and 90 is increasing with irradiation time. The slope for the photoisomerization of 52 is more severe than that for 49 indicating that the back isomerization is more efficient in the former case. This observation is in good agreement with magnitudes of the calculated quantum yields.

III. Summary

The photoisomerizations of several iminium salts were studied quantitatively by high field ^1H NMR spectroscopy and were found to be highly regioselective. It was found that in conjugated iminium salts, the efficiencies of these photoisomerizations decreases as the chain length increases. Differing substitution on nitrogen had little effect on the efficiency for photoisomerization in the simple iminium salts studied, but had a large effect on the photoisomerization efficiency in retinylidene iminium salts.

The method of analysis in this work, high field ^1H NMR spectroscopy, was found to be accurate and far superior to previously used HPLC/hydrolysis techniques. Furthermore, the use of non-nucleophilic perchlorate anions and solvent (methylene chloride), assured

that thermal cis/trans isomerizations which have plagued previous photochemical studies of all-trans retinylidene iminium salts did not occur. This combination of ^1H NMR spectroscopy, anion and solvent should be the only combination used in future studies of these complex polyene systems, where several possible photoisomerizations are possible.

Using the ^1H NMR technique, quantum yields for only the all-trans to 11-cis photoisomerizations in retinylidene iminium salts were determined. This is the first time a quantum yield for a specific c=C bond photoisomerization has been determined for retinylidene ions. In the case of the t-butyl retinylidene iminium salt 52, a quantum yield of 0.25 was found for this process, essentially the same efficiency as that in bacteriorhodopsin.

EXPERIMENTAL METHODS

Chapter 4

EXPERIMENTAL METHODS

I. Materials

The reagents used in this work were commercially available. Diethyl ether was distilled from $LiAlH_4$ and stored over 3Å molecular sieves. Methylene chloride was distilled from P_2O_5, and stored over molecular sieves. Tertiary butylamine and n-butylamine were distilled and kept over 3Å molecular sieves. Tertiary butylamine was stored in the refrigerator.

Cinnamaldehyde (Kodak), 2,4-hexadienal (Aldrich), and β-ionone (Aldrich) were distilled prior to use. All-trans retinal (Aldrich or Fluka) was assayed by analytical HPLC (>98% pure) and used without further purification. Dimethyl ammonium perchlorate was prepared from dimethylamine and perchloric acid and stored in a dessicator prior to use.

Deuterated methylene chloride, used in all quantitative ^1H NMR experiments, was purchased in sealed 1 gram ampules (MSD Isotopes) and used without further purification.

II. Instrumentation

1. ^1H NMR Spectra

All ^1H NMR spectra were obtained at 90 MHz on a Varian EM390

spectrometer, 250 MHz on a Bruker WM250 spectrometer or 500 MHz on a Bruker AM500 spectrometer. Unless otherwise noted the acquisition temperature was 21°C.

Deuterated methylene chloride was used as an internal reference for most spectra. The residual $C\underline{H}DCl_2$ in this solvent was centred at 5.32 ppm and appeared as a triplet.

The ^1H NMR spectral simulation of iminium salt 24 was carried out in the absence of the chemical shift of C(1)H and its coupling to C(2)H due to a lack of memory size in the progam.

ii. Solution ^{13}C NMR Spectra

Spectra were obtained at 20.1 MHz on a Bruker WP80 spectrometer, 62.9 MHz on a Bruker WM250 spectrometer or 125.8 MHz on a Bruker AM500 spectrometer. Unless otherwise noted, spectra were acquired at 21°C. Deuterated methylene chloride was used as an internal standard in most spectra, the central peak of the quintet being centred at 53.8 ppm.

The various resonances of all compounds were assigned by broadband decoupling, spin-echo and $\{^{13}C\}^1H$ correlation experiments. Concentrations ranged from 0.03 M to 0.4 M.

iii. Solid State ^{13}C NMR Spectra

Solid state ^{13}C NMR spectra of the iminium salts 34, 41-44, 48, 51 52, and 54 were obtained using cross polarization magic angle spinning (CPMAS) on crystalline samples. Samples were packed into alumina rotors in a nitrogen atmosphere. Spectra were acquired at 25.1 MHz on a Bruker

MSL100 spectrometer or at 50.3 MHz on a Bruker MSL200 spectrometer. Spectra obtained on this latter instument were provided by Dr. R.E. Wasylishen of the Department of Chemistry at Dalhousie University, Halifax, Nova Scotia. Spinning rates were approximately 4000-4500 Hz. Methyl and quaternary carbon resonances were assigned using the delay without decoupling pulse sequence of Opella and Frey (201). Adamantane was used as an external reference, having chemical shifts of 29.50 ppm (CH) and 38.56 ppm (CH_2) with respect to tetramethylsilane (263).

iv. Solution and Solid State Absorption Spectra

Solution absorption spectra were obtained at 21°C using a Hewlett Packard 8451A diode array spectrophotometer, Perkin-Elmer Lambda 9 spectrophotometer or Pye Unicam SP8-100 UV-Vis spectrophotometer. Concentrations of approximately 10^{-5} M in methylene chloride were employed.

Solid state absorption spectra were obtained on microcrystalline samples using the method of Kobayashi et al (206). A thin layer of freshly crystallized iminium salt was placed on a glass or quartz slide. A similar slide or one coated with KBr was used as a reference.

v. Infrared Spectra

Solid and solution infrared spectra were measured using a Nicolet 7199 FT-IR spectrometer. Solid spectra were obtained for iminium salts as thin KBr discs.

vi. Liquid Chromatography

Preparative and analytical high pressure liquid chromatography of all retinal isomers was carried out in a dark room using a Varian 5000 liquid chromatograhic system with a Varian Vista 402 data station. In analytical experiments, a silica phase Varian Si-5, 15 cm x 4 mm i.d. column was used. Preparative experiments used a similar Si-10 column, having dimensions of 30 cm x 8 mm i.d.. The solvent system used was 98% hexane/2% tetrahydrofuran.

Quantitative analysis of retinal isomers was carried out at 254 nm and 365 nm. The composition of isomers was corrected using the relative extinction coefficient method of Waddell and West (170). The elution order of isomers was 13-cis, 11-cis, 9-cis and all-trans having relative retention times of 0.54:0.65:0.72:1.0 at a flow rate of 1.0 ml/min and column pressure of 36 psi.

III. Synthesis

The imines 26-29 and 45-47 were synthesized using a modified method of Blatz et al (32). The corresponding iminium salts 30-33 and 48-53 were prepared by addition of an ethereal solution of the desired acid to the imine dissolved in ether. The iminium salts 34, 41-44 and 54 were prepared following the procedures of Leonard and Paukstelis (193). The protonated aldehydes 38 and 39 were prepared by extraction from methylene chloride into FSO_3H. Sample syntheses of all classes of compounds are given below.

Physical data for the iminium salts prepared in this work are

found in Table 4-1, unless the compound has been previously reported and characterized.

i. N-t-butyl-2,4-hexadienylidene imine, 26 and N-t-butyl-2,4,6-octatrienylidene imine, 27

Tertiary butylamine (1.52 g, 21.0 mmoles) was added to a solution of 2,4-hexadienal (sorbaldehyde) (200 mg, 2.0 mmol) in dry ether (10 ml) over anhydrous K_2CO_3 under a nitrogen atmosphere. The reaction mixture was stirred for 24 hours, filtered, and ether and excess amine removed under vacuum. The yield was 267 mg, 95%.

Imine 27 was prepared by the similar condensation of t-butylamine with 2,4,6-octatrienal (150 mg, 1.23 mmol). Octatrienal was prepared from a Reformatsky reaction of bromomethylacetate with sorbaldehyde, followed by reduction with $LiAlH_4$ at 0°C and MnO_2 oxidation (overall yield, 5%).

ii. N-t-butyl-2,4-hexadienylidene iminium perchlorate, 30, and N-t-butyl-2,4,6-octatrienylidene iminium perchlorate, 31

The freshly prepared imine, 26 (above), was dissolved in dry ether (10 ml) and cooled to -40°C under nitrogen. To this an ethereal solution of $HClO_4$ was added dropwise until precipitation was complete. The resulting solid was filtered and recrystallized from CH_3CN/ether at -20°C, to yield a pale yellow solid (96 mg, 21%).

Iminium salt 31 was prepared similarly to give a yellow solid, yield 110 mg, 33%.

Table 4-1

Some Physical Data for Selected Imines and Iminium Salts

Cmpd	mp (°C)	Str. Freq. (cm^{-1})[a]		Mol. Form.	Analyses					
					Calc.			Found		
		$\nu_{C=N}$	$\nu_{C=C}$		%C	%H	%N	%C	%H	%N
30	159	1658.56	1628.45	$C_{10}H_{16}NClO_4$	47.80	7.22	-	47.71	7.23	
31	175	1653.56	1600.81	$C_{12}H_{18}NClO_4$	51.89	7.26	-	50.91	6.88	
34	106	1666.28	1630.29	$C_8H_{14}NClO_4$	42.96	6.31	6.26	42.98	6.22	6.10
41	105	1606.10	1573.90	$C_{18}H_{16}NCl_3O_2$	56.20	4.19	3.64	43.77	3.68	2.26
41[b]				$C_{20}H_{17}NCl_6O_4$	43.80	3.13	2.56	43.77	3.68	2.26
42	185	1628.45	1585.46	$C_{16}H_{16}NClO_4$	59.73	5,01	4.35	59.82	5.01	4.17
43	115	1612.39	1574.60	$C_{18}H_{15}NCl_4O_2$	51.59	3.60	3.34	40.45	2.95	1.53
43[b]		1612.39	1574.60	$C_{20}H_{16}NCl_7O_4$	41.24	2.77	2.40	40.45	2.95	1.53
44	151	1621.63	1578.11	$C_{16}H_{15}NClO_4$	53.95	4.24	3.93	53.96	4.15	3.96
45	115	1628.01	1578.98	$C_{15}H_{12}N$	74.54	5.00	5.80	74.99	5.39	5.74
48	180	1644.38	1539.62	$C_{26}H_{38}NCl_3O_2$	62.09	7.62	2.79	59.67	7.56	2.80
51	180	1637.33	1542.56	$C_{24}H_{38}NBF_4$	67.45	8.96	-	64.28	8.74	
52	166	1635.32	1539.64	$C_{24}H_{38}NClO_4$	65.51	8.71	-	62.73	9.16	
53	146	1645.36	1550.70	$C_{25}H_{38}NF_3SO_3$	58.87	7.82	-	59.58	7.90	
54	168	1639.70	1542.45	$C_{22}H_{34}NClO_4$	64.15	8.32	-	62.64	7.90	

a KBr disc.

b with two CCl_3COOH molecules per cation

iii. N,N dimethyl-2,4-hexadienylidene iminium perchlorate, 34

N,N dimethyl ammonium perchlorate (600 mg, 4.1 mmol) was dissolved in a minimum amount of absolute ethanol (5 ml) and sorbaldehyde added dropwise (840 mg, 8.8 mmol). After stirring for 3 hours, a small amount of dry ether was added to induce precipitation, and the flask cooled in ice. The resulting pale yellow salt was filtered, recrystallized twice from ethanol/ether and dried under vacuum (yield 410 mg, 45%).

The retinylidene iminium salt 54 was prepared similarily from N,N dimethyl ammonium perchlorate (50 mg, 0.35 mmol) and all-trans retinal (200 mg, 0.70 mmol). The yield was 145 mg, 50%.

iv. Aromatic Iminium Salts, 41-44

The aromatic iminium salts 41-44 were prepared in a similar manner to 34. The method is illustrated for the perchlorate salt, 41. Cinnamaldehyde (2.0 g, 15 mmol) was stirred in ether and equimolar amounts of N-methyl aniline (800 mg, 7 mmol) and $HClO_4$ were added dropwise until precipitation was complete. The yellow salt was recrystallized twice from CH_3CN/ether and dried under vacuum. The yield was 1.06 g, 72%.

v. N-t-butyl-retinylidene imine, 46

Tertiary butylamine (2.1 g, 28.2 mmol) was added to a solution of all-trans retinal (800 mg, 2.8 mmol) in dry ether (50 ml) under a nitrogen atmosphere and in the absence of light. The reaction was

stirred at room temperature over 3Å molecular sieves for 24 hours. The mixture was filtered, and ether and excess amine removed under vacuum, yielding a pale yellow residue (910 mg, 95%).

vi. N-t-butyl-retinylidene iminium perchlorate, 52

Freshly prepared imine 47 was dissolved in dry ether (30 ml) and cooled to -40°C in the dark. To this, an ethereal solution of $HClO_4$ was added dropwise until precipitation was complete. The dark red precipitate was filtered and washed several times with ether until the fitrate was pale yellow. The salt was recrystallized twice from methylene chloride/ether at -20°C, fitered and dried overnight under vacuum (yield 440 mg, 37%).

The iminium salts 49-51 and 53 were prepared a similar fashion.

vii. Protonated aldehydes 38 and 39

The appropriate aldehyde (100 mg) was dissolved in CD_2Cl_2 (0.5 ml) in a medium walled nmr tube and cooled to -78°C in a dry ice-acetone bath. Previously cooled FSO_3H (-78°C) was added slowly down the sides of the tube. The sample was mixed using a thin glass rod and kept at -78°C until ^1H NMR analysis.

IV. Bond-Valence Calculations

All bond-valence calculations were carried out using bond lengths (R) obtained from crystallographic data. The general formula found below was used. Values for standard bond lengths (R_o) and its appropriate

fitted constant (B) are those determined by Brown and co-workers (216-220) except for that involving a conjugated C-C bond, for which no accurate value was available. This (R_o) was determined using a back calculation from known benzenoid crystal structures (264-266) and assuming that each bond (R) had a valence of 1.5 as in benzene itself. All of the parameters used are listed below.

$$s = e^{\frac{(R_o - R)}{B}}$$

Bond Type	R_o	B
C-C	1.543	0.35
C-C (conj)	1.512	0.35
C-N	1.462	0.31
C-O	1.370	0.30

V. Determination of Crystal Structures

i. Collection of Data

Crystals of the iminium salt 44 and imine 45 suitable for x-ray diffraction techniques, were obtained from distillation of diethyl ether into an acetonitrile solution of each salt at about -20°C.

The space group of each compound was determined through precession photography. These showed that crystals were monoclinic and that the space group for each was $P2_1/c$. Accurate unit cell parameters were determined from a least squares fit of X, ϕ and 2Θ. In 37, a range

of $19.6 < 2\theta < 31.3$ was used for 15 reflections. For 38, 15 reflections where $18.6 < 2\theta < 25.9$ were used. Radiation was graphite monochromatic MoK_α, $\lambda = 0.71069$ Å, and reflection intensity data was measured using a Syntex $P2_1$ diffractometer having a coupled θ(crystal)-2θ(counter) scan. Selection of scan rates and initial data treatment were as previously described (267,268). Corrections for Lorentz-polarization factors were made, but not for absorption. This will make the maximum error in F_o 1.0% in 37 and 38. All crystal data are summarized in Table 4-2.

ii. Solution of Structures

In the iminium salt 44, chlorine atoms were found from a three-dimensional Patterson synthesis and all other atoms were located from electron difference syntheses. The chlorine atom in the imine 45 was found by direct methods using 164 reflections with $|E| > 1.1$ and 20 sets of starting phases. All remaining atoms were found from the subsequent difference map. Coordinates of all non-hydrogen atoms were defined using full-matrix least-squares minimizing $\Sigma\omega(|F_o| - |F_c|)^2$, until the maximum shift/error was < 0.1. Throughout, the scattering curves were taken from those in the International Tables (269). Secondary extinction corrections were applied from SHELX. Positional parameters for non-hydrogen atoms of both structures are found in Tables 4-3 and 4-4. Anisotropic temperature factors, hydrogen positional parameters and observed (F_o) and calculated (F_c) reflection intensities for 44 and 45 can be found in the Appendix.

Table 4-2

Crystal Data

	44	45
Compound	$(C_{16}H_{15}NCl^+)(ClO_4^-)$	$C_{15}H_{12}NCl$
F.W.	356.17	241.72
Crystal Size (mm)	0.30 x 0.30 x 0.25 rough cube	0.30 x 0.30 x 0.10 plate
Systematic Absences	0k0 k=2n+1	0k0 k=2n+1
	h01 l=2n+1	h01 l=2n+1
Space Group	$P2_1/c$	$P2_1/c$
Unit Cell (Å and deg)	a= 7.811 b=16.811 b=113.26 c=13.876	a=14.438 b=14.348 b=101.57 c= 6.240
Volume ($Å^3$)	1673.97	1266.39
Z	4	4
pcalc (g cm^{-3})	1.413	1.268
μ (cm^{-1})	3.53	2.34
Max. 2θ, reflctns meas	45°, h,k,>l	55°, h,k,>l
Standard reflctns (esd)	1 0 4 (0.041) 2 5 1 (0.015)	4 -3 2 (0.012) 1 6 -2 (0.009)
Temp, (°C)	22	22
No. unique reflctns	1927	2922
No. with I>0	1317	1393
Final R_1, R_2	0.0980, 0.0542	0.0920, 0.0764
Final shift/error max (avg)	.044	.020
x (secondary extinction)	0.00438	0.01092
Final difference map		
max (e. $Å^{-3}$); location	0.64 .20 .74 .84	0.26 .08 .88 .76
min (e. $Å^{-3}$); location	-0.60 .38 .80 .32	-0.57 .10 .66 .52
Weighting	$w=\sigma(F)^{-2}$	$w=(\sigma F^2 + 0.000659F^2)^{-1}$
Error in an obs of unit wt	2.5385	1.3278

$R_1 = \Sigma||F_o|-|F_c||/\Sigma|F_o|$; $R_2 = [\Sigma\omega(|F_o|-|F_c|)^2/\Sigma\omega F_o^2]^{1/2}$

Table 4-3

Atomic positional parameters and temperature factors ($Å^2$)

for C15H12ClN, 45.

Atom	X(x10^4)	Y(x10^4)	Z(x10^4)	Ueq(x10^3)
CL	-1048.9(6)	1564.6(7)	9267(1)	75.3(5)
C(1)	-6222(2)	1102(1)	12906(4)	49(1)
C(2)	-5250(2)	1050(2)	12657(4)	51(1)
C(3)	-4984(2)	1160(1)	10756(4)	50(1)
C(4)	-4019(1)	1192(1)	10376(4)	43(1)
C(5)	-3239(2)	875(2)	11915(4)	49(1)
C(6)	-2331(2)	974(2)	11572(5)	55(1)
C(7)	-2189(2)	1393(1)	9673(4)	48(1)
C(8)	-2940(2)	1686(2)	8084(4)	50(1)
C(9)	-3843(2)	1581(2)	8459(4)	50(1)
C(10)	-7413(1)	1150(1)	14905(4)	45(1)
C(11)	-7649(2)	1625(2)	16666(4)	52(1)
C(12)	-8574(2)	1680(2)	16918(5)	58(1)
C(13)	-9278(2)	1251(2)	15429(6)	62(1)
C(14)	-9050(2)	762(2)	13709(5)	65(1)
C(15)	-8131(2)	719(2)	13431(5)	53(1)
N	-6446(1)	1104(1)	14780(3)	50.6(9)

Table 4-4.

Atomic positional parameters and temperature factors ($Å^2$) for C16H15Cl2NO4, 44.

Atom	X(x10^4)	Y(x10^4)	Z(x10^4)	Ueq(x10^3)
CL(1)	3975(2)	8062(1)	3580(1)	57.5(4)
CL(2)	3179(2)	3881(1)	4157(1)	79.0(5)
O(1)	5235(9)	8621(3)	3614(5)	175(1)
O(2)	2750(8)	7983(2)	2582(3)	184(1)
O(3)	4956(6)	7360(2)	4021(3)	74(1)
O(4)	3120(9)	8358(4)	4179(4)	143(2)
C(1)	-649(9)	7353(3)	-340(4)	41(1)
C(2)	451(9)	6891(3)	537(4)	48(1)
C(3)	-222(8)	6193(3)	674(4)	44(1)
C(4)	671(7)	5638(3)	1523(4)	32(1)
C(5)	-103(8)	4882(3)	1483(4)	52(1)
C(6)	646(8)	4340(3)	2280(4)	51(1)
C(7)	2199(8)	4556(3)	3139(4)	48(1)
C(8)	2978(8)	5292(4)	3189(4)	60(1)
C(9)	2256(8)	5829(3)	2387(4)	45(1)
C(10)	-1460(8)	8447(3)	-1534(4)	41(1)
C(11)	-2277(9)	8010(4)	-2438(4)	54(1)
C(12)	-3513(10)	8365(4)	-3324(5)	66(2)
C(13)	-3934(10)	9160(5)	-3320(5)	74(2)
C(14)	-3092(13)	9603(4)	-2420(8)	54(1)
C(15)	-1837(10)	9257(3)	-1486(5)	49(1)
C(16)	1593(12)	8449(4)	40(6)	85(1)
N(1)	-202(6)	8059(3)	-600(3)	43(1)

VI. Quantum Yield Measurements

The light source used for the determination of quantum yields for the iminium salts 30 and 34 was an Osram HBO 200W super pressure mercury lamp in a Kratos LHM 150/1 housing. The power source was a Kratos LPS 251HR Universal Arc Lamp Supply. A Kratos GM 100-1 monochrometer with 11.4 nm bandwidth entrance and exit slits was used. The collimated light beam was passed through a filter with a transmission window of 308-400 nm (Corning #5970) to a beam splitter inside of a light tight box.

The light source used for the irradiation of the iminium salts 49 and 52 was an Osram XBO 150W/S high pressure xenon lamp placed in a PRA ALH215 Arc Lamp Housing, and operated with a PRA M303X Lamp Power Supply. The light was passed through a PRA ALH1 Jacketed Infrared Filter. A PRA B102 monochrometer with 20 nm bandwidth entrance and exit slits was used, followed by a 425 nm cut-off filter (Corning #3389). Collimated light was passed through a beam splitter to the samples.

In both cases a UV-enhanced silicon chip diode detector placed behind each of the sample and comparison channels was used to assess the amount of light passing through each sample. These were connected to a "home-built" digital integrater.

Samples of each iminium salt were carefully weighed (3-10 mg) and dissolved in CD_2Cl_2 (0.5 mls) in 22-mm-od x 2-mm quartz "lollipop" cells. All work was carried out in a dark room.

Quantum yields were determined using ferrioxalate actinometry at 313 nm for salts 30 and 34 and 468 nm for 49 and 52. Photon flux was determined before and after each series of four irradiations and was

found not to vary by more than 5%. The quantum yield for 54 to 93 was determined relative to the conversion of 49 to 87 at 350 nm. After each irradiation the entire sample was placed in a 5-mm-o.d., thin walled tube for 250 MHz or 500 MHz ^{1}H NMR analysis. The resulting spectrum was assayed for the presence of the trans isomer and any photochemically formed cis isomers. Evaluation of these compounds was accomplished using the relative areas of the C(2')H resonance for 30 to 77, C(1)H for 34 to 83 and C(20)H for 49 to 87, 52 to 90 and 54 to 93. The areas of these resonances were integrated by both a cut and weigh and relative peak height techniques. The relative differences in these techiques was approximately 5% and represents the approximate error in this method of measurement. Raw quantum yield data are presented in Table 4-5.

$$\Phi_{t\rightarrow c} C_t \varepsilon_t = \Phi_{c\rightarrow t} C_c \varepsilon_c \qquad (50)$$

Quantum yields for 87 to 49 and 90 to 52 were calculated from equation 50, where $\Phi_{t\rightarrow c}$ is the measured quantum yield for the trans to cis process, C_t and C_c are the concentrations of the trans and cis isomers respectively at the photostationary state, and ε_t and ε_c are their respective extinction coefficients. C_t and C_c were approximated from an extended irradiation at 468 nm and the ratio of ε_t to ε_c was determined (in CH_2Cl_2) from literature values. The remaining variable $\Phi_{c\rightarrow t}$ can be calculated from a manipulation of equation 40 to give an approximate quantum yield for the cis to trans process.

Table 4-5

Primary Quantum Yield Data

Reaction	Wgt (gm) $\times 10^3$	Moles $\times 10^5$	% Conv.	Moles Conv. $\times 10^6$	Einsteins $\times 10^6$	Φ
30 → 77	6.70	2.669	2.97	0.793	1.404	0.565
"	6.75	2.689	4.96	1.33	2.445	0.545
"	6.83	2.721	6.53	1.78	3.398	0.523
"	6.60	2.629	8.01	2.11	4.226	0.498
34 → 83	8.55	3.817	2.31	0.883	1.631	0.541
"	8.85	3.951	2.94	1.16	2.283	0.509
"	8.60	3.839	3.86	1.48	2.990	0.496
"	8.75	3.906	5.84	2.28	4.831	0.473
49 → 87	2.25	0.511	2.00	0.102	0.716	0.143
"	2.32	0.527	2.56	0.135	0.988	0.137
"	2.22	0.505	2.99	0.151	1.121	0.135
"	2.28	0.518	3.36	0.185	1.288	0.135
52 → 90	7.45	1.693	1.42	0.240	1.097	0.219
"	7.67	1.743	1.75	0.305	1.716	0.178
"	7.30	1.659	2.18	0.362	2.030	0.178
"	7.55	1.716	2.47	0.424	2.756	0.154

VII. Kinetic Measurements

1. Isomerization Rate Constants

The rate constant for the isomerization of 83 to 34 was determined in duplicate at 22±0.5°C in CD_2Cl_2. In each case the iminium salt 34 (10 mg) was dissolved in 0.5 ml of solvent in a medium walled nmr tube. The sample was then irradiated at 300 nm in a Rayonet Photochemical Reactor (Southern New England Ultraviolet Co., RPR-100) until approximately equal amounts of the 2-cis isomer, 83, and the starting material 34 were present, as assayed by ^1H NMR. The peak heights of the singlet resonances corresponding to one of the N-methyl groups in each isomer, δ 3.77 in 83 and δ 3.68 in 34, were used to quantitate the reaction. A ^1H NMR spectrum was obtained during several timed intervals of the reaction. The ratio of the cis isomer to the total iminium salt was determined and ln (ratio) plotted against time, Figure 3-5. Each run had a good linear correlation (r=0.99). The slopes of these graphs were equal to the first-order rate constant for the reaction. An average rate constant of 1.15×10^{-5} sec^{-1} for the two experiments was obtained. Raw data are given in Table 4-6. The difference in rate constants was 5%, which was the approximate error for the experiment.

Since the reaction times of the isomerization was relatively short, it was assumed that the total concentration of iminium salt did not vary substantially. The volume of CD_2Cl_2 remained constant throughout the experiment. The reaction was monitored for 1.5 half-lives at which time the N-methyl resonance for 83 became too small to

measure accurately.

A similar experiment was performed for the iminium salt 30. The major difference was that measured amounts of dimethyl ammonium chloride (> 10 fold excess) were added to each of four samples in order to catalyse isomerization. This was done after approximately 50% of the 2-cis isomer 77 had been generated photochemically. In the absence of chloride salt no thermal cis/trans isomerization was noted at 22°C. Several measurements were made during a 24 hour period and showed only a general scatter of 10% in the amount of 2-cis isomer. The reaction was monitored using the t-butyl peak heights at δ 1.54 for 77 and δ 1.51 for 30. The ratio of cis to total iminium salt was measured a minimum of three times for each catalysed reaction and ln (ratio) plotted against time to obtain four linear correlations (r=0.99 for all) and four observed pseudo first order rate constants (k_{obs}). These were plotted against the concentration of chloride for each respective run to obtain the second order rate constant 4.37×10^{-4} sec^{-4} M^{-1} (r=0.99), Figure 3-4.

Table 4-6

Rate Constant Data for the Isomerization of 83 → 34

Time (min)	% Cis	Ratio[a]	-ln (ratio)
0	42.6	1	0
30	41.9	0.98	.017
60	39.9	0.94	.065
120	37.6	0.88	.125
300	32.6	0.77	.268
360	30.6	0.72	.331
420	30.9	0.73	.321
600	26.8	0.63	.463
1380	16.8	0.39	.930

a Ratio = $\frac{Cis}{Cis_{t=0}}$

APPENDIX

Hydrogen atom positional parameters and temperature factors ($\AA^2$) for C15H12ClN, 45.

Atom	X(x10^4)	Y(x10^4)	Z(x10^4)	U(x10^3)
H(1)	-679(2)	114(1)	1149(4)	79(1)
H(2)	-481(2)	95(2)	1389(5)	100(1)
H(3)	-548(2)	126(1)	950(4)	65(1)
H(4)	-330(1)	60(1)	1327(4)	51(1)
H(5)	-170(2)	77(2)	1270(5)	103(1)
H(6)	-279(1)	196(1)	677(4)	74(1)
H(7)	-434(1)	180(2)	750(4)	64(1)
H(8)	-719(1)	192(1)	1765(4)	63(1)
H(9)	-879(2)	203(2)	1824(5)	92(1)
H(10)	-993(2)	125(2)	1546(5)	97(1)
H(11)	-955(2)	45(2)	1264(5)	90(1)
H(12)	-802(1)	41(1)	1227(4)	57(1)

Hydrogen atom positional parameters and temperature factor($\mathring{A}^2$)
for C16H15Cl2NO4 44.

Atom	X(x10^4)	Y(x10^4)	Z(x10^4)	U(x10^3)
H(1)	-179(5)	706(2)	-97(3)	55(3)
H(2)	156(7)	708(3)	111(3)	[illegible](3)
H(3)	-132(5)	600(2)	10(2)	36(3)
H(5)	-106(6)	475(2)	92(3)	61(3)
H(6)	6(6)	381(2)	227(3)	60(3)
H(8)	398(7)	546(3)	376(3)	74(3)
H(9)	293(6)	644(2)	248(3)	70(3)
H(11)	-191(7)	738(3)	-236(3)	80(3)
H(12)	-426(8)	802(3)	-406(4)	134(3)
H(13)	-490(6)	948(2)	-401(3)	61(3)
H(14)	-322(11)	1004(3)	-227(6)	133(3)
H(15)	-90(8)	950(3)	-61(4)	112(3)
H(16)	140(9)	869(3)	62(4)	114(3)
H(17)	249(11)	813(4)	30(6)	174(3)
H(18)	173(10)	896(3)	-16(5)	140(3)

Anisotropic temperature factors ($Å^2 \times 10^3$) for C16H15Cl2NO4, 44.

Atom	U11	U22	U33	U12	U13	U23
CL(1)	63(1)	67(1)	64(1)	5(1)	9(9)	14(1)
CL(2)	100(1)	84(1)	70(1)	20(1)	7(1)	4(1)
O(1)	122(5)	114(4)	337(9)	123(5)	20(5)	9(4)
O(2)	230(6)	118(4)	83(3)	-31(3)	-51(4)	67(4)
O(3)	81(3)	71(2)	111(3)	28(2)	17(2)	27(2)
O(4)	185(6)	283(8)	106(4)	34(4)	61(4)	159(6)
C(1)	73(5)	59(4)	58(4)	-2(3)	28(3)	-5(3)
C(2)	68(4)	62(4)	57(3)	11(3)	18(3)	3(4)
C(3)	54(4)	63(4)	55(3)	3(3)	17(3)	2(3)
C(4)	50(4)	51(3)	63(3)	-0.(3)	28(3)	2(3)
C(5)	50(4)	70(4)	57(4)	-7(3)	8(3)	-7(3)
C(6)	58(4)	52(3)	71(4)	4(3)	12(3)	-4(3)
C(7)	54(4)	60(4)	58(3)	-2(3)	12(3)	1(3)
C(8)	57(4)	79(5)	57(4)	-10(3)	6(3)	-3(4)
C(9)	51(4)	62(4)	58(3)	-3(3)	15(3)	-12(3)
C(10)	59(4)	74(4)	50(3)	16(3)	25(3)	-9(3)
C(11)	80(5)	78(4)	50(3)	6(4)	20(3)	-0.(4)
C(12)	88(6)	95(6)	78(5)	13(4)	26(4)	-10(4)
C(13)	75(5)	122(7)	78(5)	38(5)	23(4)	-0.(5)
C(14)	107(6)	70(5)	126(7)	39(6)	60(5)	18(5)
C(15)	98(5)	61(4)	85(4)	20(4)	41(4)	-3(4)
C(16)	92(6)	76(5)	81(5)	5(4)	-2(5)	-31(5)
N(1)	64(3)	63(3)	52(2)	1(2)	21(2)	-6(3)

Anisotropic temperature factors ($Å^2 \times 10^3$) for $C_{16}H_{15}ClN$

Atom	U11	U22	U33	U12	U13	U23
CL	67.8(6)	99.1(7)	109.0(8)	-8.4(6)	41.5(5)	-8.8(5)
C(1)	53(1)	51(1)	52(1)	-1(1)	8(1)	-0.(1)
C(2)	56(1)	56(1)	52(1)	-0.(1)	10(1)	1(1)
C(3)	51(1)	52(1)	54(1)	-1(1)	5(1)	2(1)
C(4)	54(1)	40(1)	44(1)	-0.(1)	7(1)	1(1)
C(5)	58(1)	56(1)	50(1)	12(1)	14(1)	8(1)
C(6)	59(1)	58(1)	65(2)	4(1)	15(1)	9(1)
C(7)	58(1)	46(1)	69(1)	-7(1)	25(1)	-1(1)
C(8)	78(2)	52(1)	51(1)	-1(1)	25(1)	-2(1)
C(9)	62(1)	52(1)	45(1)	2(1)	7(1)	3(1)
C(10)	53(1)	42(1)	52(1)	5(1)	11(1)	5(1)
C(11)	67(1)	54(1)	54(1)	2(1)	15(1)	-1(1)
C(12)	81(2)	64(2)	69(2)	-1(1)	35(1)	6(1)
C(13)	58(1)	67(2)	99(2)	1(1)	31(1)	4(1)
C(14)	54(1)	70(2)	86(2)	-9(1)	13(1)	-9(1)
C(15)	62(1)	55(1)	64(1)	-13(1)	17(1)	-3(1)
N	53(1)	60(1)	50(1)	-1(1)	10(1)	4(1)

REFERENCES

1. G. Wald, Nature, 132, 316 (1933).
2. R. Hubbard, J. Gen. Physiol., 37, 381 (1954).
3. F.J.M. Daemen, W.J. de Grip and P.A.A. Jansen, Biochim. Biophys. Acta, 271, 419 (1972).
4. F.J.M. Daemen, Biochim. Biophys. Acta, 300, 255 (1973).
5. N.G. Abdulaev, I.D. Artamonov, A.S. Bogachuk, M.Yu. Feigina, M.B. Kostina, A.B. Kudelin, V.I. Martynov, A.I. Miroshnikov, A.S. Zolotarov and Yu.A. Ovchinnikov, Biochem. Int., 5, 693 (1982).
6. S. Tsunasawa, K. Narita and H. Shichi, Am. Soc. Photobiol., Abstr.71 (1979).
7. P.A. Hargrave and S.L. Fong, J. Supramol. Struct. 6, 559 (1977).
8. P.A. Hargrave, S.L. Fong, J.H. McDowell, M.T. Mas, D.R. Curtis, J.K. Wong, E. Juszczak and D.P. Smith, Neurochem. Int. 1, 231 (1980).
9. H. Shichi, M.S. Lewis, F. Irreverre and A.L. Stone, J. Biol. Chem., 244, 529 (1969).
10. M. Azuma and Y. Kito, Ann. Rep. Biol. Works Fac. Sci. Osaka Univ., 15, 59 (1967).
11. M.D. Bownds and G. Wald, Nature, 205, 254 (1965).
12. R. Fager, P. Sejnowsli and E.W. Abrahamson, Biochim. Biophys. Res. Commun., 47, 1244 (1972).

13. M.D. Bownds, Nature, 216, 1178 (1967).

14. M. Akhtar, P.T. Blosse and P.B. Dewhurst, Chem. Commun., 631 (1967).

15. R. Hubbard and G. Wald, J. Gen. Physiol., 36, 269 (1962).

16. G. Wald, P.K. Brown, R. Hubbard and W. Orosnik, Proc. Natl. Acad. Sci. U.S.A., 41, 438 (1955).

17. W.J. de Grip, R.S.H. Liu, V. Ramamurthy and A.E. Asato, Nature, 262, 416 (1976).

18. H. Matsumoto, R.S.H. Liu, C.J. Simmons and K. Seff, J. Am. Chem. Soc., 102, 4261 (1980).

19. R.S.H. Liu, A.E. Asato, M. Denny and D. Mead, J. Am. Chem. Soc., 106, 8298 (1964).

20. P. Blatz, M. Lin, P. Balasubramaniyan, V. Balasubramaniyan, P.B. Dewhurst, J. Am. Chem. Soc., 91, 5930 (1969).

21. H. Matsumoto and T. Yoshizawa, Nature, 258, 524 (1975).

22. K. Nakanishi, A.P. Yudd, R. Crouch, G.L. Olson, H-C Cheung, R. Govindjee, T.G. Ebrey and D.J. Patel, J. Am. Chem. Soc., 98, 236 (1976).

23. N.A. Sokolova, B.I. Mitsner and V.I. Zakis, Bioorg. Khim. 5, 1053 (1979).

24. D.R. Lewin and N.J. Thomson, Biochem. J., 103, 36P (1967).

25. M. Azuma, K. Azuma and Y. Kito, Biochim. Biophys. Acta, 295, 520 (1973).

26. R.S.H. Liu, A.E. Asato and M. Denny, J. Am. Chem. Soc., 99, 8095 (1977).

27. G. Wald and P.K. Brown, J. Gen. Physiol., 37, 189 (1953).

28. W. Dawson and E.W. Abrahamson, J. Phys. Chem., 66, 2542 (1962).

29. W.H. Waddell, A.M. Schaffer and R.S. Becker, J. Amer. Chem. Soc., 99, 8456 (1977).

30. R. Morton and G. Pitt, Biochem. J., 59, 128 (1955).

31. C.S. Irving and P.A. Leermakers, Biochemistry, 9, 858 (1970).

32. P.E. Blatz, J.H. Mohler and H.V. Navangul, Biochemistry, 11, 848 (1972).

33. P.E. Blatz and J.H. Mohler, Biochemistry, 11, 3240 (1972).

34. P.E. Blatz and J.H. Mohler, Biochemistry, 14, 2304 (1975).

35. J. Favrot, J.M. Leclercq, R. Roberge, C. Sandorfy and D. Vocelle, Photochem. Photobiol., 29, 99 (1979).

36. J. Favrot, D. Vocelle and C. Sandorfy, Photochem. Photobiol., 30, 417 (1979).

37. F.I. Harosi, J. Favrot, J.M. Leclercq, D. Vocelle and C. Sandorfy, Rev. Can. Biol., 37, 257 (1978).

38. A. Lewis, M.A. Marcus, B. Ehrenberg and H. Crespi, Proc. Natl. Acad. Sci. U.S.A., 75, 4642 (1978).

39. R.H. Callender, A. Doukas, R. Crouch and K. Nakanishi, Biochemistry, 15, 1621 (1976).

40. R. Callender and B. Honig, Ann. Rev. Biophys. Bioeng., 6, 33 (1977).

41. A.R. Oseroff and R.H. Callender, Biochemistry, 13, 4243 (1974).

42. J. Shriver, G. Mateescu, R. Fager, D. Torchia and E.W. Abrahamson, Nature, 17, 271 (1977).

43. J. Shriver, E.W. Abrahamson and G.D. Mateescu, J. Am. Chem. Soc., 98, 2407 (1976).

44. B. Honig, U. Dinur, K. Nakanishi, V. Balogh-Nair, M.A. Gawinowicz, M. Arnaboldi and M.A. Motto, J. Am. Chem. Soc., 101, 7086 (1979).

45. C. Longstaff and R.R. Rando, Biochemistry, 24, 8137 (1985).

46. R.D. Gilardi, I.L. Karle and J. Karle, Acta Cryst., B28, 2605 (1972).

47. R. Mathies, A.R Oseroff and L. Stryer, Proc. Natl. Acad. Sci. U.S.A., 73, 1 (1976).

48. G.S. Harbison, P.P.J. Mulder, H. Pardoen, J. Lugtenburg, J. Herzfeld and R.G. Griffen, J. Am. Chem. Soc., 107, 4809 (1985).

49. B. Honig, B. Hudson, B.D. Sykes and M. Karplus, Proc. Natl. Acad. Sci. U.S.A., 68, 1289 (1971).

50. A.H. Schaeffer, W.H. Waddell and R.S. Becker, J. Am. Chem. Soc., 96, 2063 (1974).

51. R. Rowan and B.D. Sykes, J. Am. Chem. Soc., 96, 7000 (1974).

52. J.W. Shriver, G.D. Mateescu and E.W. Abrahamson, Biochemistry, 18, 4785 (1979).

53. H. Akita, S.P. Tanis, M. Adams, V. Balogh-Nair and K. Nakanishi, J. Am. Chem. Soc., 102, 6370 (1980).

54. Y. Inoue, Y. Tokito, R. Chujo and Y. Miyoshi, J. Am. Chem. Soc., 99, 5592 (1977).

55. M.E. Heyde, D. Gill, R.G. Kilponen and L. Rimai, J. Am. Chem. Soc., 93, 6776 (1971).

56. M.-J. Mantione and B. Pullman, Int. J. Quantum Chem., 5, 349

(1971).

57. L. Salem and P. Bruckmann, Nature, 258, 526 (1975).

58. T. Kakitani and H. Kakitani, J. Phys. Soc. Japan, 38, 1455 (1975).

59. H.J.A. Dartnall, Vision Res., 8, 339 (1968).

60. W.H. Waddell, A.P. Yudd and K. Nakanishi, J. Am. Chem. Soc., 98, 238 (1976).

61. T. Yoshizawa and G. Wald, Nature 197, 1279 (1963).

62. G. Eyering, B. Curry, A. Broek, J. Lugtenburg and R. Mathies, Biochemistry, 21, 384 (1982).

63. B. Mao, M. Tsuda, T.G. Ebrey, H. Akita, V. Balogh-Nair and K. Nakanishi, Biophys. J., 35, 543 (1981).

64. R.R. Birge, Ann. Rev. Biophys. Bioeng., 10, 315 (1981).

65. A.G. Doukas, B. Aton, R.H. Callender and T.G. Ebrey, Biochemistry, 17, 2430 (1978).

66. R. Uhl and E.W. Abrahamson, Chem. Rev., 81, 291 (1981).

67. J.S. George and W.A. Hagins, Nature, 303, 344 (1983).

68. P.S. Zurer, Chem. Eng. News, 61, 24 (1983).

69. M.D. Bownds, Photochem. Photobiol., 32, 487 (1980).

70. V.P. Skulachev, FEBS Lett., 146, 244 (1982).

71. A. Sitaramayya, J. Harkness, J.H. Parkes, C. Gonzalez-Oliva and P.A. Liebman, Biochemistry, 25, 651 (1986).

72. K.L. Puckett and S.M. Golden, Biochemistry, 25, 1739 (1986).

73. D. Oesterhelt and W. Stoekenius, Nature New Biol., 233, 149 (1971).

74. B. Honig, Ann. Rev. Phys. Chem., 29, 31 (1978).

75. R. Henderson, Ann. Rev. Biophys. Bioeng., 6, 87 (1977).

76. G.S. Harbison, S.O. Smith, J.A. Pardoen, P.P.J. Mulder, J. Lugtenburg, J. Herzfeld, R. Mathies and R.G. Griffin, Biochemistry, 23, 2662 (1984).

77. D. Oesterhelt, M. Meentzen and L. Schuhmann, Eur. J. Biochem., 40, 453 (1973).

78. M.J. Pettei, A.P. Yudd, K. Nakanishi, R. Hesselman and W. Stoekenius, Biochemistry, 16, 1955 (1977).

79. G.S. Harbison, S.O. Smith, J.A. Pardoen, C. Winkel, J. Lugtenburg, J. Herzfeld, R. Mathies and R.G. Griffin, Proc. Natl. Acad. Sci. U.S.A., 81, 1706 (1984).

80. C.R. Goldschmidt, O. Kalisky, T. Rosenfeld and M. Ottolenghi, Biophys. J., 17, 179 (1977).

81. B. Becher and T.G. Ebrey, Biophys. J., 17, 185 (1977).

82. T. Rosenfeld, B. Honig, M. Ottolenghi, J. Hurley and T.G. Ebrey, Pure Appl. Chem., 49, 341 (1977).

83. R.H. Lozier, R.A. Bogomolni and W. Stoeckenius, Biophys. J., 15, 955 (1975).

84. M. Braiman and R. Mathies, Proc. Natl. Acad. Sci. U.S.A., 79, 403 (1982).

85. S.O. Smith, J. Lugtenburg and R.A. Mathies, J. Membrane Biol., 85, 95 (1985).

86. S.O. Smith, A.B. Meyers, J.A. Pardoen, C. Winkel, P.P.J. Mulder, J. Lugtenburg, R. Mathies, Proc. Natl. Acad. Sci. U.S.A., 81, 2055 (1984).

87. K.J. Kaufmann, P.M. Rentzepis, W. Stoeckenius and A. Lewis,

Biochem. Biophys. Res. Commun., 68, 1109 (1976).

88. M.L. Applebury, K.S. Peters and P.M. Rentzepis, Biophys. J., 23, 375 (1978).

89. R.H. Lozier and W. Niederberger, Fed. Prod., Fed. Am. Soc. Exp. Biol., 36, 1828 (1977).

90. Y. Shichida, S. Matuoka, Y. Hidaka and T. Yoshizawa, Biochim. Biophys. Acta, 723, 240 (1983).

91. H.J. Polland, M.A. Franz, W. Zinth, W. Kaiser, E. Kolling and D. Oesterhelt, Biophys. J., 49, 651 (1986).

92. D.L. Narva, R.H. Callender and T.G. Ebrey, Photochem. Photobiol. 33, 567 (1981).

93. P.V. Argade and K.J. Rothschild, Biochemistry, 22, 3460 (1983).

94. M.A. Slifkin and S.R. Caplan, Nature, 253, 56 (1975).

95. Q.Q. Li, R. Govindjee and T.G. Ebrey, Proc. Natl. Acad. Sci. U.S.A., 81, 7079 (1984).

96. M.A. Marcus and A. Lewis, Biochemistry, 17, 4722 (1978).

97. M. Braiman and R. Mathies, Biochemistry, 19, 5421 (1980).

98. K. Schulten and P. Tavan, Nature, 272, 85 (1978).

99. J. Terner, C.L. Hsieh, A.R. Burns and M.A. El-Sayed, Biochemistry, 18, 3629 (1979).

100. S.O. Smith, J.A. Pardoen, P.P.J. Mulder, B. Curry, J. Lugtenburg and R. Mathies, Biochemistry, 22, 6141 (1983).

101. J.M. Fang, J.D. Carricker, V. Balogh-Nair and K. Nakanishi, J. Am. Chem. Soc., 105, 5162 (1983).

102. E. Kolling, W. Gartner, D. Oesterhelt and L. Ernst, Angew. Chem.

Int. Ed. Engl., 23, 81 (1984).

103. M. Sheves, N. Friedman, A. Albeck and M. Ottolenghi, Biochemistry, 24, 1260 (1985).

104. B. Chance, M. Porte, B. Hess and D. Oesterhelt, Biophys. J., 45, 913 (1975).

105. R.H. Lozier, W. Niederberger, R.A. Bogomolni, S. Hwang and W. Stoeckenius, Biochim. Biophys. Acta, 440, 545 (1976).

106. R.H. Lozier, R.A. Bogomolni and W. Stoeckenius, Biophys. J., 15, 955 (1975).

107. B. Becher and T.G. Ebrey, Biophys. J., 17, 185 (1977).

108. J.B. Hurley, T.G. Ebrey, B. Honig and M. Ottolenghi, Nature, 270, 540 (1978).

109. H.G. Khorana, G.E. Gerber, W.C. Herlihy, C.P. Gray, R.J. Anderegg, K. Nihei and K. Biemann, Proc. Natl. Acad. Sci. U.S.A., 76, 5046 (1979).

110. Yu. A. Ovchinnikov, N.G. Abdulaev, M.Yu. Feigina, A.V. Kiselev and N.A. Lobanov, FEBS Lett., 100, 219 (1979).

111. R. Henderson and P.N.T. Unwin, Nature, 257, 28 (1975).

112. H. Michel and D. Oesterhelt, Proc. Natl. Acad. Sci. U.S.A., 77, 1283 (1980).

113. H. Michel, EMBO J., 1, 1267 (1982).

114. H. Michel, J. Mol. Biol., 158, 567 (1982).

115. N. Unwin and R. Henderson, Sci. Amer., ,78 (1983).

116. B.A. Lewis, C.S. Harbison, J. Herzfeld and R.G. Griffin, Biochemistry, 24, 4671 (1985).

117. D. Oesterhelt and L. Schuhmann, FEBS Lett., 44, 262 (1974)

118. F. Tokunga, R. Govindjee, T.G. Ebrey and R. Crouch, Biophys. J., 19, 191 (1977).

119. F. Tokunaga, T.G. Ebrey and R. Crouch, Photochem. Photobiol., 33, 495 (1981).

120. M. Muradin-Szweylcowska, J. A. Pardoen, D. Dobbelstein, J.P.L. Van Amsterdam and J. Lugtenburg, Eur. J. Biochem., 140, 173 (1984).

121. K. Kouyama, T. Kinosita and A. Ikegami, J. Mol. Biol., 165, 91 (1983).

122. K.J. Rothschild, P.V. Argade, T.N. Earnest, K.S. Huang, E. London, M.J. Laio, H. Bayley, H.G. Khorana and J. Herzfeld, J. Biol. Chem., 257, 8592 (1982).

123. S.O. Smith, A.B. Meyers, R.A. Mathies, J.A. Pardoen, C. Winkel, E.M.M. Van Den Berg and J. Lugtenberg, Biophys. J., 47, 653, (1985).

124. G.S. Harbison, J. Herzfeld and R.G. Griffin, Biochemistry, 22, 1 (1983).

125. J.A. Pardoen, P.P.J. Mulder, E.M.M. Van den Berg and J. Lugtenburg, Can. J. Chem., 63, 1431 (1985).

126. T. Hamanaka, T. Mitsui, T. Ashida and M. Kakudo, Acta Cryst., B28, 214 (1972).

127. P. Tavan, K. Schulten and D. Oesterhelt, Biophys. J., 415 (1985).

128. G.S. Harbison, S.O. Smith, J.A. Pardoen, J.M.L. Courtin, J. Lugtenburg, J. Herzfeld, R.A. Mathies and R.G. Griffin, Biochemistry, 24, 6955 (1985).

129. R. Hubbard, Nature, 221, 432 (1969).

130. V. Balogh-Nair and K. Nakanishi, in "New Comprehensive Biochemistry", Vol. 3, C. Tamm, ed., Elsevier Biomedical Press, Amsterdam, p. 283 (1982).

131. N.J. Turro, in "Modern Molecular Photochemistry", Benjamin/Cummings Publishing, Menlo Park, California, U.S.A., p. 91 (1978).

132. D. Cossette and D. Vocelle, Can. J. Chem., 65, 661 (1987).

133. A.M. Arnaboldi, M.G. Motto, K. Tsujimoto, V. Balogh-Nair and K. Nakanishi, J. Am. Chem. Soc., 101, 7082 (1979).

134. H. Kakitani, T. Kakitani, H. Rodman and B. Honig, Photochem. Photobiol., 41, 471 (1985).

135. M. Sheves, K. Nakanishi and B. Honig, J. Am. Chem. Soc., 101, 7086 (1979).

136. M.G. Motto, M. Sheves, K.Tsujimoto, V. Balogh-Nair and K. Nakanishi, J. Am. Chem. Soc., 102, 7947 (1980).

137. M. Sheves and K. Nakanishi, J. Am. Chem. Soc., 105, 4033 (1983).

138. K. Nakanishi, V. Balogh-Nair, M. Arnaboldi, K. Tsujimoto and B. Honig, J. Am. Chem. Soc., 102, 7945 (1980).

139. V. Balogh-Nair, J.D. Carricker, B. Honig, V. Kamat, M.G. Motto, K. Nakanishi, R. Sen, M. Sheves, M. Arnaboldi Tanis and K. Tsujimoto, Photochem. Photobiol., 33, 483 (1981).

140. J.L. Spudich, D.A. McCain, K. Nakanishi, M. Okabe, N. Shimizu, H. Rodman, B. Honig and R. A. Bogomolni, Biophys. J., 49, 479 (1986).

141. J. Lugtenburg, M. Muradin-Szweykowska, C. Heeremans, J. A. Pardoen, G.S. Harbison, J. Herzfeld, R.G. Griffin, S.O. Smith and R.A.

Mathies, J. Am. Chem. Soc., 108, 3104 (1986).

142. F. Derguini, D. Dunn, L. Eisenstein, K. Nakanishi, K. Odashima, V. J. Rao, L. Sastry and J. Termini, Pure & Appl. Chem., 58, 719 (1986).

143. B. Honig, A.D. Greenberg, U. Dinur and T.G. Ebrey, Biochemistry, 15, 4593 (1976).

144. R. van der Steen, P.L. Biesheuvel, R.A. Mathies and J. Lugtenburg, J. Am. Chem. Soc., 108, 6410 (1986).

145. M. Ottolenghi, in Advances in Photochemistry, Vol. 12, J.N. Pitts, G.S. Hammond, K. Gollnick and D. Grosjean, ed., Wiley-Interscience, New York, 1980, p97.

146. A.G Doukas, M.R. Junnarkar, R.R. Alfano, R.H. Callender, T. Kakitani and B. Honig, Proc. Natl. Acad. Sci. U.S.A., 81, 4790 (1984).

147. T. Kouyama, K. Kinosita and A. Ikegami, Biophys. J., 47, 43 (1985).

148. M.M. Fischer and K. Weiss, Photochem. Photobiol., 20, 423 (1974).

149. W.H. Waddell, A.M. Schaffer and R.S. Becker, J. Am. Chem. Soc., 95, 8223 (1973).

150. J. Michl, Mol. Photochem., 4, 243 (1972).

151. T. Rosenfeld, B. Honig, M. Ottolenghi, J. Hurley and T.G. Ebrey, Pure & Appl. Chem., 49, 341 (1977).

152. V. Bonacic-Koutecky, P. Bruckmann, P. Hiberty, J. Koutecky, C. Leforestier and L. Salem, Angew. Chem. Int. Ed. Engl., 14, 575 (1975).

153. L. Salem, Acc. Chem. Res., 12, 87 (1979).

154. P. Bruckmann and L. Salem, J. Am. Chem. Soc., 98, 5037 (1976).

155. M.C. Bruni, J.P. Daudey, J. Langlet, J.P. Malrieu and F. Momicchioli, J. Am. Chem. Soc., 99, 3587 (1977).

156. F. Dietz, A. Tadjer and N. Tyutyulkov, Chem. Phys. Lett., 99, 120 (1983).

157. A. Warschel and M. Karplus, Chem. Phys. Lett., 32, 11 (1975).

158. A. Warschel, Nature, 260, 679 (1976).

159. R.M. Weiss and A. Warschel, J. Am. Chem. Soc., 101, 6131 (1979).

160. R.R. Birge and L. Hubbard, J. Am. Chem. Soc., 102, 2195 (1980).

161. R.S.H. Liu, D. Mead and A.E. Asato, J. Am. Chem. Soc., 107, 6609 (1985).

162. R.S.H. Liu and D.T. Browne, Acc. Chem. Res., 19, 41 (1986).

163. R.S.H. Liu, H. Matsumoto, A.E. Asato and D. Mead, 108, 3796 (1986).

164. R.A. Mathies, Photochem. Photobiol., 43S, 46S (1986).

165. S.O. Smith, I. Hornung, R. van der Steen, J.A. Pardoen, M.S. Braiman, J. Lugtenburg and R.A. Mathies, Proc. Natl. Acad. Sci., 83, 967 (1986).

166. M. Sheves, A. Albeck, M. Ottolenghi, P.H.M. Bovee-Guerts, W.J. De Grip, C.M. Einterz, J.W. Lewis, L.E. Schaechter and D.S. Kliger, J. Am. Chem. Soc., 108, 6440 (1986).

167. A.E. Asato, M. Denny and R.S.H. Liu, J. Am. Chem. Soc., 108, 5032 (1986).

168. W.H. Waddell, R. Crouch, K. Nakanishi and N.J. Turro, J. Am. Chem. Soc., 98, 4189 (1976).

169. W.H. Waddell, P.M. Dawson, D.L. Hopkins, K.L. Rach, M. Uemura and

J. West, 2, 1205 (1979).

170. W.H. Waddell and J. West, J. Phys. Chem., 84, 134 (1980).

171. W.H. Waddell and K. Chihara, J. Am. Chem. Soc., 103, 7389 (1981).

172. T. Rosenfeld, A. Alchalel and M. Ottolenghi, Photochem. Photobiol., 20, 121 (1974).

173. R.S. Becker, K. Freedman and G. Causey, J. Am. Chem. Soc., 104, 5797 (1982).

174. R.S. Becker and K. Freedman, J. Am. Chem. Soc., 107, 1477 (1985).

175. R.S. Becker and K. Freedman, J. Am. Chem. Soc., 108, 1245 (1986).

176. K. Freedman, R.S. Becker, D. Hannak and E. Bayer, Photochem. Photobiol., 43, 291 (1986).

177. J.M. Donahue and W.H. Waddell, Photochem. Photobiol., 40, 399 (1984).

178. H. Kessler, Tetrahedron, 30, 1861 (1974).

179. D. Cremer, J. Gauss, R.F. Childs and C.J. Blackburn, J. Am. Chem. Soc., 107, 2435 (1985).

180. S. Seltzer, J. Am. Chem. Soc., 109, 1627 (1987).

181. J.E. Johnson, N.M. Silk, E.A. Nalley, M. Arfan, J. Org. Chem., 46, 546 (1981).

182. H. Gusten and D. Schulte-Frohlinde, Z. Naturforsch., 34B, 1556 (1979).

183. W.B. Jennings, S.A. Showiman, M.S. Tolley and D.R. Boyd, J. Chem. Soc. Perk. II, 1535 (1975).

184. C. Pattaroni and J. Lauterwein, Helv. Chim. Acta, 64, 1969 (1981).

185. M. Sheves and T. Baasov, J. Am. Chem. Soc., 106, 6840 (1984).

186. M. Pankratz and R.F. Childs, J. Org. Chem., 50, 4553 (1985).

187. P.C. Mowery and W. Stoeckenius, J. Am. Chem. Soc., 101, 414 (1979).

188. R.F. Childs and B.D. Dickie, J. Am. Chem. Soc., 105, 5041 (1983).

189. D. Lukton and R.R. Rando, J. Am. Chem. Soc., 106, 258 (1984).

190. D. Lukton and R.R. Rando, J. Am. Chem. Soc., 106, 4525 (1984).

191. R. Hubbard, J. Biol. Chem., 241, 1814 (1966).

192. B.S. Fulton and R.R. Rando, Biochemistry, 26, 110 (1987).

193. N.J. Leonard and J.V. Paukstelis, J. Org. Chem., 28, 3021 (1963).

194. G.M. Sharma and O.E. Roels, J. Org. Chem., 38, 3649 (1973).

195. M. Bissonnette, H.L. Thanh and D. Vocelle, Can. J. Chem., 62, 1459 (1984).

196. H.L. Thanh and D. Vocelle, Chem. Phys. Lett., 111, 501 (1984).

197. M. Bissonette and D. Vocelle, Chem. Phys. Lett., 111, 506 (1984).

198. C. Rabiller and D. Danho, Helv. Chim. Acta, 67, 1254 (1984).

199. R.F. Childs and B.D Dickie, J. Chem. Soc. Chem. Comm., 1268 (1981).

200. D.D. Muccio, W.G. Copan, E.W. Abrahamson and G.D. Mateescu, Org. Mag. Resl, 22, 121 (1984).

201. S.J. Opella and M.H. Frey, J. Am. Chem. Soc., 101, 5854 (1979).

202. R.F. Childs, B.D. Dickie, C.A. Fyfe, C.J.L. Lock, and R.E. Wasylishen, J. Cryst. Spect. Res., 15, 73 (1985).

203. G.D. Mateescu, E.W. Abrahamson, J.W. Schriver, W. Copan, D. Muccio, M. Iqbal and V. Waterhaus, in "Spectroscopy of Biological Molecules", C. Sandorfy and T. Theophanides, ed., D. Reidel Publishing Co., Boston, U.S.A., p. 257 (1984).

204. C.S. Yannoni, Acc. Chem. Res., 15, 201 (1982).

205. K. Shibata in "Methods in Biochemical Analysis", D. Glick, ed., Intersciences Publishing co., New York, p.77 (1959).

206. H. Kobayashi, Y. Vanagawa, H. Osada, S. Minami and M. Shiziwa, Bull. Chem. Soc. Japan, 46, 1471 (1972).

207. Tables of Interatomic Distances and Configurations of Molecules and Ions, Chem. Soc. London, Spec. Publ. No. 11, p. M196 (1959).

208. J. Bernstein and I. Izak, J. Chem. Soc. Perkin II, 429 (1976).

209. L.M. Trefonas, R.L. Flurry, R. Majeste, E.A. Meyers and R.F. Copeland, J. Am. Chem. Soc., 88, 2145 (1966).

210. J.O. Selzer and B.W. Matthews, J. Phys. Chem., 80, 631 (1976).

211. B.W. Matthews, R.E. Stenkamp and P.M. Colman, Acta Cryst., B29, 449 (1973).

212. Tables of Interatomic Distances and Configurations of Molecules and Ions, Chem. Soc. London, Spec. Publ. No. 11, p. M129 (1959).

213. ibid, p. M164.

214. H. Boehme and H.G. Viehe, in "Iminium Salts in Organic Chemistry", J. Wiley & Sons, New York, 1976.

215. L. Pauling, Acta Cryst., B36, 1898 (1980).

216. I.D. Brown, in "Structure and Bonding in Crystals", Vol. II, Academic Press, U.S.A., p. 1 (1981).

217. I.D. Brown, Acta Cryst., A32, 786 (1976).

218. I.D. Brown and K-K. Wu, Acta Cryst., B32, 1957 (1976).

219. I.D. Brown, Chem. Soc. Rev., 7, 359 (1978).

220. I.D. Brown, J. Chem. Soc. Dalton, 1118 (1980).

221. P.J. MacDougall, personal communication.

222. R.F. Childs, R. Faggiani, C.J.L. Lock and C.V. Rogerson, J. Org. Chem., 26, 3043 (1983).

223. R.F. Childs, R. Faggiani, C.J.L. Lock and M. Mahendran, J. Am. Chem. Soc., 108, 3616 (1986).

224. F.H. Allen and A.J. Kirby, J. Am. Chem. Soc., 106, 6197 (1984).

225. R. Gopal, W.D. Chandler and W.D. Robertson, Can. J. Chem, 58, 658 (1980).

226. R.F.W. Bader, T-H. Tang, Y. Tal and F.W. Biegler-Konig, J. Am. Chem. Soc., 104, 946 (1982).

227. R.F. Childs, M. Mahendran, S.D. Zweep, G.S. Shaw, S.K. Chadda, N.A.D. Burke, B.E. George, R. Faggiani and C.J.L. Lock, Pure Appl. Chem., 58, 111 (1986).

228. M. Karplus and J.A. Pople, J. Chem. Phys., 38, 2803 (1963).

229. D.G. Farnum, Adv. Phys. Org. Chem., 11, 123 (1975).

230. A. Cornelius and P. Laszlo, Org. Mag. Res., 5, 99 (1973).

231. W. Adam, A. Grimison and G. Rodriguez, J. Chem. Phys., 50, 645 (1969).

232. A.J. Sarewicz, B.K. Bobertson and E.A. Meyers, J. Phys. Chem., 69, 1915 (1965).

233. C.H. Wei, Cryst. Struct. Comm., 6, 525 (1977).

234. V.H. Hartl, Acta Cryst., B31, 1781 (1975).

235. R.F. Childs, R. Faggiani, C.J.L. Lock, M. Mahendran and S.D. Zweep, J. Am. Chem. Soc., 108, 1692 (1986).

236. S.K. Chadda, R.F. Childs, R. Faggiani and C.J.L. Lock, J. Am. Chem. Soc., 108, 1694 (1986).

237. R.F. Childs, R. Faggiani, C.J.L. Lock and S.D. Zweep, unpublished results.

238. S. Malhotra and M. Whiting, J.Chem. Soc., 3812 (1960).

239. T.S. Sorensen, J. Am. Chem. Soc., 87, 5075 (1965).

240. F. Sondheimer, D. Ben-Efraim and R. Wolovsky, J. Am. Chem. Soc., 83, 1675 (1961).

241. T.E. Hogen-Esch and J. Smid, J. Am. Chem. Soc., 88, 307 (1966).

242. D.H. O'Brien, C.R. Russell and A.J. Hart, J. Amer. Chem. Soc., 101, 633 (1979).

243. J.B. Grutzner, J.M. Lawlor and L.M. Jackman, J. Amer. Chem. Soc., 94, 2306 (1972).

244. H.V. Carter, B.J. McClelland and E. Warhurst, J. Chem. Soc. Faraday, 56, 456 (1960).

245. A. Streitwieser and J.I. Brauman, J. Amer. Chem. Soc., 85, 2633 (1963).

246. R.H. Cox, H.W. Terry and L.W. Harrison, J. Amer. Chem. Soc., 93, 3297 (1971).

247. C.S. Choi, H.J. Prask and E. George, J. Phys. Chem., 61, 3523 (1974).

248. R.R. Birge, L.P. Murray, R. Zidovetzki and H.M. Knapp, J. Amer. Chem. Soc., 109, 2090 (1987).

249. B.D. Dickie, Ph.D. Thesis, McMaster University, Hamilton, Ontario (1982).

250. R.G. Pearson, J. Chem. Educ., 45, 581 (1968).

251. J. Langlet, B. Pullman and H. Berthod, J. Mol. Structure, 6, 139

(1970).

252. C.H. Stam and C.H. MacGillivary, Acta Cryst., 16, 62 (1963).

253. T. Hamanaka, T. Mitsui, T. Ashida and M. Kakudo, Acta Cryst., B28, 214 (1972).

254. C.J. Simmons, R.S.H. Liu, M. Denny and K. Seff, Acta Cryst., B37, 2197 (1981).

255. W.E. Oberhansli, W.E. Wagner and O. Isler, Acta Cryst., B30, 161 (1974).

256. C.H. Cram, Acta Cryst., B28, 2936 (1972).

257. E.L. Eichorn and C.H. MacGillivary, Acta Cryst., 12, 872 (1959).

258. H. Gunther in "NMR Spectroscopy", John Wiley & Sons, New York, 1980, p41.

259. M. Pankratz, Ph.D. Thesis, McMaster University, Hamilton, Ontario (1986).

260. R.F. Childs, G.S. Shaw and M. Mahendran, unpublished results.

261. R.R. Rando and A.J. Chang, J. Am. Chem. Soc., 105, 2979 (1983).

262. J. Langlet and J-P. Malrieu, Theor. Chim. Acta, 33, 307 (1974).

263. W.L. Earl and D.L. Vander Hart, J. Magn. Res., 48, 35 (1982).

264. P. Deltaren, Cryst. Struct., Comm., 5, 31 (1976).

265. A.N. Talukdar, Acta Cryst., B32, 803 (1976).

266. T. Ishida, J.C.S. II, 297 (1984).

267. B. Lippert, C.J.L. Lock, B. Rosenberg and M. Zvagulis, Inorg. Chem., 16, 314 (1977).

268. R.P. Hughes, N. Krishnamachari, C.J.L. Lock, J. Powell and G. Turner, Inorg. Chem., 16, 1525 (1977).

269. D.T. Cromer, J.T. Waber in "International Tables for X-ray Crystallography", J.A. Ibers and W.C. Hamilton, eds., Kynoch Press, Birmingham, England, p. 99 (1974).